Università degli Studi di Pavia - Dipartimento di Scienze della Terra edell'Ambiente

SCUOLA DI DOTTORATO IN SCIENZE E TECNOLOGIE

DOTTORATO DI RICERCA IN SCIENZE DELLA TERRA

Jakub Fedorík

Titolo della tesi: The Sicilian Channel: fault geometry and tectonic structures, 3D, analogue and numerical modelling, geodynamic mechanism. Consequences for seismic hazard assessment.

Anno Accademico 2017-2018

Ciclo XXX

Coordinatore

Prof. Roberto Sacchi

Tutore

Prof. Silvio Seno

Co-tutore

Dott. Giovanni Toscani

Dott. Emanuele Lodolo

Contents

Abstract

Analysis of multichannel seismic reflection profiles acquired in the northern part of the Sicilian Channel allows a 3D reconstruction of a NS-trending tectonic lineament which displays a mainly transcurrent structural character, and it is constituted of two major strike-slip fault systems. The western fault (Capo Granitola Fault) system does not show clear evidence of present-day tectonic activity, and toward the south, the NS-trending tectonic lineament merges into the Graham Bank. The eastern fault (Sciacca Fault) system is structurally more complex, showing active deformation at the sea-floor, particularly evident along the Nerita Bank. The Sciacca Fault is constituted of a primary fault and splay faults compatible with right-lateral kinematics. A set of analogue models has been carried out to better constrain the tectonic processes that led to the structural setting seen from seismic data. Complex right-lateral structure and uplift/subsidence patterns generated by the models are compatible with the 3D model obtained from seismic reflection profiles. Nevertheless, actual stress field derived from GPS measurements in the study area does not support the present-day right-lateral kinematics along the Sciacca Fault system. Moreover, seismic events show focal mechanisms with the left-lateral component. All these information in a coherent reconstruction show that the reconstructed fault pattern formed under a right-lateral regime; in recent times a change of the slip direction along the Sciacca Fault occurred, due to a change of the direction of principal horizontal stress.

Three-dimensional mechanical simulations of the Sciacca Fault system produce deformation that matches geologic observations and demonstrate the first order impact of fault kinematics, on uplift patterns and slip potential. Incorporating 3D fault geometry in regional will provide a more accurate understanding of active faulting in the northern part of Sicilian Channel, which is critical for hazard modelling that is used to identify regions most susceptible to earthquake damage. Two boundary-element method models have been tested, to verify subsurface structure interpretation of and slip potential. The preliminary results of the first model where both segments of the Sciacca Fault was tested show the difference in the slip potential. The northern segment of the fault system shows limited displacement while the southern segment slip. Similar activity is observed along the Sciacca Fault, where the southern segment, which comprises Nerita and the Eastern side of the Terrible Bank show active sea-floor deformation, however, the northern segment does not show any recent tectonic activity. Also, the seismological data confirm the difference of activity

along the Sciacca Fault. The second model, where we intentionally locked the northern segment and let freely slide the southern segment, show fair match between the uplift pattern seen in the model and Sicilian Channel.

Scaled sandbox models were used to investigate the 4D evolution (XRCT technique) of strike-slip dominated structure and its interaction with pre-existing thrust belt. The analysed tectonic regimes are pure strike-slipe, transpression and transtension. Transpressional models consist of two downward converging faults with a reverse slip component which dip angle values decrease with the higher amount of obliquity. Pure strike-slip model is built by similar two downward converging faults and one sub-vertical fault which is positioned above the velocity discontinuity of the model. The transtensional models present the evolution from primary and splay faults mechanism (lower angle of obliquity) to two faults with steep dip angles bounding several minor sub-vertical faults mechanism (higher angle of obliquity). The evolutional model of splay faults which are positioned only on the one side of the primary fault is proposed. Similar structural styles we observe in the strike-slip dominated part of our models were compared to several natural cases.

Ph.D overview

1st year:

The first year have been devoted initially to study the existing literature on analogue models and study area, creating a 3D model from the available seismic dataset and running clay analogue models in the laboratory of structural geology at the University of Pavia. The first task was the transformation of the seismic lines from scanned pdf formats to SEGY files in order to be uploaded in MOVE software for further structural analysis. Then the specific area of interest was selected as some areas were poorly imaged. The further structural analysis was focused on transcurrent Transfer zone of the Sicilian Channel. Analogue modelling simulating the interaction between strike-slip dominated structures and thrust front was carried out simultaneously with the seismic interpretation. At the end of the first year, all clay analogue models were performed and almost 80% of the seismic data was interpreted.

2nd year:

At the beginning of the 2nd year, the 3D fault pattern based on the seismic interpretation was built. I pursued my PhD as visiting scholar at the University of Massachusetts in Amherst (USA) during six months. The principal goal of this visiting period was learning the numerical modelling which was used during the analysis of tectonic activity seen along the Sciacca Fault. During my stay in the USA, I was led by Prof. Michele Cooke (http://www.geo.umass.edu/faculty/cooke/), who introduced me the technique which was applied on the fault pattern built from the seismic dataset. Additionally, I followed several courses and seminars, with the focus on structural geology, geomechanics and geophysics. After my return back to Europe I spent five weeks at the University of Bern (Switzerland), where X-ray computed tomography (XRCT) imaging was used to analyse sandbox analogue models. I wanted to use this technique as I could not obtain the internal structures of the fault patterns from the clay models. These new models were performed with the collaboration with Prof. Guido Scheurs (http://www.geo.unibe.ch/people/schreurs/index_ger.html) and Dr. Frank Zwaan.

3rd year

The beginning of the third year had a focus on the finalising the first manuscript which presents the results of the clay modelling and 3D modelling. A new technique for XRCT dataset interpretation was developed, in order to obtain 3D fault pattern. These results with a comparison of Sicilian Channel and several other natural cases are merged in the second manuscript. Lastly, I finalise the analysis of the numerical model, which validates the interpretation of the seismic profiles and clarify the understanding of active and non-active areas along the Sciacca Fault.

Ph. D activities

Courses attended

ENI - The role of structural geology in O&G exploration

One day lecture - Milan, Italy

Gianreto Manatschal (Univ. of Strasbourg - CNRS) - Tectonic evolution of rifted margins

Three days short course – Pavia, Italy

Jean Philippe Avouac (Univ. of Cambridge) - Earthquakes and crustal deformation

Three days short course – Rome, Italy

Michele Cooke (Mechanical Modelling of Faulting and Fractures)

Three days short course – Pavia, Italy

Michele Cooke (Rock Fracture Mechanics - GEO-SCI 631)

100 hours of class with lecturing, practical work – Amherst (MA), USA

Mike Williams (Tectonics - GEO-SCI 531)

The course involved 3 hours of lecture/discussion per week (total 39 hours) plus additional outside reading and research involving 3-6 hours per week – Amherst (MA), USA

Shell Global Solutions - Applications of carbonate diagenesis to hydrocarbon exploration and production

3/2 day short course – Parma, Italy

Shell Global Solutions - Applications of structural geology to hydrocarbon exploration and production

3/2 day short course – Parma, Italy

Presentations at congresses

2017:

GNGTS - 36° Convegno Nazionale, Trieste, Italy (presentation)

AAPG - Structural Styles in the Middle East, Muscat, Oman

Analog Modelling of Tectonic Processes, Austin, USA (poster)

2016:

25th Earth Science Meeting, Caen, France (presented by Prof. Odonne – University of Paul Sabatier, France)

Geomod, Montpellier, France (poster)

2015:

Geomod-IT Workshop dedicated to the analogue modelling in Italy

Annual reunion of Italian Structural Geologist group, Catania, Italy (poster)

7th International Symposium on Submarine Mass Movements and Their Consequences, Wellington, New Zealand (presented by Prof. Odonne – University of Paul Sabatier, France)

AGU fall meeting, San Francisco, USA (poster)

Teaching activity

- Co-Tutor of the M.Sc. Thesis of Giacomo Turini at the University of Pavia

- Teaching assistant during the short course of Prof. Michele Cooke at the University of Pavia

Grants and awards

- Grant for “Pavia-Boston project” from the University of Pavia (November 2015-April 2016).

- Grant for “International Mobility of Ph.D students” from the University of Pavia (June 2016).

- Awarded with “Licio Cernobori award” during the 36th Congress of GNGTS (Gruppo Nazionale Geofisica della Terra Solida). Trieste, 14-16 November 2017.

Thesis structure

The Ph. D thesis will be organised following the same order of my research activities and will be mainly composed of two scientific articles and one extended abstract.

The first article (chapter 2) deals with the natural case from Sicilian Channel. The 3D fault geometries obtained from seismic interpretation were compared to results from clay analogue modelling performed in the structural laboratory at the University of Pavia. The article describing these results was published in the journal of *Tectonophysics* (https://doi.org/10.1016/j.tecto.2017.11.014). This research and some preliminary results from the numerical modelling (chapter 3) were presented during the 36th Congress of GNGTS in Trieste (14-16 November 2017) and awarded with the "Licio Cernobori award"in the section of Geodynamics.

The preliminary results from the numerical modelling will be described in chapter 3 as an extended abstract. Final results from these models are not available yet as the fault surfaces need to be re-meshed and corrected.

Sandbox analogue models carried out to describe and study the general geological process of strike-slip dominated fault system and its interaction with thrust belt structure. This study is presented in a second paper (chapter 4) which will be submitted to *Journal of Structural Geology.*

1- Introduction

The Sicilian Channel is an area where three possible tectonic regimes occur and simultaneously interact (Fig. 1). Normal faulting mostly pronounced by Pantelleria, Malta and Linosa grabens and compressive structure, which is known as Sicilian-Maghrebian Chain, are interacting with a NS Transfer zone (Argnani, 1990; Casero and Roure, 1994; Antonelli et al., 1988 among others). The onshore part of the Transfer zone was recently analysed and the results of an integrated stratigraphic, structural, geophysical, and geochemical study reveal the presence of a crustal discontinuity in western Sicily that, at present, runs roughly N-S along a band from San Vito Lo Capo to Sciacca (Di Stefano et al., 2015). The offshore part of the Transfer zone was discussed by the main part of authors studying the Sicilian Channel. Even this structure was recognised by several authors (Argnani, 1990; Casero and Roure, 1994; Antonelli et al., 1988; Nigro and Renda, 2002; Finetti, 2003; Lentini et al., 2006 and Ghisetti et al., 2009), only a few seismic lines crossing the Transfer zone were interpreted and no structural model describing the formation of such important structure was proposed. The primary aim of this PhD is to analyse and understand the geological history and kinematics of this structure which possible onshore extension produced the 6^{th} most devastating earthquake in the modern Italian history (The 1968 Belice earthquake sequence). Calo & Parisi (2014) suggest a seismological linkage between onshore and offshore parts of the Transfer zone and in addition, they show that some areas of the Transfer zone are still active. Soumaya et al. (2015) present their focal mechanisms with the left-lateral strike-slip component of displacement for the offshore segment. This NS component of displacement fit well with nowadays NW-SE principal horizontal stress. However, Mantovanni et al. (2014) present its evolution since Middle Miocene. The authors show that during period Middle – Lower Miocene, the principal horizontal stress had NE-SW direction.

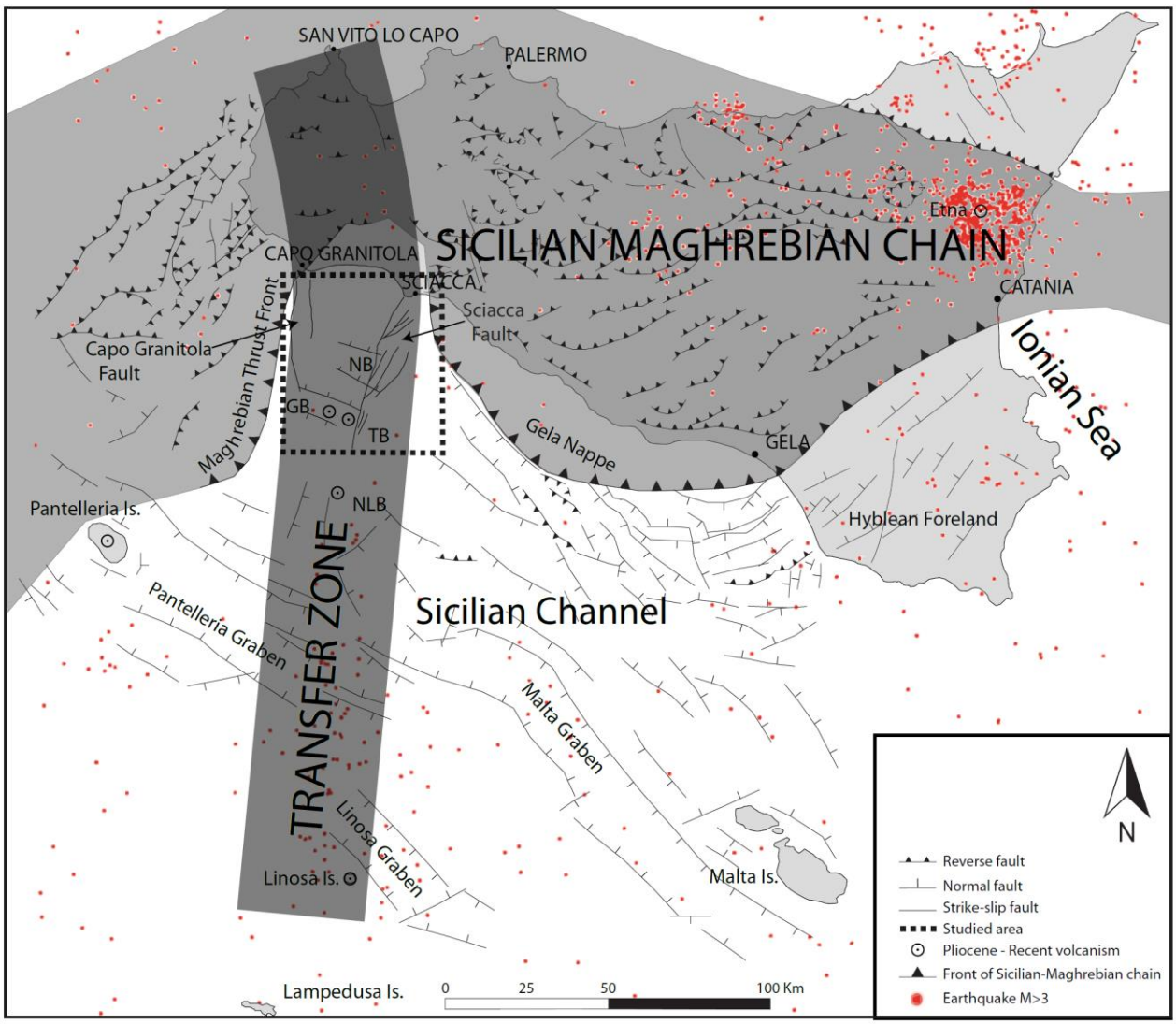

Figure 1: Simplified structural sketch map of Sicily (after Barreca et al., 2014; Di Stefano et al., 2015) and the Sicilian Channel (after Antonelli et al., 1988; Lodolo et al., 2012; Civile et al., 2014). The location of Transfer zone and Sicilian Maghrebian chain are highlighted. The dashed rectangle is the study area where the tectonic structures described in the text are reported. Epicentral earthquake locations (M>3, between 1985 and 2017; data from ISIDE, ''Italian Seismic Instrumental and parametric DatabasE'' - http://iside.rm.ingv.it/) are highlighted with red points. GB, Graham Bank; NB, Nerita Bank; NLB, Nameless Bank; TB, Terrible Bank.

Dataset available from the ViDEPI project (http://unmig.sviluppoeconomico.gov.it/videpi/videpi.asp) proposed fair coverage of seismic and well data in the northern part of Sicilian Channel where the Transfer zone is present. The area between the three central depressions (Pantelleria, Linosa and Malta grabens) of Sicilian Channel,

was also affected by the Transfer zone, however, the dataset available in this zone is insufficient. For this reason, the 3D model build started in the northern part of the Sicilian Channel. Seismic lines uploaded on the ViDEPI website were high definition scans of original paper documentation produced by different exploration companies. The seismic profiles were transformed into SEG-Y files in order to be processed to the interpretation step. The software used for profiles transformation was SegyMAT (https://cultpenguin.gitbooks.io/segymat/content/). For the interpretation and 3D fault, geometries build, MOVE software (https://www.mve.com/) for structural geologist was used.

Based on previous work of several authors, seismostratigraphic interpretation (Civile et al., 2012, 2014) was quickly incorporated into the 3D model as well as seismic interpretation (Argnani, 1990 and Ghisetti et al., 2009). Two important transcurrent broadly NS trending lineaments incorporated in the Transfer zone were mapped. The western lineament called after the city of Capo Granitola was observed between the mentioned city and Graham Bank volcanic area. This fault system is composed of positive flower structure in the Northern area. The full 3D fault pattern was not built as the quality of the seismic dataset was insufficient. The Eastern lineament, called Sciacca Fault system, was crossing seismic profiles with higher quality and 3D fault geometry was obtained. At the same time, the clay analogue model was performed in order to understand the sense of the motion along this transcurrent fault system. This model assumed the interaction between pre-existing thrust front and newly formed transcurrent structure as a fixed plate with L-shape was under slid by a moving plate which simulated the different transcurrent tectonic regimes. In addition, pure strike-slip, transpression 10° and transtension 10° tectonic regimes were tested. Comparison between the 3D model and clay model showed fair similarities. Observed splay faults seen mostly on the one side of the primary fault in analogue and 3D model define the sense of deformation which produced the Sciacca Fault system. The right-lateral deformation also fit with the principal horizontal stress which was oriented in NE-SW direction during the Middle Miocene – Early Pliocene period when the first transcurrent episode along the Sciacca Fault system occurred. Nevertheless, the analogue models did not provide enough information to understand if the deformation seen in Sicilian Channel was transpressive, transtensive or pure strike-slip as all models showed splay-primary faulting and positive flower structures.

Seismic profiles from the study area also revealed the presence of some normal faults with the same orientation as seen within the Pantelleria, Malta and Linosa grabens. This normal faulting crosscutting the transcurrent system, possibly affected the strike direction as the Sciacca Fault system can be divided into two segments, and the difference of the strike angle between these two segments is approximately 11 degrees. Additionally, seismic and chirp profiles show that the southern sector, which comprises Nerita and the Eastern side of the Terrible Bank, is active nowadays, while the northern one does not present any active tectonics. Numerical model used within this PhD program was developed to validate the interpretation of seismic profiles and for better understanding of fault activity seen along the Sciacca Fault system. The software used for the numerical model is Poly3D, which is a fast, user-friendly 3D stress modelling tool based on the boundary element method (BEM). The analysed fault pattern was obtained from the seismic interpretation in the Sicilian Channel. The preliminary results from the model show the same sense of the displacement as from the seismological analysis and confirm the tectonic activity differences along the Sciacca Fault. The results of the first model where both segments of the Sciacca Fault was tested show the difference in the slip potential. The southern segment shows a higher slip potential than the northern one. The second model, where we intentionally locked the northern segment and let freely slide the southern one, shows fair match between the uplift pattern seen in the model and Sicilian Channel.

Lastly, sand analogue models were used to investigate the 4D evolution of a strike-slip dominated structure and its interaction with a preexisting thrust front. These models were performed, as the internal fault system and its evolution could not be analysed with clay models. An analysis of 7 models applying (i) pure strike-slip, (ii) transtension (10/20/30 degrees) and (iii) transpression (10/20/30 degrees) kinematics shows important structural variations in the area of strike-slip faults. Some models closely resemble the geometries of natural interaction observed between the transcurrent Transfer zone of the Sicilian Channel and the Sicilian Maghrebian chain. The experimental apparatus consisted of a box with three independent rigid base plates. During the first phase of deformation, the thrust front was created as the upper plate was sliding on the fixed plate. In the second phase, the lowest plate was sliding under the fixed one. The analogue models were analysed by X-Ray Computed Tomography (XRCT). This technique allows visualisation of the interior of a model during deformation without destroying it (4D analysis). The strike-slip fault structures obtained from the analogue models and its comparison with fault pattern from the

Sicilian Channel demonstrated a fair match between the models and natural case. Also, the results of 4D analyses of analogue models give a new perspective of fault development under different strike-slip tectonic regimes.

Results from the wet-clay and sand analogue models could be used in different areas where thrust belt interact with the transcurrent structures. Two other examples apart the Transfer zone of Sicilian Channel show unexpectedly high level of seismicity and can be found along Maghreabian Chain. The first one, the Molise-Gondola shear zone (Di Bucci et al., 2006), show two not linked seismologically active segments of the shear zone in the foreland and inside of the thrust belt. The second, Vizzini-Scicli shear zone (Di Bucci et al., 2010) deforms only the foreland of the Maghreabian Chain while the inside area of the thrust belt the do not show any seismicity. These two examples show fair similarities with the wet-clay and sand models described in this thesis.

2- Sicilian Channel and clay models

Structural analysis and Miocene-to-Present tectonic evolution of a lithospheric-scale, transcurrent lineament: The Sciacca Fault (Sicilian Channel, Central Mediterranean Sea)

Jakub Fedorik[1]*, Giovanni Toscani[1], Emanuele Lodolo[2], Dario Civile[2], Lorenzo Bonini[3-4], Silvio Seno[1]

[1] *Dipartimento di Scienze della Terra e dell'Ambiente, Università di Pavia, Pavia, ITALY*

[2] *Istituto Nazionale di Oceanografia e di Geofisica Sperimentale, Trieste, ITALY*

[3] *Dipartimento di Matematica e Geoscienze, Università di Trieste, ITALY*

[4] *INGV- Roma, ITALY*

***Corresponding author email**: *jakub.fedorik01@universitadipavia.it*

Abstract

Seismo-stratigraphic and structural analysis of a large number of multichannel seismic reflection profiles acquired in the northern part of the Sicilian Channel allowed a 3-D reconstruction of a regional NS-trending transfer zone which displays a transcurrent tectonic regime, and that is of broad relevance for its seismotectonic and geodynamic implications. It is constituted of two major transcurrent faults delimiting a 30-km-wide, mostly undeformed basin. The western fault (Capo Granitola) does not show clear evidence of present-day tectonic activity, and toward the south it is connected with the volcanic area of the Graham Bank. The eastern fault (Sciacca) is structurally more complex, showing active deformation at the sea-floor, particularly evident along the Nerita Bank. The Sciacca Fault is constituted of a master and splay faults compatible with right-lateral kinematics. Sciacca Fault is superimposed on an inherited weakness zone (a Mesozoic carbonate ramp), which borders to the east a 2.5-km-thick Plio-Quaternary basin, and that was reactivated during the Pliocene.

A set of scaled claybox analogue models was carried out in order to better understand the tectonic processes that led to the structural setting displayed by seismic data. Tectonic structures and uplift/subsidence patterns generated by the models are compatible with the 3-D model obtained

from seismic reflection profiles. The best fit between the tectonic setting deriving from the interpretation of seismic profiles and the analogue models was obtained considering a right-lateral movement for the Sciacca Fault. Nevertheless, the stress field in the study area derived from GPS measurements does not support the present-day modelled right-lateral kinematics along the Sciacca Fault. Moreover, seismic events along this fault show focal mechanisms with a left-lateral component.

We ascribe the slip change along the Sciacca Fault, from a right-lateral transcurrent regime to the present-day left-lateral kinematics to a change of principal horizontal stress direction starting from Late Pliocene.

KEYWORDS: Sicilian Channel; active tectonics; fault kinematics; analogue models; 3-D reconstructions

1- Introduction

The Sicilian Channel and the front of the Sicilian-Maghrebian Chain represent two key-elements for the comprehension of the Central Mediterranean geodynamics. In particular, the north-western part of the Sicilian Channel and the front of the Sicilian-Maghrebian Chain are affected by a wide NS-trending, lithospheric-scale transfer zone which separates sectors characterized by different structural setting and tectonic evolution (Fig. 1) (Argnani et al., 1988; Argnani, 1990; Civile et al., 2014; Di Stefano et al., 2015 and references therein). Offshore south-western Sicily, the NS trending transfer zone is bounded by the Capo Granitola Fault (CGF) to the west and by the Sciacca Fault (SF) to the east. The latter (SF) was formerly identified by several authors (Argnani, 1990; Casero and Roure, 1994; Antonelli et al., 1988; Nigro and Renda, 2002; Finetti, 2003; Lentini et al., 2006; Ghisetti et al., 2009), but its tectonic evolution and kinematics are still debated.

In this paper, we present a detailed structural study of this transfer zone with a particular focus on the SF, based on the interpretation of a large number of offshore multichannel seismic reflection profiles and well logs made available by the Italian Ministry of the Economic Development in the framework of the ViDEPI project (http://unmig.sviluppoeconomico.gov.it/videpi/). Interpretation of seismic data allowed us to compile a structural map of the study area and a 3-D model of the SF system. In order to understand fault kinematics, we carried out a set of scaled analogue models useful to understand the regional tectonic regime acting from Late Miocene.

The study area is a key point for Central Mediterranean geodynamics for the presence of regional tectonic lineaments and is also the place: (i) where some authors (e.g. Mantovani et al., 2014) found that maximum stress directions reoriented through times, (ii) that separates different sectors of the Sicilian-Maghrebian Chain characterized by different tectonic evolution, deformation age and thrusts vergence (Argnani et al., 1988; Argnani, 1993), (iii) that separates in two parts the Sicilian Channel Rifting Zone (a western area where the Pantelleria Graben took place and an eastern sector characterized by the presence of the Linosa and Malta troughs, e.g. Civile et al., 2010), (iv) where several recent submarine volcanic centers are present (Civile et al., 2008; Lodolo et al., 2012; Coltelli et al., 2016) and (v) where present-day seismicity is recorded (Calò and Parisi, 2014). In addition, the study area represents the offshore extension of the zone affected by the 1968 Belice earthquake (Monaco et al., 1996). All these data and their

interpretations depict a complex geodynamic setting where recent volcanism, rifting zones and compressive structures coexist. This work aims at a better comprehension of the tectonic evolution of the area and of its present-day kinematics, to better constrain seismic hazard assessment in the Sicilian Channel and southwestern Sicily. Moreover, the kinematics of transcurrent faults with associated splay reconstructed in this paper can be of help also when studying comparable geological settings worldwide to understand better transcurrent fault kinematics and, in a more general view, to define better and reconstruct the geodynamic setting of the Mediterranean region. Looking at the Central and Western Mediterranean region, kinematic changes along transcurrent fault systems are present also in other sectors of the Mediterranean basin. At the western end of the convergence between Africa and Eurasia, Maldonado et al. (1999) describe a change in the African-Eurasian convergence motion from N–S to NW–SE, which was responsible for strike-slip structures emplaced during the Plio-Quaternary. Also, Medialdea et al. (2004, 2009) and Zitellini et al. (2009) report regional strike-slip transfer zones in the Gulf of Cadiz that, on a regional scale, could be the complementary structures of the left-lateral transfer zone in the Sicilian Channel, accommodating the Late Pliocene-Quaternary NW-SE African-Eurasian convergence.

2- Regional tectonics framework

The Sicilian Channel is located in the northern sector of the African continental plate, between Sicily and Tunisia (Fig. 1), close to a major convergent margin represented by the Nubia-Eurasia plate boundary (Boccaletti et al., 1987; Dewey et al., 1989; Corti et al., 2006). Along this margin, the SSE-verging Sicilian-Maghrebian Chain originated by the deformation of the former African paleomargin (Roure et al., 1990). The outermost thrust sheet, represented by the offshore Gela Nappe is interpreted as a complex imbricate wedge, involving the Miocene-Pliocene sedimentary succession of the foredeep basin originally located NW of the Hyblean Plateau, as imaged by several seismic reflection profiles and tectonic reconstructions (Lentini, 1982; Argnani, 1987; Antonelli et al., 1988; Trincardi and Argnani, 1990; Argnani, 1993; Catalano et al., 1996, 2000, 2013; Ghisetti et al., 2009; Lavecchia et al., 2007; Cavallaro et al., 2016).

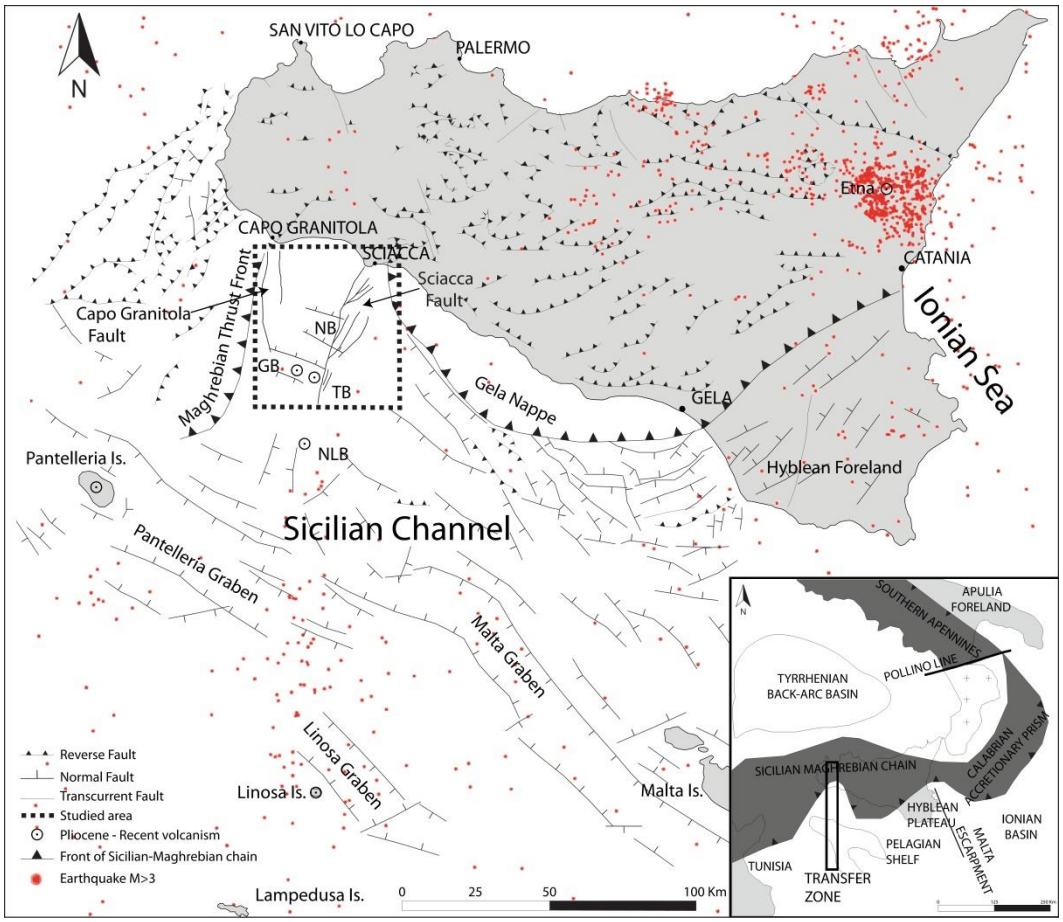

Figure 1: Simplified structural sketch map of Sicily (after Barreca et al., 2014; Di Stefano et al., 2015) and the Sicilian Channel (after Antonelli et al., 1988; Lodolo et al., 2012; Civile et al., 2014). The dashed rectangle is the study area where the tectonic structures described in the text are reported. Inset box (right-bottom) indicates the main geodynamic features of Southern Italy. Epicentral earthquake locations (M > 3, between 1985 and 2017; data from ISIDE, "Italian Seismic Instrumental and parametric DatabasE" - http://iside.rm.ingv.it/) are highlighted with red points. GB, Graham Bank; NB, Nerita Bank; NLB, Nameless Bank; TB, Terrible Bank.

The study area (Fig. 1), interpreted by several authors as a lithospheric transfer zone (Argnani, 1990; Civile et al., 2008, 2010, 2014; Calò and Parisi, 2014), is located off the south-west coast of Sicily in correspondence with the pronounced onshore indenter of the Sicilian-Maghrebian Chain, developed during Late Oligocene-to-Pleistocene times (Nigro and Renda, 2001), and separates the Late Miocene NS trending Maghrebian Thrust Front to the west from the Plio-Pleistocene Gela Nappe to the east. The stratigraphic succession of the Sicilian Channel consists of sedimentary deposits ranging from Triassic to Plio-Quaternary. A broad lithological distinction can be made between the successions ranging from Triassic to Paleogene,

predominantly carbonate, and the successions ranging from Miocene to Quaternary, predominantly siliciclastic (Civile et al., 2014). One of the main structure of the study area is represented by the Sciacca Fault (SF, same name in Antonelli et al., 1988), an almost NS-trending, sub-vertical transcurrent fault with several high angle splays (Argnani, 1990; Finetti, 2003) which is the eastern boundary of the lithospheric transfer zone. The western boundary is named in this paper Capo Granitola Fault (CGF), (Belice Fault in Antonelli et al., 1988). WNW–ESE trending normal faults are also present in the study area (e.g. Antonelli et al., 1988) and their orientation is almost parallel to the tectonic depressions of the Sicilian Channel Rift Zone (Pantelleria, Linosa and Malta grabens). This was interpreted by some authors as the result of an intraplate rifting process which affected the Sicilian Channel during the Neogene-Quaternary (Reuther and Eisbacher, 1985; Boccaletti et al., 1987; Cello, 1987; Argnani, 1990; Civile et al., 2010). The rifting process was accompanied by a widespread volcanic activity mainly concentrated on the islands of Pantelleria and Linosa. Other submarine volcanic manifestations have been recognized in the Adventure Plateau, Graham and Nameless banks (Colantoni, 1975; Carapezza et al., 1979; Beccaluva et al., 1981; Calanchi et al., 1989; Rotolo et al., 2006; Lodolo et al., 2012; Civile et al., 2015, 2016; Coltelli et al., 2016). In particular, the Ferdinandea volcanic shoal (whose last eruption occurred in 1831; Gemmellaro, 1831; Washington, 1909) is one of the two shoals of a wider volcanic field (Graham Bank) characterized by several centers that together depict a NS oriented belt (Coltelli et al., 2016), located along the CGF. Instrumental seismicity shows that the Sicilian Channel is dominated by strike-slip focal mechanisms, with some oblique-normal seismic events (Calò and Parisi, 2014; Soumaya et al., 2015). Most of the seismicity is distributed along an elongated cluster depicting a large NS-oriented belt (transfer zone) extending from Lampedusa Island to the south, to the Sciacca offshore to the north.

Several studies investigated the possible structural onshore-offshore link between the tectonic structures of Western Sicily and those of the Sicilian Channel. Casero and Roure (1994) describe a NW-SE trending regional shear zone (Segesta Fault) crossing the Sicilian-Maghrebian Chain from San Vito Lo Capo to the Sciacca offshore. Nigro and Renda (2001, 2002) show the emplacement of thin deep-water sediments thrusted onto Meso-Cenozoic shelf carbonates with an overall lateral ramp geometry along a Meso-Cenozoic fault-controlled paleo-margin. Di Stefano et al. (2008, 2015) suggest the presence of a shelf to deep water transition in the Sciacca area corresponding to a segment of the rifted southern passive margin of the Permo-Triassic Ionian Tethys that, at present, runs roughly NS from San Vito Lo Capo to Sciacca. This paleo-margin

separated a continental crust characterized by a thick Permo-Triassic carbonate platform succession to the west from a thinned continental crust covered by deep-water carbonate deposits to the east. This weakness zone may have been reactivated as a major right-lateral strike-slip fault on the basis of the variable direction of the stress field acting in the Central Mediterranean area since Late Miocene (Mantovani et al., 2014). The presence of this weakness zone produced sectors of the Sicilian-Maghrebian Chain characterized by different deformation ages, shortenings, distinct structural trends and tectonic evolution (Argnani et al., 1988; Argnani, 1993). The present-day configuration of the grabens forming the Sicilian Channel Rift Zone could be related to the presence of this tectonic structure representing the boundary line between a western sector where only one graben is present (Pantelleria Graben) and the eastern one where two grabens are present (Malta and Linosa graben) (Civile et al., 2010). Calò and Parisi (2014) provide evidence of a wide active sub-vertical fault zone (at least 200–250 km long) crossing western Sicily and the Sicilian Channel (M > 3 events between 1985 and 2017 have been plotted in Fig. 1; data from ISIDE, "Italian Seismic Instrumental and parametric DatabasE"). This fault should affect the entire continental crust and the upper mantle to a depth of at least 70 km, as suggested by relocated seismicity and geochemical evidence (Caracausi et al., 2005). Anderson and Jackson (1987) relocated the largest earthquakes recorded in western Sicily during the last century and infer a NS alignment. Others studies provided possible faulting mechanisms that range from thrusting on a WSW–ENE striking plane to right lateral transpression on a NNW–SSE striking plane (McKenzie, 1972; Bottari, 1973; Gasparini et al., 1982; Monaco et al., 1996; Frepoli and Amato, 2000). Evidence of recent and ongoing NW–SE compressive tectonic activity is also shown in the Capo Granitola zone (Barreca et al., 2014).

In the offshore area, according to Soumaya et al. (2015), the focal mechanisms show a pure left-lateral, strike-slip stress regime associated with NS trending sub-vertical planes. In summary, these studies suggest the presence of a wide shear zone in the northwestern Sicilian Channel that could be a main segment of a NS-trending regional tectonic lineament extended from San Vito Lo Capo to Lampedusa Island.

3- Materials and methods

The available seismic data of the Sicilian Channel were collected and georeferenced in order to analyze the structural setting of the northern part of the NS-trending transfer zone (Fig. 2). The dataset contains 2-D multichannel seismic reflection profiles (Italian Commercial Zones “G” and “C”) collected during the 70s and 80s by oil companies for commercial purposes, some site surveys seismic lines, and several well composite logs both made available from the ViDEPI project. The data quality of all these profiles is very inhomogeneous because they were acquired at different times, with different acquisition systems, parameters and purposes. The first step was to convert the raster files to SEG-Y format files using a MatLab free script. Afterward, the SEG-Y files were georeferenced, uploaded and interpreted using the MOVE® software. Some significant seismic profiles are described in the text (always using TWT, in milliseconds, as vertical scale unit) while a part of the interpreted dataset is available online (Supplementary Material, data repository).

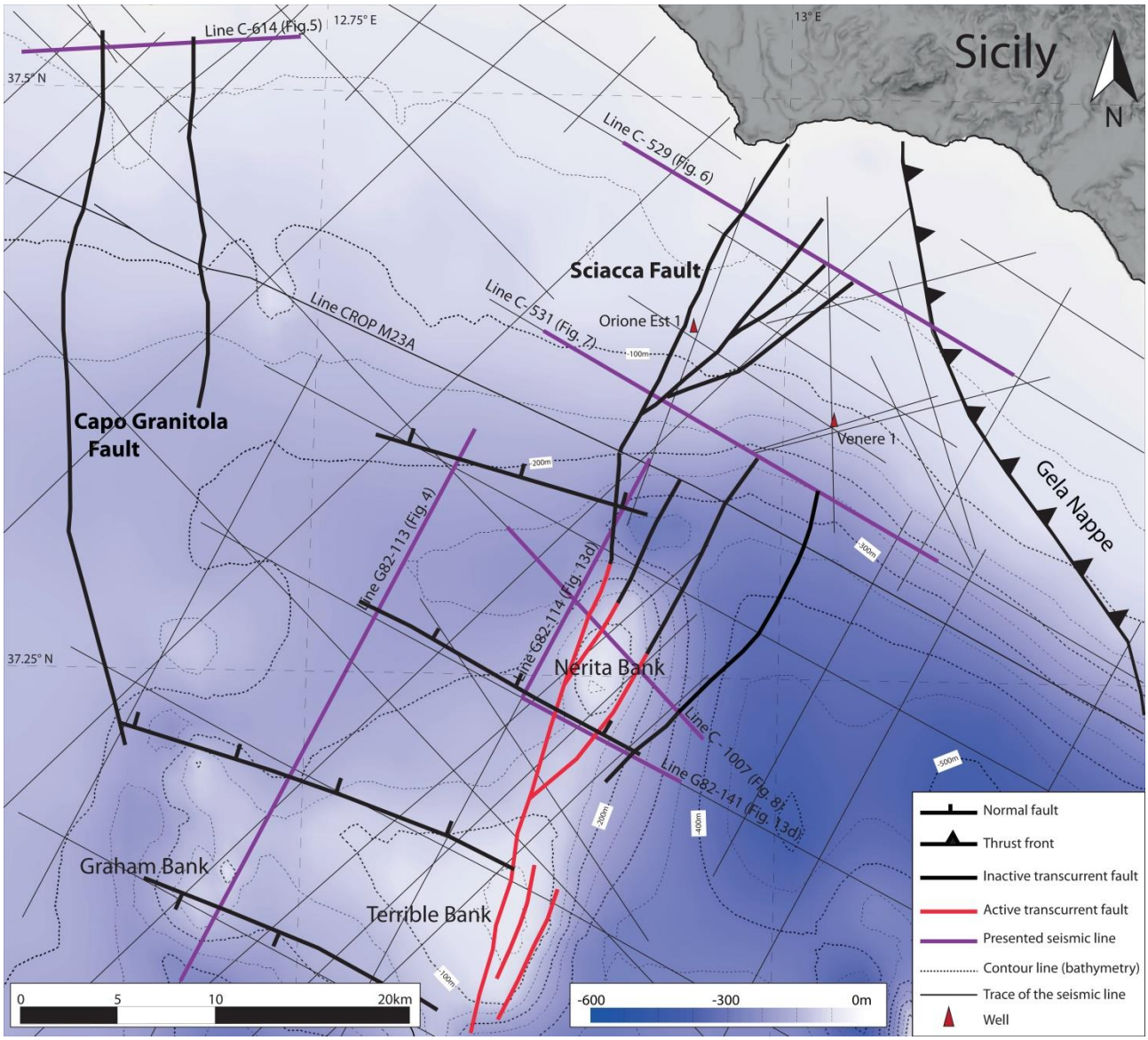

Figure 2: Bathymetric map (extracted from GEBCO dataset) of the study area with the position of the available seismic lines. Interpreted fault segments of the Capo Granitola and the Sciacca Faults are reported along with the position of the thrust front of the Gela Nappe and the major NW–SE trending normal faults identified in the study area.

4- Seismo-stratigraphic and structural interpretation

Seismic interpretation was calibrated using available well data; two simplified stratigraphic columns are shown in Fig. 3 to highlight the inferred depth of the interpreted seismic horizons and thickness variations in the well-log. Two main prominent reflectors, assigned to the Messinian unconformity and Top of Meso-Cenozoic carbonate succession, have also been identified on the basis of literature information (Ghisetti et al., 2009; Civile et al., 2014; Cavallaro et al., 2016).

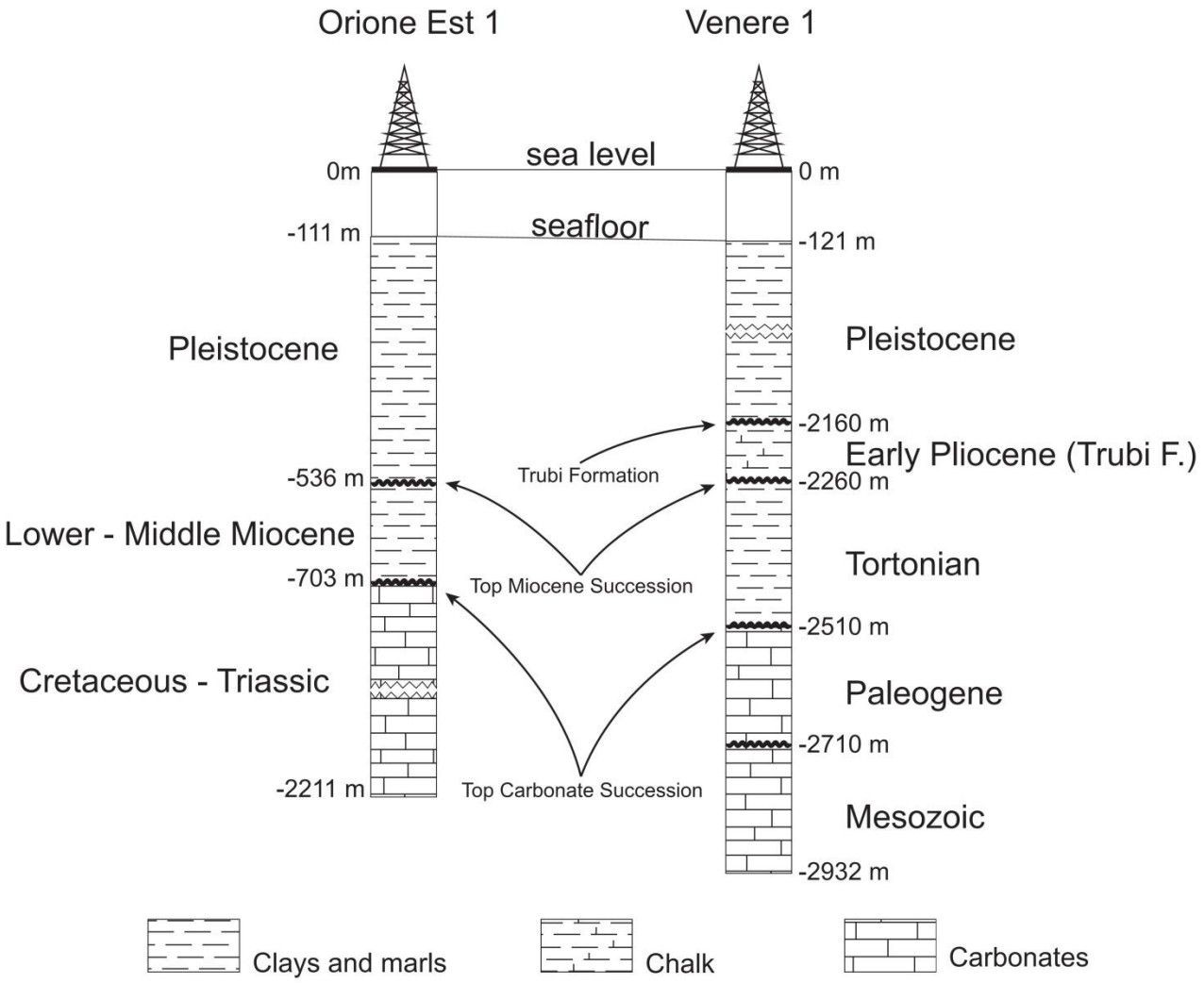

Figure 3: Simplified stratigraphy of two wells located in the northern part of the study area and used to calibrate the seismic profiles. The three interpreted horizons in the seismic lines are reported. Location of wells in Fig. 2.

4.1- Normal Faults

In the study area, four major NW-SE trending normal faults, not less 15 km long, were mapped. These structures can be observed along the northern part of seismic line G82-113 (Fig. 4). The faults display different times of activation. The northernmost one offsets the TCS (Top Carbonate Succession), while TMS (Top Miocene Succession) seems to be undeformed. All remaining normal faults of Fig. 4 offset both TCS and TMS. It is worth to be noted that the fault bounding the northern side of the Graham Bank also shows a Pliocene-Quaternary syn-tectonic sequence. The seismic line crosses the Graham Bank which seems to be affected by huge magmatic intrusions whose seismic facies are characterized by limited acoustic penetration, with

discontinuous and chaotic reflectors, velocity pull-up and tilting of the reflectors around the magmatic intrusions. The normal faults recognized in the study area terminate within the perpendicularly oriented SF.

Pliocene NW-SE trending normal faults bound Pantelleria, Malta and Linosa grabens of the Sicilian Channel Rift Zone (Civile et al., 2010). A similar fault orientation was observed in the north-central sector of the Sicilian Channel, in front of the Gela Nappe, by Cavallaro et al. (2016), which interpreted these structures as Miocene normal faults reactivated during Zanclean-Piacenzian time by dextral strike-slip motion.

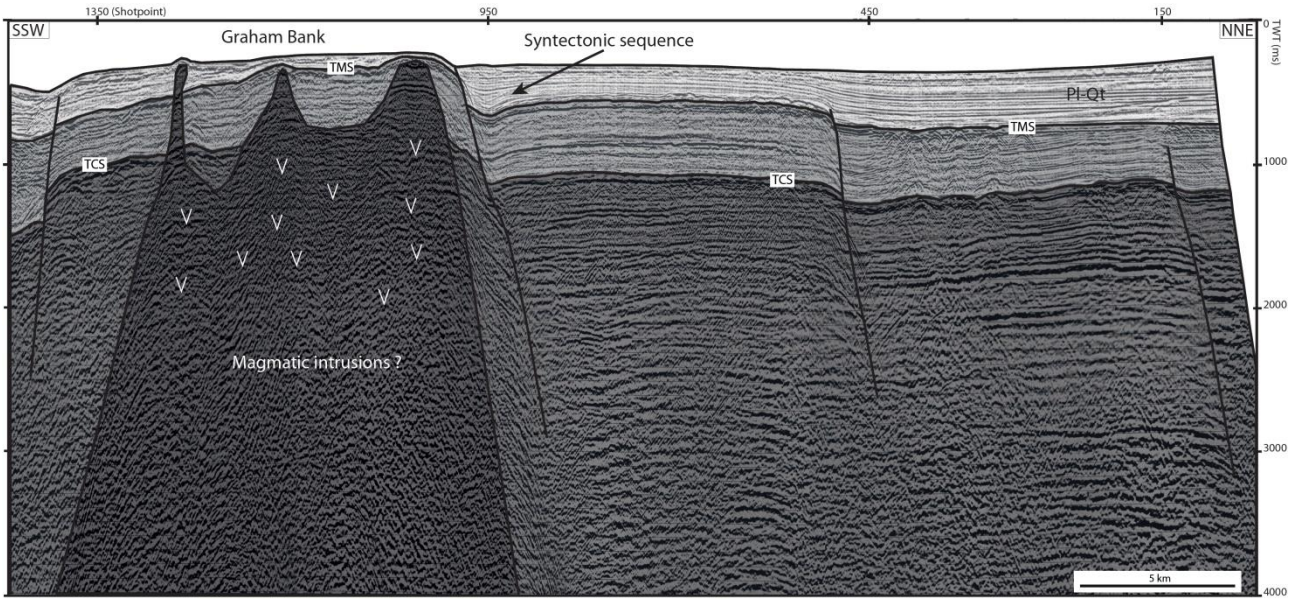

Figure 4: NNE-part of the seismic line G82-113, showing NW-SE-oriented normal faults. Two seismo-stratigraphic horizons are reported: Top Carbonate Succession (TCS) and Top Miocene Succession (TMS). Moreover, the lower part of the Plio-Quaternary cover (Pl-Qt) shows syn-tectonic features at the fault bounding the northern side of the Graham Bank. The NNW-half of the presented seismic line crosscut the Graham Bank where a huge magmatic intrusion has been supposed. Location of seismic profile in Fig. 2.

4.2- Capo Granitola Fault System

Within the available seismic dataset, 16 profiles crossing the CGF at different angles were selected in order to reconstruct its structure, kinematics and (eventual) morphological expression at the sea-floor. This tectonic structure extends for about 50 km in the NS direction starting from the offshore area of Capo Granitola to the Ferdinandea shoal, after which it is no longer

recognizable even if its southward extension could be supposed on the basis of the occurrence of a NS oriented volcanic belt (Civile et al., 2008; Coltelli et al., 2016). The seismic Line C-614 (Fig. 5) crosses the northern part of the CGF where a positive flower structure affecting the Mesozoic-Miocene succession can be identified. It is composed of a sub-vertical master fault with three related west dipping splay faults on the eastern side and two east dipping splay fault on the western side. The lower part of the Plio-Quaternary succession shows the presence of growth strata which allow to hypothesize that the formation of the positive flowers structure occurred during the Early Pliocene time. The uppermost part of the Plio-Quaternary succession seems to seal it. Along the publicly available seismic reflection profiles crossing CGF, clear evidence of active tectonics (i.e., faults displacing Quaternary sediments and/or sea-floor) have not been observed, but in other papers (e.g. Barreca et al., 2014) this fault system seems to be presently active near its intersection with the coastline where the sea-floor is slightly deformed.

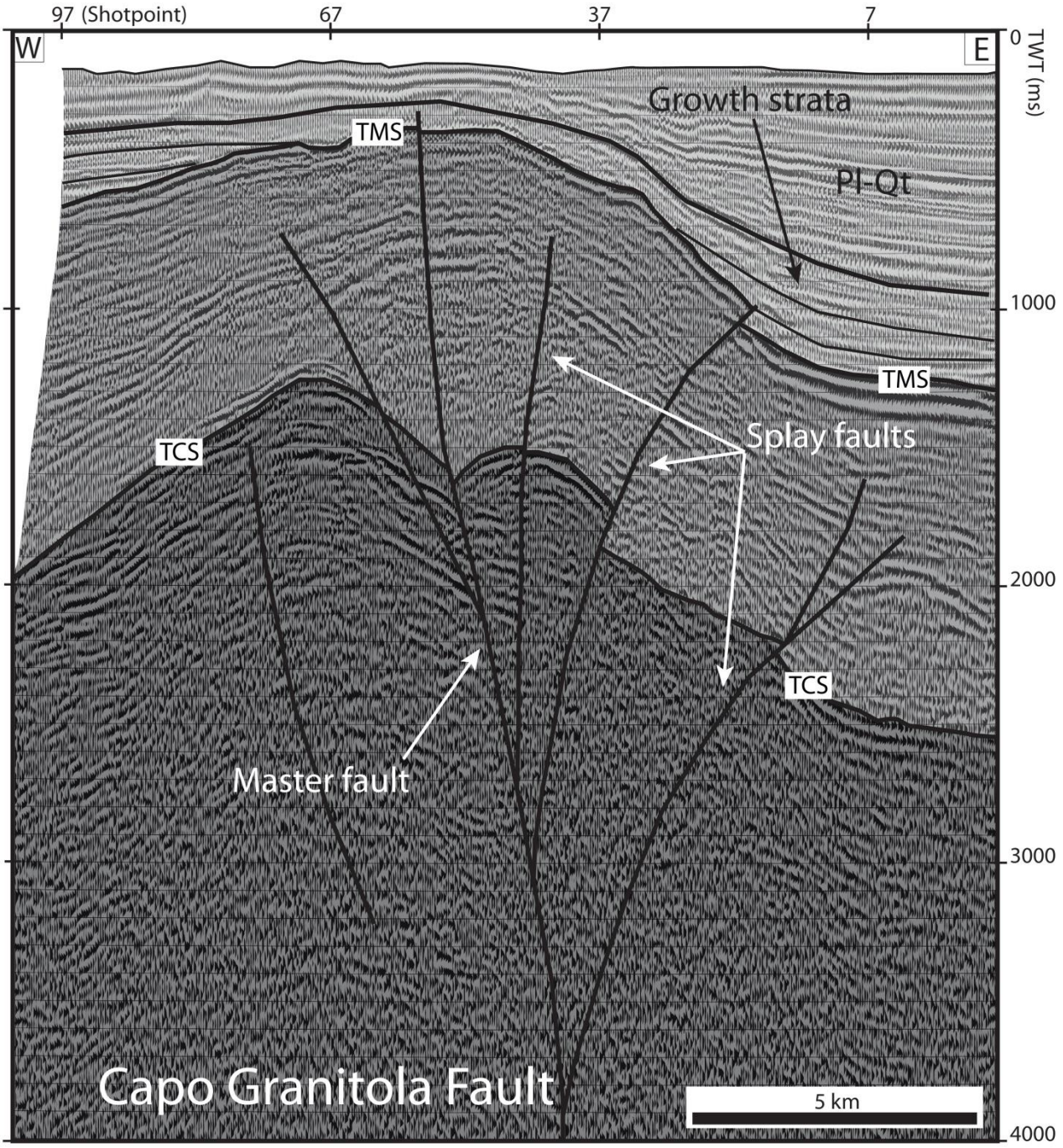

Figure 5: Seismic line C-614, showing a positive flower structure associated with the Capo Granitola Fault. This structure consists of a sub-vertical master fault and several splay faults. Location of seismic profile in Fig. 2. Two seismostratigraphic horizons are reported: Top Carbonate Succession (TCS) and Top Miocene Succession (TMS). The lowermost part of the Plio-Quaternary succession (Pl-Qt) shows growth strata.

4.3- Sciacca Fault System

The seismic dataset available along the SF allowed us to produce a 3-D model of this tectonic structure. The evidence of transcurrent tectonics along this fault is observable at least for 70 km, from the Sicily coastline to the southern margin of the Terrible Bank. Following our interpretation, this tectonic lineament consists of a sub-vertical NNE-SSW trending master fault with several splays. The dip angle of the master fault (measured on TWT sections) ranges from 80° to 60°, moving from the northern to the southern sector of the study area. Ghisetti et al. (2009) interpret the northern part of the SF as a NNE-SSW trending left-lateral transpressive flower structure, based on CROP data (see Fig. 2 for location). Based on the interpretation of the same CROP profile Finetti (2003) suggests that the left-lateral transcurrent SF affects the whole crust probably reaching the upper part of the mantle.

The seismic line C-529 (Fig. 6) crosses the northern part of the SF which is located close to the thrust front of the Gela Nappe. The positive flower structure recognized along this line affects the top of the Miocene succession and the Early Pliocene deposits corresponding to the Trubi Formation which is usually well identified on seismic lines due to its typical semi-transparent acoustic character (Ghisetti et al., 2009; Cavallaro et al., 2016). The Early Pliocene deposits are also deformed by the thrust of the Gela Nappe. The thickness of the Miocene succession ranges from about 200 ms to over 500 ms.

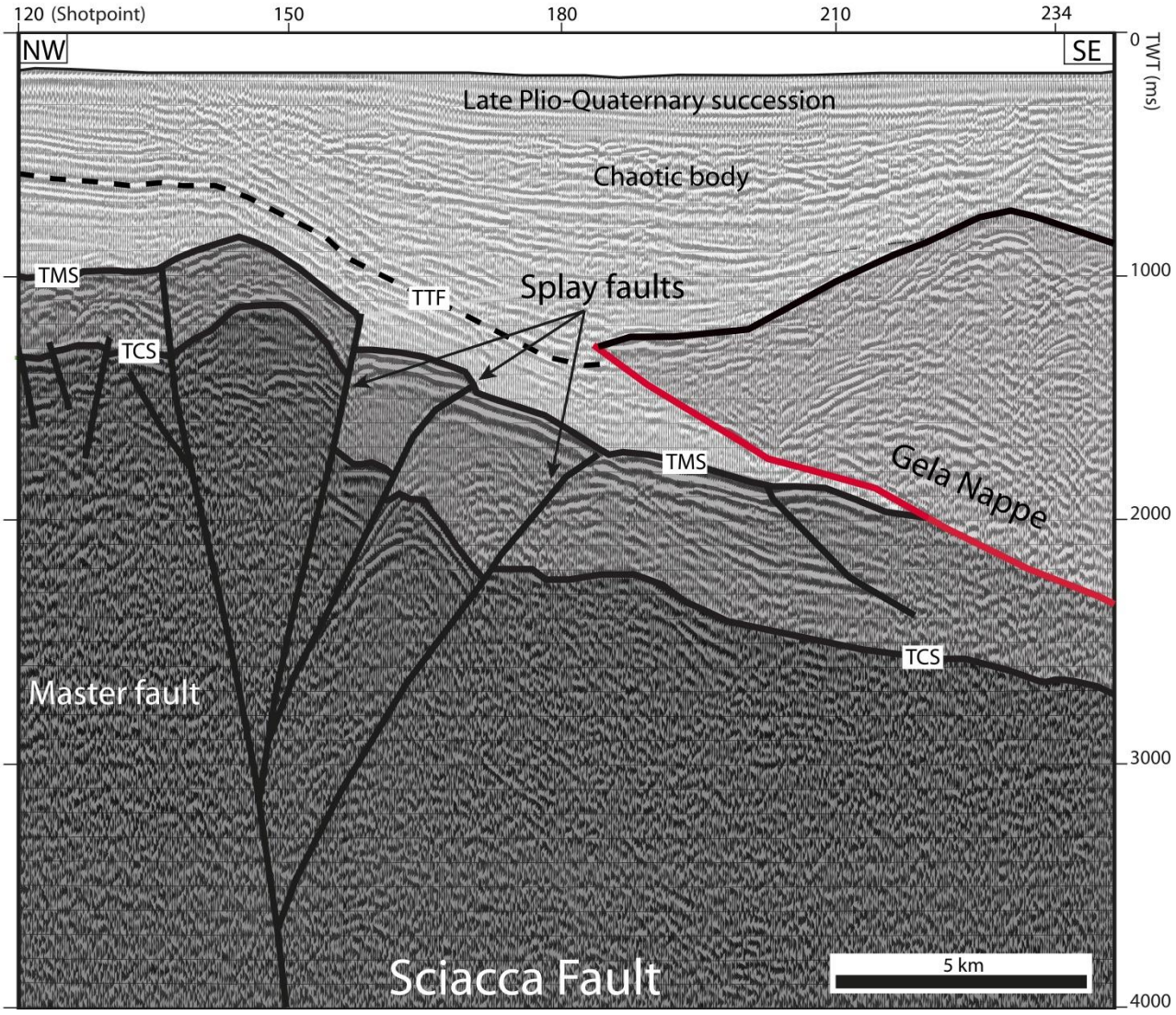

Figure 6: Western part of the seismic line C-529, showing a positive flower structure associated with the Sciacca Fault. It is composed of a sub-vertical master fault and four splay faults. On the S-E part of the seismic profile, the front of the Gela Nappe is present. Location of seismic profile in Fig. 2. Three seismo-stratigraphic horizons are reported: Top Carbonate Succession (TCS), Top Miocene Succession (TMS), and top of the Trubi Formation - Early Pliocene (TTF). Red line shows the basal thrust of the Gela Nappe. The Late Pliocene-Quaternary succession represents shelf margin-basin depositional system subsequently tilted by the load of the southward advancing Sicilian-Maghrebian Thrust Chain.

Along the seismic line C-531 (Fig. 7), that is parallel to the previous one but located 12.5 km to the south (see location in Fig. 2), the SF still shows a positive flower structure geometry affecting the Mesozoic-Miocene sediments and the lower Pliocene Trubi Formation. The Miocene succession shows a considerable thickness variation between the western and eastern sides of the

master fault probably produced by a previous extensional tectonic phase. The flower structure is covered by an undeformed upper-Pliocene-Pleistocene succession.

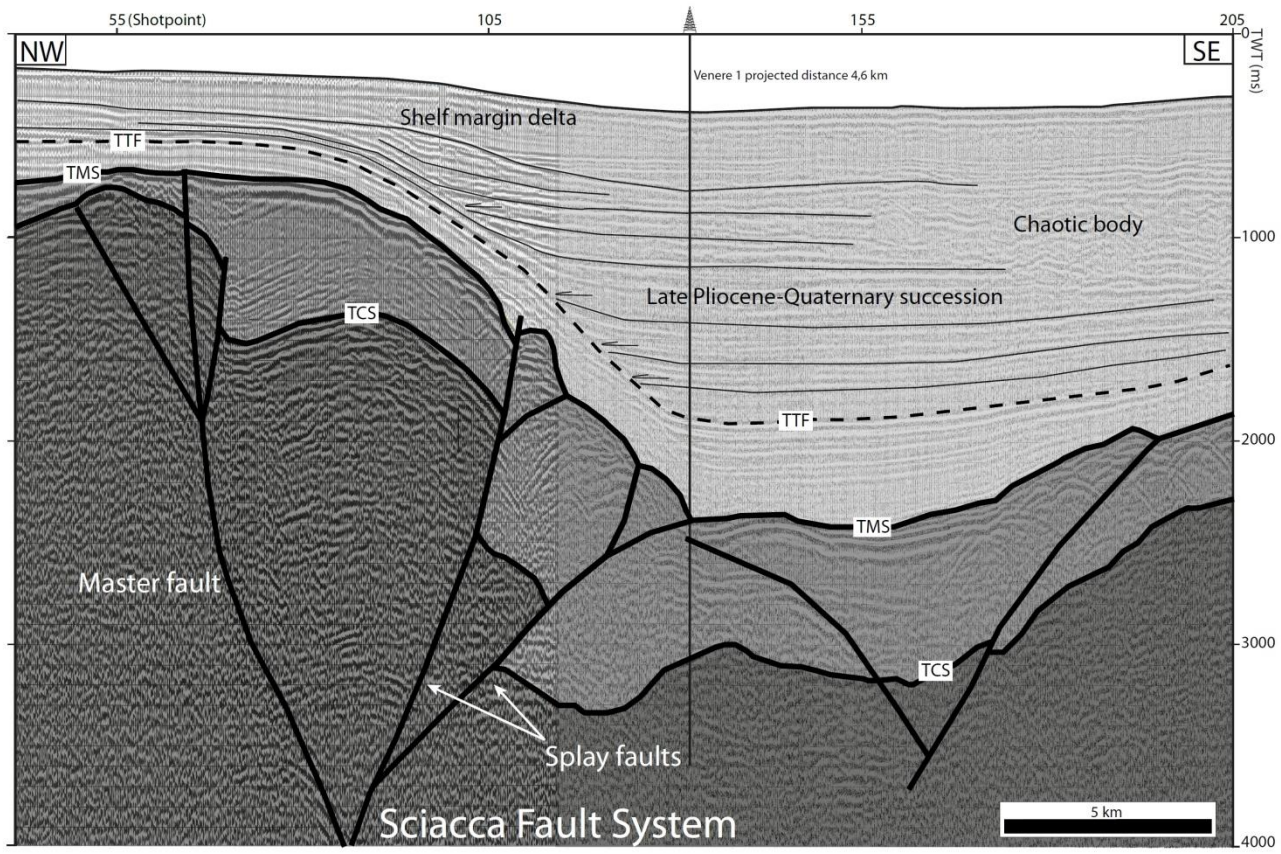

Figure 7: Western part of the seismic line C-531. The Sciacca Fault is composed of a SE dipping master fault, two main NW-dipping and one smaller SE-dipping splay faults. The considerable thickness variation of the Miocene succession suggests a possible tectonic inversion of the master fault from normal fault to transcurrent fault. Location of profile in Fig. 2. Three seismo-stratigraphic horizons are highlighted: Top Carbonate Succession (TCS), Top Miocene Succession (TMS), and Top Trubi Formation - Early Pliocene (TTF).

The seismic line C-1007 (Fig. 8), located along the northern margin of the Nerita Bank (see Fig. 2), shows the presence of a large positive flower structure that also affects the sea-floor. The most eastern splay faults of this structure are buried.

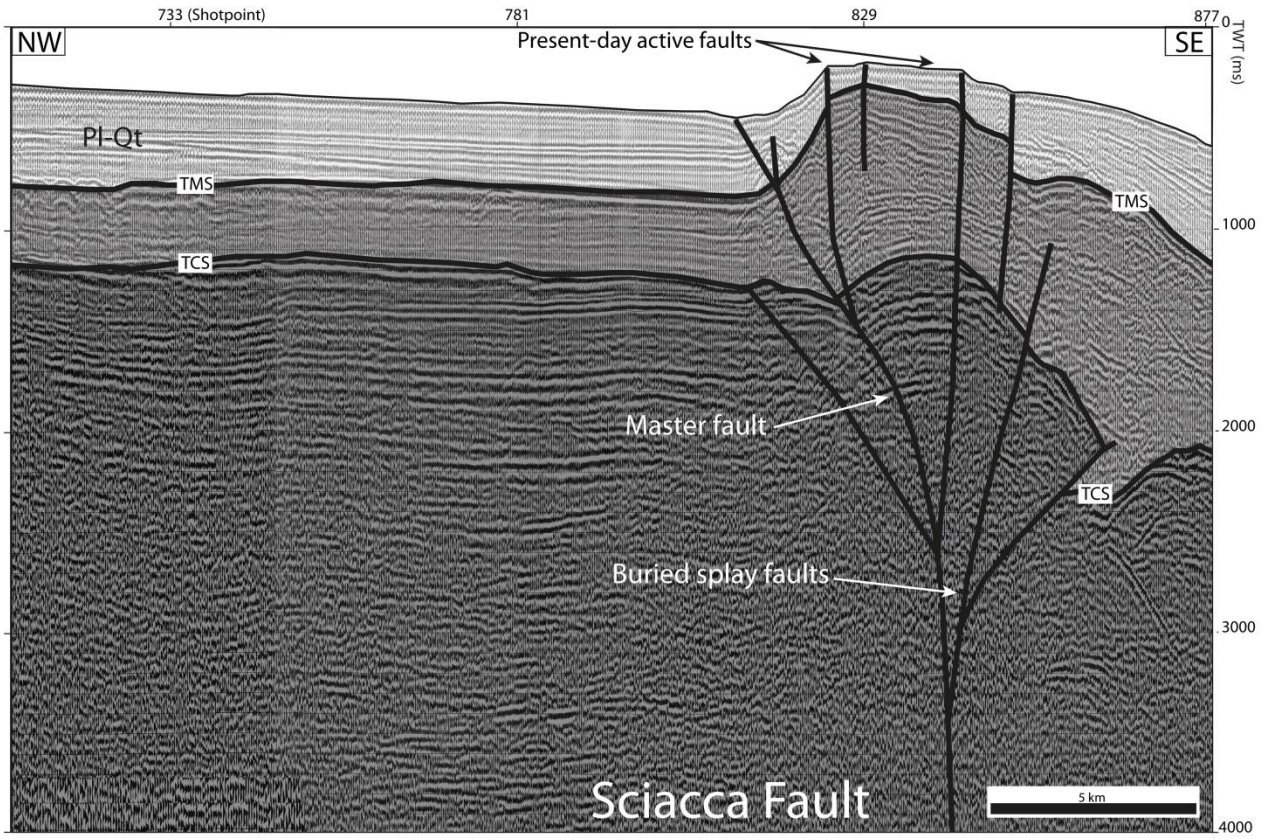

Figure 8: Eastern part of the seismic line C-1007, crossing the southern part of the Sciacca Fault (Nerita Bank). Two seismo-stratigraphic horizons are reported: Top Carbonate Succession (TCS) and Top Miocene Succession (TMS). Moreover, the Plio-Quaternary cover (Pl-Qt) is also indicated. Significant variation of Miocene thickness in the area of the Sciacca Fault can be linked to the tectonic inversion from normal to transcurrent fault. The present-day deformation affecting the sea-floor may be related to the hypothesized recent kinematic change of the Sciacca Fault from right-lateral to left-lateral motion. Location of seismic profile in Fig. 2.

On the basis of the available data, the SF could be divided in northern and southern parts. Along the northern segment, extended between the Sicilian coast and the northern margin of the Nerita Bank, the SF seems sealed by Late Pliocene-Quaternary deposits. The southern segment, extended between the Nerita and Terrible banks, shows clear evidence of active tectonics. In addition, it is remarkable to note that the two segments have different orientations, N 17° for the southern portion, and N 28° for the northern one. This change of direction occurs in correspondence of the northernmost WNW-ESE normal fault reported in Fig. 2.

5- Model setup and description

5.1- Methods

A set of scaled analogue claybox models was carried out and compared with the reconstructed 3-D pattern of the SF, and the tectonic regime drawing this deformation stile was successively simulated. Wet kaolin was chosen to perform analogue deformative simulations, as also preferred by other authors, due to the proper response of this material to simulated stress field (Miller and Mitra, 2011; Cooke and van der Elst, 2012). Until a few years ago, glass microbeads or silicone were used to simulate pre-existing discontinuities in analogue models (Sassi et al., 1993; Faccenna et al., 1995; Dubois et al., 2002; Del Ventisette et al., 2006; Ahmad et al., 2014; Toscani et al., 2014; Di Domenica et al., 2014, among others). Recently, a new technique to introduce pre-existing discontinuities in clay models was proposed for strike-slip tectonics (Cooke et al., 2013), and successfully applied also in extensional regimes (Paul and Mitra, 2013; Bonini et al., 2015, 2016), by cutting wet kaolin with an electrified blade before starting the deformation process. The cut, ~200 μm thick, separates the clay creating a water film along the cut and it effectively acts as a physical discontinuity.

The subsequent scale relationships were referred to well established models (Hubbert, 1937; Ramberg, 1981). Analogue material (kaolin) has been impregnated with 60% of water content by mass, reaching a density of 1.65 g/cm^3, and permitting us to assume a cohesion in the range of 60-140 Pa (Eisenstadt and Sims, 2005). Assuming a natural rock density of ~2500 kg/m^3 and a natural cohesion of 10-20 MPa, the length ratio varies from 10^{-4} to 10^{-5}, so that 1 cm corresponds to about 0.1-1.0 km in nature. The model deformation velocity must also be properly set up. We deformed the models at 0.02 mm/s, a strain rate in a range allowing wet kaolin to deform as a bi-viscoelastic Burgers material (Cooke and van der Elst, 2012). Using this velocity, i.e. this strain rate, wet kaolin is about 0.6 as frictional coefficient (Henza et al., 2010). This value is within the range of natural rocks frictional coefficient (0.55 - 0.85) at slow slip rate (Handin, 1966; Byerlee, 1978).

5.2- Setup and description

The experimental apparatus consists in a 90 x 60 cm rectangular box with two metal plates: a fixed and a mobile ones whose movements is mechanically controlled (Fig. 9a and 9b). The fixed plate is 75 cm long and 50 cm wide. One quadrant of this plate was removed in order to give it an L-shape. The free quadrant (lower right in Fig. 9b) is occupied by the moving plate, sliding under the fixed one. In this way we can simulate a rock volume (offshore Sicily), where a regional discontinuity is present (SF) moving toward a thrust front (Sicilian Maghrebian Front). A homogeneous clay cake, 5 cm thick, is deposited above the two plates leaving a free space between the clay cake and the experimental apparatus walls in order to avoid boundary effects (Fig. 9c and 9d). Afterwards, a N-S striking and 30° dipping rectilinear cut is introduced into the clay cake, simulating a pre-existing thrust front (Fig. 9c and 9d). In the first model (Fig. 9e), the moving plate moves perpendicularly to the thrust front in order to simulate the pure strike-slip tectonic regime along the separation line between the fixed and moving plates. Changing the moving plate direction of motion by 10° with respect to the separation line (see fig. 9b), transpressional (Fig. 9f) and transtensional (Fig. 9g) tectonic regimes were modeled.

The underlying plate, in all models, was moved by 10 cm creating similar sets of faults visible on the model surface. Deformation appears to be concentrated along a master transcurrent fault in every model (Fig. 9e, f, g) and a clear, much more complex, distributed pattern of splay faults is visible on the deformed surface. The linkage between master transcurrent fault and the splay faults is not evident in all models, but we suppose their connection beneath the surface. The position of the splays regarding the master fault is always on the side of the fixed plate.

The surface scans were performed using a structured light beamer and a HD detector device to analyze subsidence/uplift pattern along the fault systems. The pure strike-slip experiment (Fig. 9e) produces homogenous uplift on the moving plate. No positive change of elevation was observed between splay faults. The highest uplift pattern was obtained during the transpressional experiment (Fig. 9f), but as with pure strike-slip experiment, no elevation change was seen between the splay faults. Transtensional experiment presents a small change in elevation. Due to a compression associated with the thrust front, the subsidence along the fault system is modest, and by contrast some areas inside of the fault system show uplift (Fig. 9g).

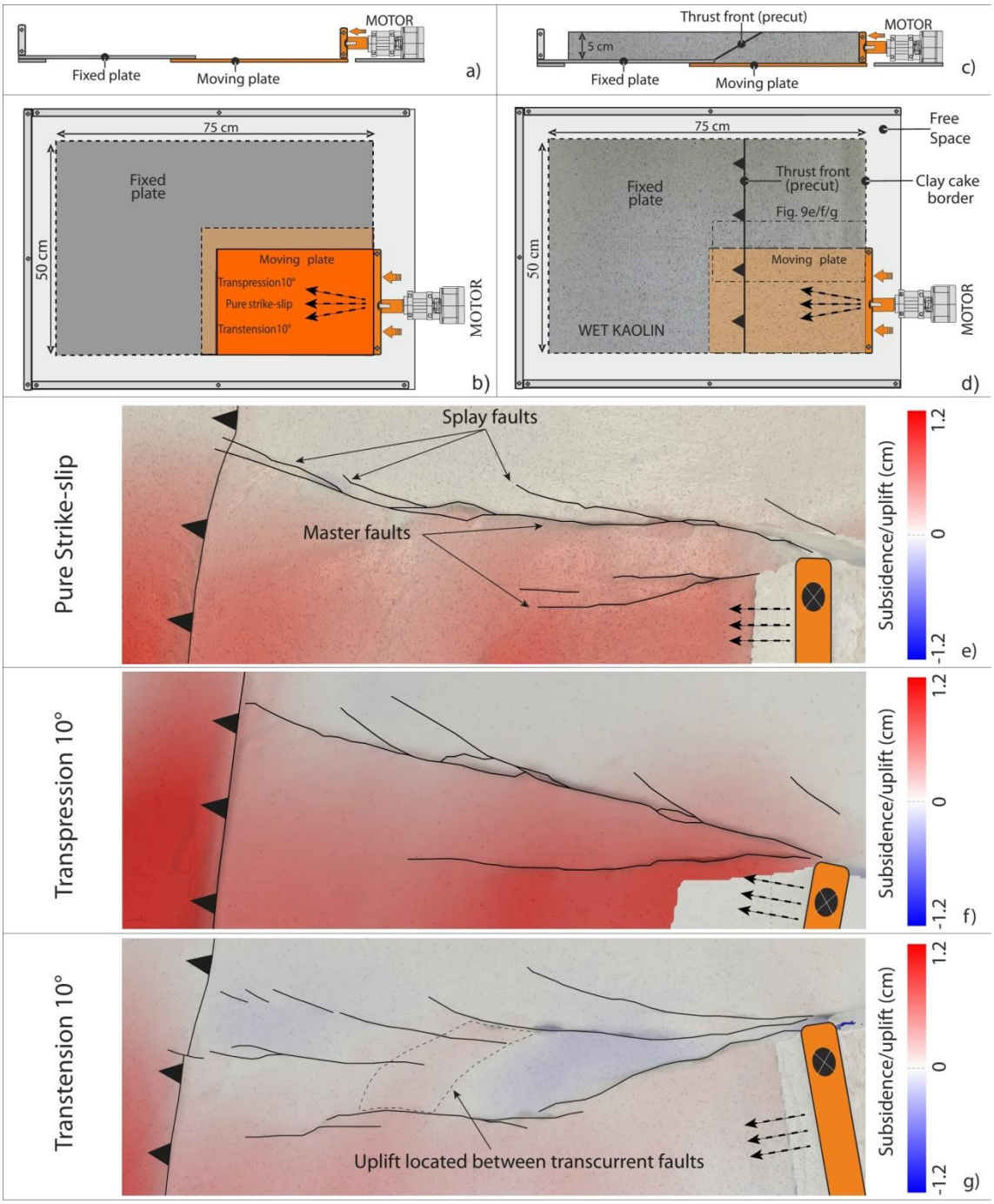

Figure 9: Set up and results of scaled clay analogue models. (a) Section view of the empty clay box; (b) map view and setup of the empty clay box showing three tectonic regimes: right-lateral pure strike-slip, transpression 10° and transtension 10°; (c) section view of the clay box showing the dip of the precut (thrust front); (d) wet kaolin have been put in the clay box and the cut has been created before moving the model (pre-existing thrust fault, black thick line); (e) fault pattern with elevation plot resulting after 7 cm of deformation under pure strike-slip, (f) transpression 10° and (g) transtension 10° tectonic regimes.

6- Comparison between structural setting and analogue models

A 3-D model of the structural setting of the SF was reconstructed by the interpretation of a series of WNW-ESE and NW-SE trending seismic profiles by using the MOVE software (Fig. 10). Some authors suggested right-lateral (Antonelli et al., 1988; Casero and Roure, 1994; Nigro and Renda, 2002) and others left-lateral (Reuther et al., 1993; Finetti, 2003; Lentini et al., 2006; Ghisetti et al., 2009) direction of motion for this fault. The available seismic lines show that the SF consists of a roughly N–S trending master fault with several splay faults developed mainly on its eastern side (Fig. 10). Applying right-lateral kinematics, the three analogue models (pure strike-slip, transpression 10°, and transtension 10°) show a comparable setting for the SF (in map view). The splay faults in our analogue models are on the right side (that is the eastern side of the SF) with respect to the master fault and to the moving basal plate. Discrimination among pure strike-slip movement and transpressional/transtensional regimes remains an open question that requires more detailed analysis. The presence of a compressional system (the analogue for the Sicilian-Maghrebian Chain) in front of the moving plate generates uplift on the left side of the transcurrent fault in all analogue models (side of the moving basal plate). Under the transtensional regime, a general subsidence between the master fault and its splays is expected. Nevertheless, the transtensional model (Fig. 9g) shows a localised uplifted area between transcurrent faults.

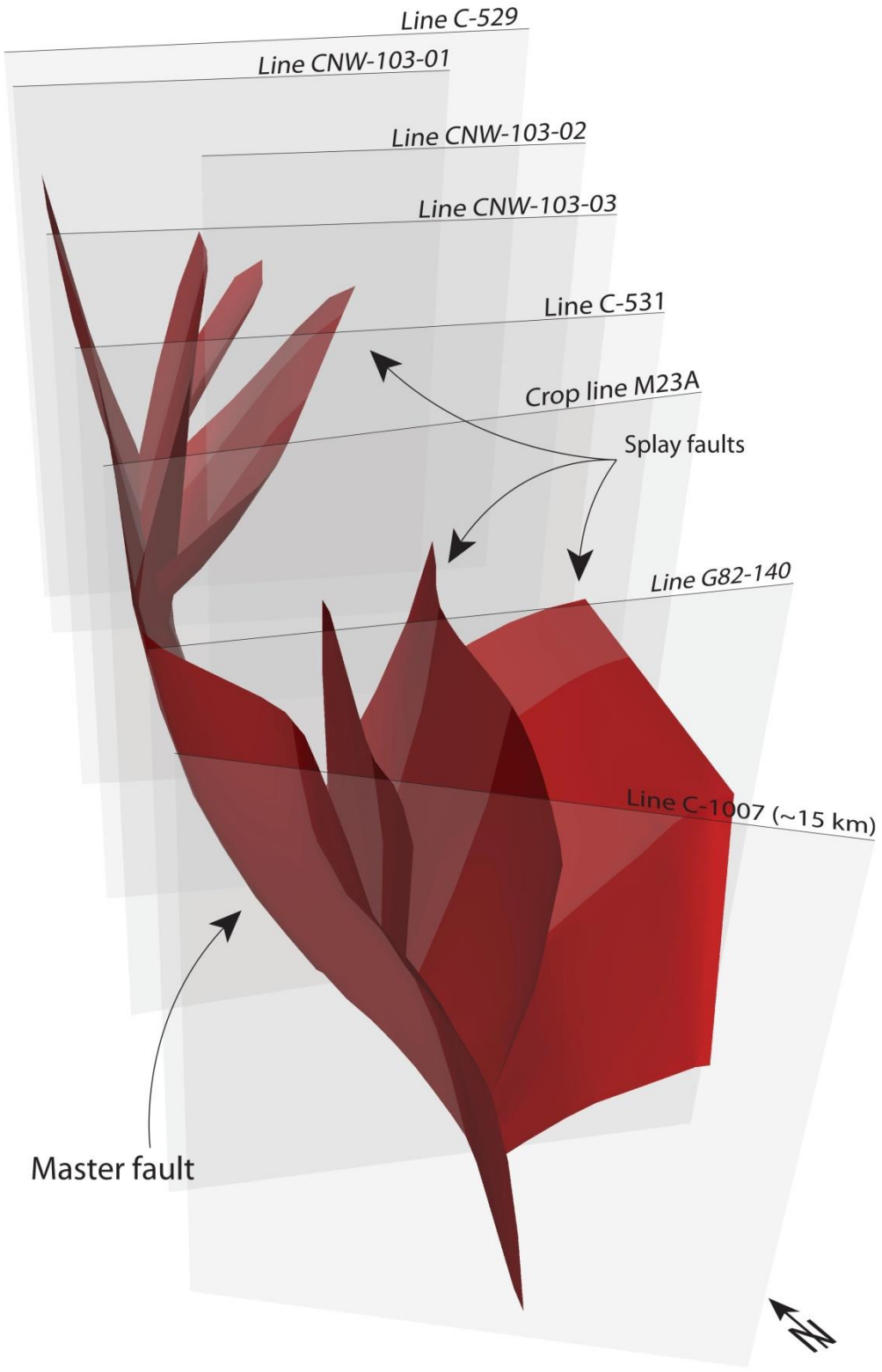

Figure 10: Three dimensional view of the structural framework of the Sciacca Fault comprised of seismic lines C - 529 and C - 1007. The most important splay faults were identified on the eastern side of the master fault. A 3-D, PDF version of this figure is available online (Supplementary material).

7- Discussion

A large dataset of seismic reflection profiles was used to analyze and reconstruct the structural setting of two main, roughly NS trending, tectonic lineaments, CGF and SF, located in the north-western Sicilian Channel, between the coast of Sicily and the Graham and Terrible banks. These lineaments bound a wide, lithospheric-scale regional shear zone from San Vito lo Capo (northern Sicily) to Lampedusa Island. This sector of the Central Mediterranean Sea shows a complex geodynamic setting, characterized by the coexistence of a compressional zone to the north, represented by the Sicilian-Maghrebian Chain, and of an extensional zone to the south, that is the Sicilian Channel Rift Zone. We hypothesize that the SF develops along the offshore extension of an inherited Permian-Triassic weakness zone recognized in western Sicily and interpreted as a platform-to-basin paleo-margin (Di Stefano et al., 2008, 2015).

Different kinematics were simulated by analogue models considering: (i) pure strike-slip, (ii) transpression 10°, and (iii) transtension 10°. The geometry of the SF system, following our 3-D model based on the interpretation of seismic profiles, show a main sub-vertical master fault and several splay faults in its eastern side. It matches quite well with the deformation pattern in the analogue models.

Scholz et al. (2010) show several examples of master faults and associated splays almost parallel to the main stress direction. In their examples, splays are present on one side only of the master fault (the side on which they can complete the plate motion circuit or, in the intraplate case, a circuit to an adjacent fault system). To understand this feature of splay faulting associated with a master fault, a three- or four-dimensional analysis of further analogue models is required. Additionally, the position of the uplifted areas observed in the analogue models is comparable to those identified in the study area. In particular, the uplifted areas are located close to the intersections between master and splay faults. Detected positive flower structures are probably the result of an Early Pliocene reactivation of a previous extensional tectonic lineament induced by a right-lateral transcurrent motion, which is compatible with the tectonic regime of the Central Mediterranean in that period (Mantovani et al., 2014). According to Di Stefano et al., 2015 the previous extensional activity of the lineament went on up to Miocene and it is highlighted by the considerable thickness variations observed in the Miocene succession with respect to the master fault.

Nowadays, focal mechanisms recorded in the Sciacca offshore show a pure left-lateral strike-slip stress regime associated with NS trending sub-vertical planes (Soumaya et al., 2015), while GPS data (Hollenstein et al., 2003; Devoti et al., 2011; Palano et al., 2012) suggest the occurrence of NW-SE oriented maximum stress. According to Mantovani et al. (2014), a change of the main stress direction occurred after the Early Pliocene, from a NE-SW to NW-SE direction. This could explain the change from right-lateral, with a component of compression, to present-day left-lateral motion along the SF (Fig. 11).

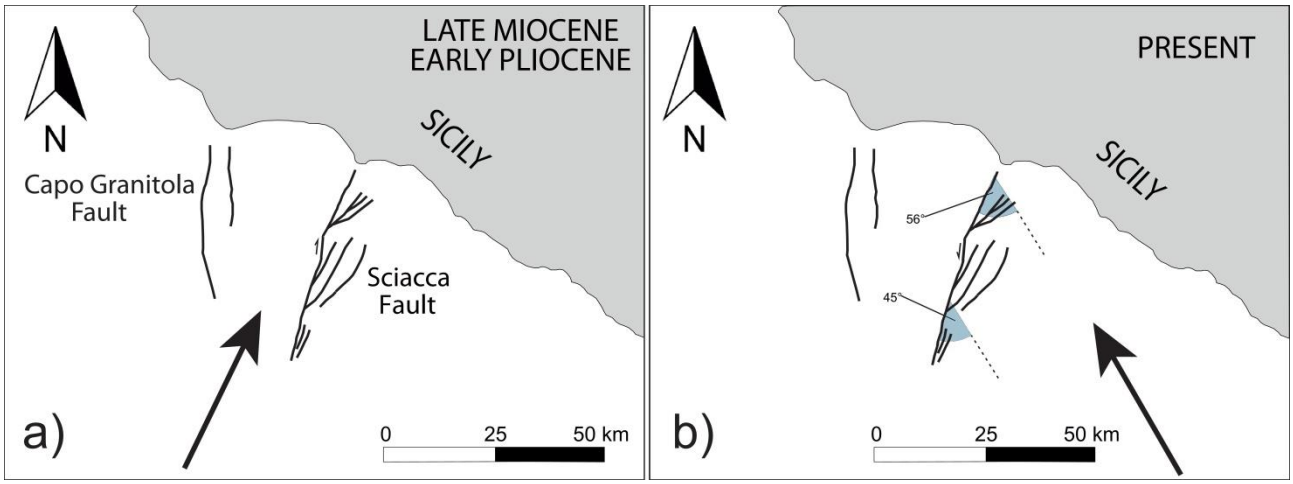

Figure 11: (a) Structural map of the Sciacca Fault and maximum stress direction (black arrow) during the Late Miocene-Early Pliocene (stress direction from Mantovani et al., 2014). Under this tectonic setting, the Sciacca Fault shows a right-lateral transcurrent kinematics; (b) Structural map of the Sciacca Fault and GPS direction represented by black arrow (from Hollenstein et al., 2003). This tectonic setting induces a left-lateral motion along the Sciacca Fault. Not being rectilinear, the southern and northern segments of the Sciacca Fault form angles of 45° and 56°, respectively, with the GPS direction. Strike-slip reactivation is favored along the southern segment where maximum stress angle of incidence is lower.

The coincidence between maximum stress orientation at Late Miocene time (NE-SW) and splay fault directions is in good agreement with the kinematics and splay geometries described both in natural cases (Scholz et al., 2010) and in analogue models (Di Bucci et al., 2007). Presently, the main stress direction is NW-SE oriented and if compared with the different strikes of the southern and northern part of the SF it generates different angles (45° in the southern segment, 56° in the northern one). These angles have been obtained comparing SF segments orientation and direction of principal horizontal stress derived from GPS data (Hollenstein et al., 2003). This

could explain: (i) the present-day seismic activity recorded along the southern segment of the SF (Calò and Parisi, 2014; Soumaya et al., 2015), where the sea-floor appears deformed; (ii) the reduced seismicity along the northern segment of the SF having a higher angle to the main stress direction (Ghisetti and Sibson, 2012).

The deformation pattern produced by the tectonic phases affecting the study area - in the Early Pliocene - is well recognizable if we consider the TWT contour map of the top of the Miocene succession (Fig. 12). This horizon is clearly detectable on all seismic reflection profiles (due to its high amplitude seismic signal). In particular, in the contour map are evident the NS oriented offset between the eastern and western side of the SF, the uplift sectors within the SF (Nerita Bank) and, even if with minor evidence, the offset produced by NW-SE normal faults which border the Graham Bank.

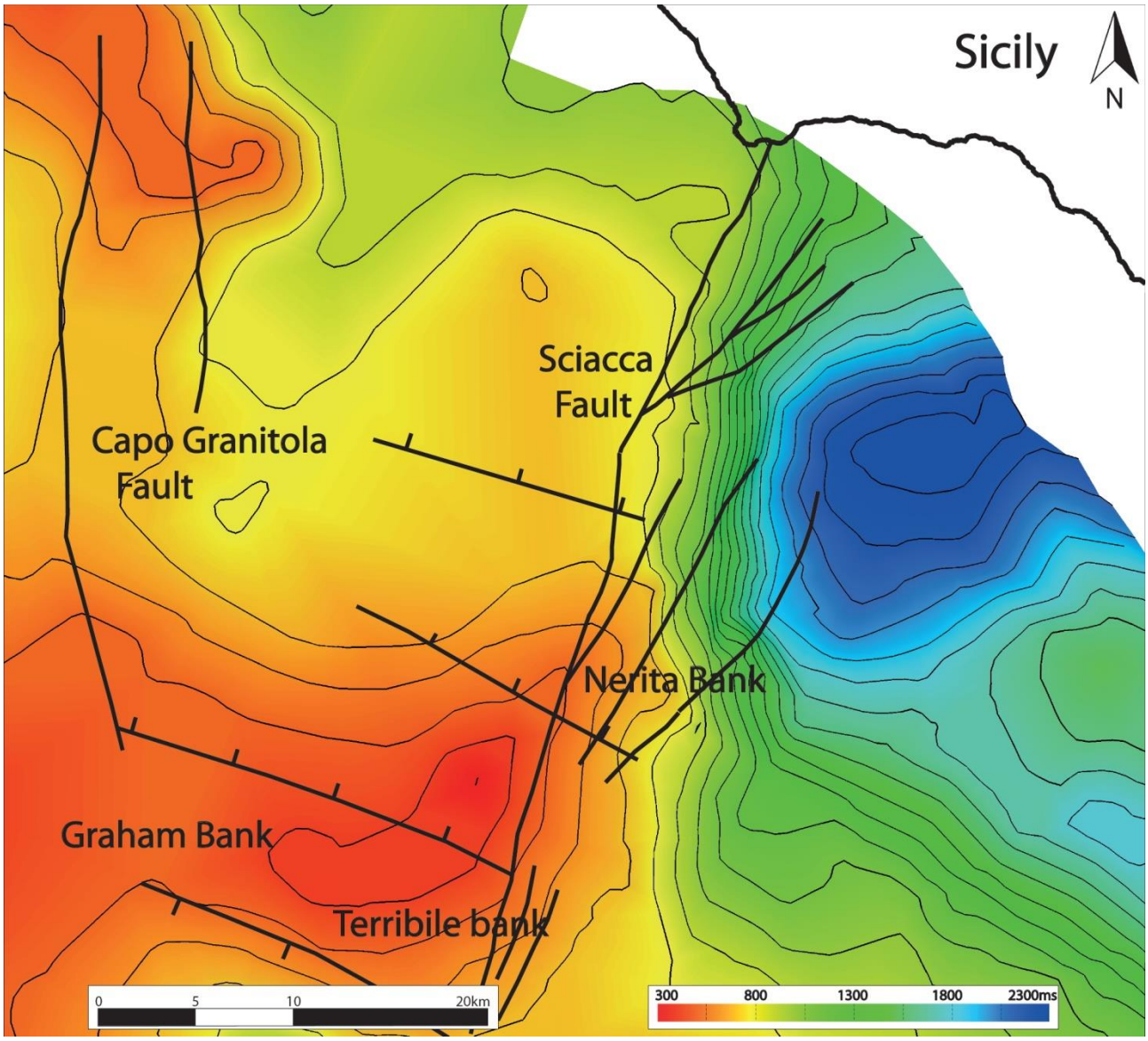

Figure 12: Map of the top of the Miocene Succession (TMS in Figs. 3–7 and 13d) obtained from the interpretation of the seismic profiles (contour lines every 100 ms). The main structural features which can be observed in the map are the following: (1) the NNE-SSW oriented significant elevation difference from the W side to the E side of the Sciacca Fault, probably built by a major normal fault, (2) the uplift sectors within the Sciacca Fault due to the presence of flower structures and, even if less evident, (3) the offset produced by NW-SE normal faults bordering the Graham Bank. The map originally coming from seismic profile interpretation was smoothed to avoid interpolation inconsistencies (smooth radius = 3 km). Data of this surface map are available in the Supplementary material.

8- Conclusions

A regional NS lithospheric-scale transfer zone located in the north-western sector of the Sicilian Channel was analysed. The structural setting, the tectonic evolution, and present-day kinematics of the transfer zone and of the Sciacca Fault, in particular, have been reconstructed in 3-D, integrating interpretation of reflection seismic profiles and analogue models (Fig. 13).

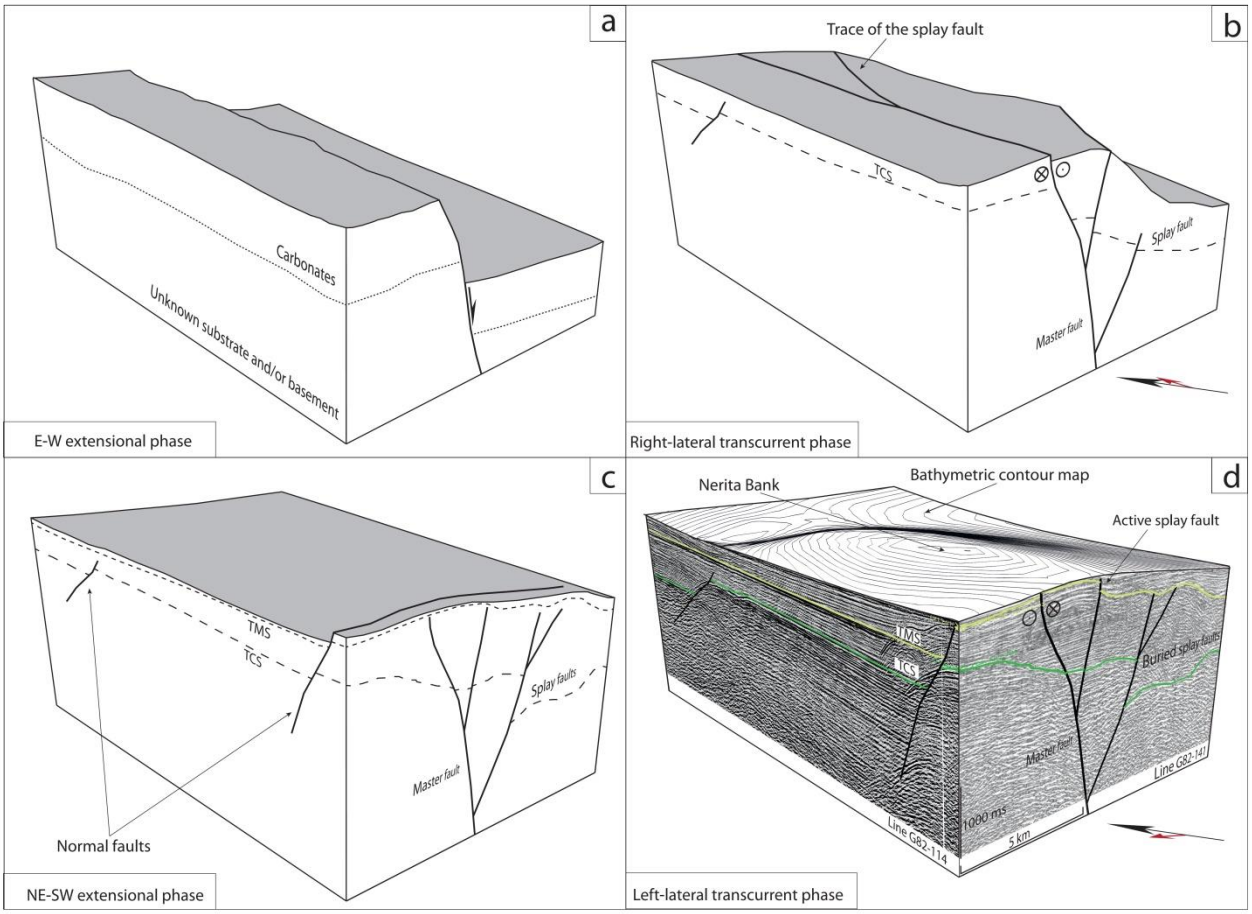

Figure 13: Block diagram illustrating the tectonic evolution of the Sciacca Fault: (a) The first step shows a major normal fault developed along the Permo-Triassic platform-to-basin paleomargin of the Pelagian block (Di Stefano et al., 2015). (b) Kinematic change from normal fault to right-lateral transcurrent fault during the Early Pliocene produced by a NE-SW orientation of the maximum stress in the Central Mediterranean area. Positive flower structures interpreted on the seismic profiles (see Figs. 6–8) occurred at this stage. The black arrow shows the N and the red arrow represents the direction of maximum horizontal stress (according to Mantovani et al., 2014). (c) NW – SE trending normal (same orientation as the Sicilian Channel Rift Zone) were developed (see map of Fig. 2). (d) Present-day 3-D view composed of two interpreted seismic profiles (lines G82-114 and G82-141) and GEBCO bathymetry. The rotation of maximum horizontal stress (red arrow)

from NE-SW to NW-SE, allowed a kinematic change along the Sciacca Fault that is reactivated as a left-lateral transcurrent structure along its southern part.

The transfer zone is made up by two tectonic N-S oriented lineaments (CG and SF) delimiting a 30 km wide area where the Plio-Quaternary succession appears poorly deformed. These two faults are inherited from a Permo-Triassic rifting phase, subsequently reactivated under transpression by the compression between Africa and Europe.

The transfer zone is made up by two tectonic NS oriented lineaments (CG and SF) delimiting a 30 km wide area where the Plio-Quaternary succession appears poorly deformed. These two faults are inherited from a Permo-Triassic rifting phase, subsequently reactivated under transpression by the compression between Africa and Europe.

The western fault (Capo Granitola Fault) does not show clear evidence of present-day tectonic activity, and toward the south it connects into the volcanic area of the Graham Bank. It is characterized in its northern part, by a buried positive flower structure involving Early Pliocene deposits. Some authors (Barreca et al., 2014) postulate that this fault is presently active near its intersection with the coastline.

The eastern fault (Sciacca Fault) is constituted of a sub-vertical master fault and several splays that together form a positive flower structures. SF probably developed along the offshore continuation of an inherited weakness zone identified in western Sicily and interpreted as a carbonate platform margin developed in Permo-Triassic times. This lineament shows active deformation at the sea-floor, particularly evident along the Nerita Bank.

A set of scaled analogue clay models was carried out in order to better constrain the tectonic processes that led to the structural setting displayed by seismic data. Tectonic structures and uplift/subsidence patterns generated by the models are compatible with the 3-D model obtained from seismic reflection profiles. The best fit between the Sciacca Fault and the analogue model was obtained with a right-lateral movement. Nevertheless, actual stress field in the study area derived from GPS measurements does not support the present-day modelled right-lateral kinematics along the Sciacca Fault. Moreover, seismic events along this fault show focal mechanisms with the left-lateral component.

We ascribe the change of the slip direction along the Sciacca Fault, from a right-lateral strike-slip regime to the present-day left-lateral kinematics as due to a change of the direction of the principal horizontal stress occurred in the Late Pliocene. The tectonic evolution of the Sciacca Fault can be summarised as follow:

(1) It was probably active up to Miocene as a high angle normal fault testified by the considerable thickness variations of the Miocene succession (Fig. 13a).

(2) Under a NE-SW oriented maximum stress direction, the previous normal fault was re-activated in the Lower Pliocene as a right-lateral transcurrent fault with a minor compressive component producing positive flower structures (Fig. 13b).

(3) WNW-ESE-oriented normal faults have been observed in the study area but their origin is unclear. These structures could be associated with the process of continental rifting developed in the Sicilian Channel since Lower Pliocene.

(4) The maximum stress direction changed its orientation starting from the Late Pliocene (Mantovani et al., 2014), so that the present-day main compressive horizontal stress in the area of the Sicilian Channel has a NW-SE direction (Fig. 13d). This change in the orientation of the maximum stress field produced a kinematic change from right-lateral to present-day left-lateral strike slip motion along the SF.

To support our interpretations, further seismic data and numerical models would be of help to confirm or modify and better define: (i) configuration and possible prolongations of the CG and SF, (ii) the origin and timing of the observed normal faults, and (iii) the distribution and extension of the active faults or fault segments, the role of which in defining the seismic hazard of this area is a fundamental issue.

Acknowledgments

The Editor Rob Govers, Luis Somoza and an anonymous reviewers are kindly acknowledged for their thoughtful revisions that greatly improved the manuscript. Carmelo Monaco, Luigi Ferranti and Giovanni Barreca are acknowledged for fruitful advices and constructive criticisms at the beginning of this research. Seismic profile interpretation, structural maps and 3-D

reconstructions were carried out using the MOVE software, provided by Midland Valley Exploration Ltd. to the University of Pavia within the ASI (Academic Software Initiative). All analogue models were carried out in the Analogue Models Lab of the University of Pavia.

Supplementary material

A 3-D, PDF version of figure 10 is available in the data repository together with a .dat file of the TMS (Top Miocene Succession, fig. 12).

References

Ahmad, M.I., Dubey, A.K., Toscani, G., Bonini, L., Seno, S., (2014). Kinematic evolution of thrust wedge and erratic line length balancing: insights from deformed sandbox models. International Journal of Earth Sciences, 103, 1, 329-347, doi:10.1007/s00531-013-0947-8.

Anderson, H. and Jackson, J., (1987). Active tectonics of the Adriatic Region. Geophysical Journal of the Royal Astronomical Society, 91, 937–983. doi:10.1111/j.1365-246X.1987.tb01675.x

Antonelli, M., Franciosi, R., Querci, A., Ronco, G. P. and Vezzani, F., (1988). Paleogeographic evolution and structural setting of the Northern side of the Sicily Channel. In: Società Geologica ltaliana, 74 Congresso Nazionale, Relazioni, 79-86.

Argnani A (1987) The Gela Nappe: evidence of accretionary melange in the Maghrebian foredeep of Sicily. Mem Soc Geol Ital 38:419–428

Argnani, A., Cornini, S., Torelli, L. and Zitellini, N., (1988). Neogene-Quaternary foredeep system in the Strait of Sicily. Mem. Soc. Geol. It., 36, 123-130.

Argnani, A., (1990). The Strait of Sicily rift zone: foreland deformation related to the evolution of a backarc basin, J. Geodyn., 12, 311-331.

Argnani, A., (1993). Neogene basins in the Strait of Sicily (central Mediterranean): Tectonic settings and geodynamic implications, in Recent Evolution and Seismicity of the Mediterranean Region, NATO ASI Ser., Ser. C, vol. 402, edited by E. Boschi, pp. 173– 187, Kluwer Acad., Dordrecht, Netherlands.

Barreca, G., V. Bruno, C. Cocorullo, F. Cultrera, L. Ferranti, F. Guglielmino, L. Guzzetta, M. Mattia, C. Monaco, F. Pepe (2014). Geodetic and geological evidence of active tectonics in south-western Sicily (Italy) J. Geodyn., 82, pp. 138–149 http://dx.doi.org/10.1016/j.jog.2014.03.004

Beccaluva, L., Colantoni, P., Di Girolamo, P. and Savelli, C., (1981). Upper-Miocene Submarine Volcanism in the Strait of Sicily (Banco Senza Nome). Bull. Volcanol., 44, 573-581.

Boccaletti, M., Cello, G., Tortorici, L. (1987). Transtensional tectonics in the Sicily Channel Journal of Structural Geology, 9 (7), pp. 869-876 DOI: 10.1016/0191-8141(87)90087-3

Bonini L., Basili R., Toscani G., Burrato P., Seno S., Valensise G., (2015). The role of pre-existing discontinuities in the development of extensional faults: an analog modeling perspective. Journal of Structural Geology, 74, 145-158, doi:10.1016/j.jsg.2015.03.004.

Bonini, L., R. Basili, G. Toscani, P. Burrato, S. Seno, Valensise, G., (2016), The effects of pre-existing discontinuities on the surface expression of normal faults: Insights from wet clay analog modeling, Tectonophysics, http://dx.doi.org/10.1016/j.tecto.2015.12.015.

Bottari, A. (1973). Attività sismica e neotettonica della Valle del Belice. Ann. Geof., XXVI (1), pp. 55-83

Byerlee, J.D. (1978). Friction of rocks. Pure and applied Geophysics, 116, 615-626

Calanchi, N., Colantoni, P., Rossi, PL., Saitta, M., Serri, G., (1989) The Strait of Sicily continental rift system: physiography and petrochemistry of the submarine volcanic centres. Marine Geol 87:55–83

Calò, M., Parisi, L., (2014). Evidences of a lithospheric fault zone in the Sicily Channel continental rift (southern Italy) from instrumental seismicity data. Geophysical Journal International, 199 (1), art. no. ggu249, pp. 219-225. DOI: 10.1093/gji/ggu249

Caracausi, A., Favara, R, Italiano, F., Nuccio, P.M., Paonita, A., Rizzo, A., (2005). Active geodynamics of the central Mediterranean Sea: tensional tectonic evidences in western Sicily from mantle-derived helium, Geophys. Res. Lett., 32, L04312, doi:10.1029/2004gl021608.

Carapezza M, Ferla P, Nuccio PM, Valenza M., (1979). Caratteri metrologici e geochimica delle vulcaniti dell'Isola Ferdinandea. Rend Soc It Min e Pet 35, 377–388

Casero, P., and F. Roure (1994). Neogene deformations at the Sicilian-North Africa plate boundary, in Peri-Tethyan Platforms, edited by F. Roure, pp. 27–45, Ed. Technip, Paris.

Catalano, R., P. Di Stefano, A. Sulli, and F. P. Vitale (1996). Paleogeography and structure of the central Mediterranean: Sicily and its offshore area, Tectonophysics, 260, 291 – 323, doi:10.1016/0040- 1951(95)00196-4.

Catalano, R., A. Franchino, S. Merlini, and A. Sulli (2000). A crustal section from the eastern Algerian basin to the Ionian ocean (central Mediterranean), Mem. Soc. Geol. Ital., 55, 71 – 85.

Catalano, R., Valenti, V., Albanese, C., Accaino, F., Sulli, A., Tinivella, U., Gasparo Morticelli, M., Zanolla, C., Giustiniani, M. (2013). Sicily's fold-thrust belt and slab roll-back: The SI.RI.PRO. seismic crustal transect. Journal of the Geological Society, 170 (3), pp. 451-464. DOI: 10.1144/jgs2012-099

Cavallaro, D., Monaco, C., Polonia, A., Sulli, A., Di Stefano, A., (2016).Evidence of positive tectonic inversion in the north-central sector of the Sicily Channel (Central Mediterranean). Natural Hazards, DOI: 10.1007/s11069-016-2515-6

Cello, G., (1987) Structure and deformation processes in the Strait of Sicily ‘‘rift zone’’. Tectonophysics 141, pp.237–247

Civile, D., lodolo, E., Tortorici, L., Lanzafame, G., Brancolini, G. (2008). Relationships between magmatism and tectonics in a continental rift: The Pantelleria Island region (Sicily Channel, Italy). Marine Geology, 251, 32-46.

Civile, D., Lodolo, E., Accettella, D., Geletti, R., Ben-Avraham, Z., Deponte, M., Facchin, L., Ramella, R., Romeo, R. (2010). The Pantelleria graben (Sicily Channel, Central Mediterranean): An example of intraplate 'passive' rift. Tectonophysics, 490 (3-4), 173-183. DOI: 10.1016/j.tecto.2010.05.008

Civile, D., Lodolo, E., Alp, H., Ben-Avraham, Z., Cova, A., Baradello, L., Accettella, D., Burca, M., Centonze, J., (2014). Seismic stratigraphy and structural setting of the Adventure Plateau (Sicily Channel). Marine Geophysical Research, 35 (1), 37-53. DOI: 10.1007/s11001-013-9205-5

Civile, D., Lodolo, E., Zecchin, M., Ben-Avraham, Z., Baradello, L., Accettella, D., Cova, A., Caffau, M. (2015). The lost Adventure Archipelago (Sicilian Channel, Mediterranean Sea): Morpho-bathymetry and Late Quaternary palaeogeographic evolution. Global and Planetary Change, 125, pp. 36-47. DOI: 10.1016/j.gloplacha.2014.12.003

Civile, D., Lodolo, E., Caffau, M., Baradello, L., Ben-Avraham, Z. (2016). Anatomy of a submerged archipelago in the Sicilian Channel (central Mediterranean Sea) Geological Magazine, 153 (1), pp. 160-178. DOI: 10.1017/S0016756815000485

Coltelli, M., Cavallaro, D., D'Anna, G., D'Alessandro, A., Grassa, F., Mangano, G., Patanè, D., Gresta, S.,(2016). Exploring the submarine graham bank in the sicily channel. Annals of Geophysics, 59 (2), art. no. S0208,DOI: 10.4401/ag-6929

Cooke, M.L., van der Elst, N.J., (2012). Rheologic testing of wet kaolin reveals frictional and bi-viscous behavior typical of crustal materials. Geophysical Research Letters, 39, http://dx.doi.org/10.1029/2011GL050186.

Cooke, M.L., Schottenfeld, M.T., Buchanan, S.W. (2013). Evolution of fault efficiency at restraining bends within wet kaolin analog experiments . Journal of Structural Geology 51, 180-192.

Colantoni, P., (1975). Note di geologia marina sul Canale di Sicilia. Giorn. Geol., 40, 181 207.

Corti, G., Cuffaro, M., Doglioni, C., Innocenti, F., Manetti, P. (2006). Coexisting geodynamic processes in the Sicily Channel. Special Paper of the Geological Society of America, 409, pp. 83-96. DOI: 10.1130/2006.2409(05)

Del Ventisette, C., Montanari, D., Sani, F., Bonini, M., (2006). Basin inversion and fault reactivation in laboratory experiments. In: Tavarnelli, E., Butler, R., Grasso, M. (Eds.), Tectonic Inversion Processes and Structural Inheritance in Mountain Belts: Journal of Structural Geology, 28, pp. 2067–2083.

Devoti, R., Esposito, A., Pietrantonio, G., Pisani, A.R., Riguzzi, F. (2011). Evidence of large scale deformation patterns from GPS data in the Italian subduction boundary. Earth and Planetary Science Letters, 311, pp. 230-241 doi: 10.1016/j.epsl.2011.09.034

Dewey, J. F., Helamn, M. L., Turco, E., Hutton, D. H. W. & Knott, S. D. (1989). Kinematics of the western Mediterranean. In: Coward, M. P., Dietrich, D. & Park, R. G. (eds) Alpine Tectonics. Geological Society, London, Special Publication, 45, 265–283.

Di Bucci, D., Ravaglia, A., Seno, S., Toscani, G., Fracassi, U., Valensise, G. (2007). Modes of fault reactivation from analogue modeling experiments: Implications for the seismotectonics of the Southern Adriatic foreland (Italy). Quanternary International, 171-172, pp. 2-13 doi: 10.1016/j.quaint.2007.01.005

Di Domenica, A., Bonini, L., Calamita, F., Toscani, G., Galuppo, C., Seno, S., (2014). Analogue modeling of positive inversion tectonics along differently oriented pre-thrusting normal faults: an application to the Central-Northern Apennines of Italy. Bull. Geol. Soc. Am., 126, 943e955. http://dx.doi.org/10.1130/B31001.1.

Di Stefano, P., Cacciatore, M.S., Zarcone, G. (2008). A Triassic carbonate platform edge in the Sciacca zone: Implications for the accretion of the Maghrebian chain in southwestern Sicily. Rendiconti Online Societa Geologica Italiana, 2, pp. 79-82.

Di Stefano, P., R. Favara, D. Luzio, P. Renda, M. S. Cacciatore, M. Calò, G. Napoli, L. Parisi, S. Todaro, and G. Zarcone (2015). A regional-scale discontinuity in western Sicily revealed by a multidisciplinary approach: A new piece for understanding the geodynamic puzzle of the southern Mediterranean, Tectonics, 34, doi:10.1002/2014TC003759.

Dubois, A., Odonne, F., Massonnat, G., Lebourg, T., Fabre, R., (2002). Analogue modelling of fault reactivation: tectonic inversion and oblique remobilisation of grabens. Journal of Structural Geology 24, 1741–1752.

Eisenstadt, G., Sims, D., (2005). Evaluating sand and clay models; do rheological differences matter? Journal of Structural Geology, 27, 1399–1412, 2005.

Faccenna, C., Nalpas, T., Brun, J.P., Davy, P., Bosi, V., (1995). The influence of pre-existing faults on normal fault geometry in nature and in experiments. Journal of Structural Geology, 17, 1139–1149.

Finetti, I. (2003). The CROP profiles across the Mediterranean Sea (CROP MARE I and II). Mem. Descr. Carta Geol. D'It., LXII, pp. 171-184.

Frepoli, A., Amato, A., (2000).Fault plane solutions of crustal earthquakes in Southern Italy (1988-1995): Seismotectonic implications. Annali di Geofisica, 43 (3), pp. 437-467.

Gasparini, C., Iannaccone, G., Scandone, P., Scarpa, R., (1982). Seismotectonics of the Calabrian Arc. Tectonophysics 84, 267–286.

Gemmellaro, C. (1831). Relazione di fenomeni del nuovo vulcano sorto dal mare fra la costa di Sicilia e l'isola di Pantelleria nel mese di luglio 1831. Catania, ne' torchi della regia Università Carmelo Pastore impresse.

Ghisetti, F. C., A. R. Gorman, M. Grasso, and L. Vezzani (2009). Imprint of foreland structure on the deformation of a thrust sheet: The Plio-Pleistocene Gela Nappe (southern Sicily, Italy), Tectonics, 28, TC4015, doi:10.1029/2008TC002385.

Ghisetti, F.C., and Sibson, R.H. (2012). Compressional reactivation of E–W inherited normal faults in the area of the 2010–2011 Canterbury earthquake sequence, New Zealand Journal of Geology and Geophysics, 55:3, 177-184, DOI: 10.1080/00288306.2012.674048

Handin, J., (1966). Strenght and ductility. In: Clark SP (ed) Handbook of physical constant. Geological Society of America Memoir, 97, 223-289

Henza, A., Withjack, M.O., Schlische, R.W., (2010). Normal-fault development during two phases of non-coaxial extension: An experimental study, J. Struct. Geol., 32, 1656–1667, doi:10.1016/j.jsg.2009.07.007.

Hollenstein, C., Kahle, H.G., Geiger, A., Jenny, S., Goes, S and Giardini, D. (2003). New GPS constraints on the Africa-Eurasia plate boundary zone in southern Italy. Geophysical Resarch Letters, 30(18), doi:10.1029/2003GL017554

Hubbert, M.K., (1937). Theory of scale models as applied to the study of geologic structures. Geological Society of America Bulletin, 48, 1459–1520.

Lavecchia, G., Ferrarini, F., de Nardis, R., Visini, F., Barbano, M.S., (2007). Active thrusting as a possible seismogenic source in Sicily (Southern Italy): Some insights from integrated structural-kinematic and seismological data. Tectonophysics, 445 (3-4), 145-167. DOI: 10.1016/j.tecto.2007.07.007

Lentini F (1982). The geology of the Mt. Etna basement. Mem. Soc. Geol. Ital., 23, 7–25

Lentini, F., Carbone, S., and Guarnieri, P., (2006). Collisional and postcollisional tectonics of the Apenninic-Maghrebian orogen (southern Italy), in Dilek, Y., and Pavlides, S., eds., Postcollisional tectonics and magmatism in the Mediterranean region and Asia: Geological Society of America Special Paper 409, p. 57–81, doi: 10.1130/2006.2409(04).

Lodolo, E., Civile, D., Zanolla, C., Geletti, R., (2012). Magnetic signature of the Sicily Channel volcanism. Marine Geophysical Research, 33 (1), 33-44. DOI: 10.1007/s11001-011-9144-y

Maldonado A, Stanley DI (1977). Lithofacies as a function of depth in the Strait of Sicily. Geology 2:111–117

Maldonado, A; Somoza, L; Pallares, L. 1999. The Betic orogen and the Iberian-African boundary in the Gulf of Cadiz: geological evolution (central North Atlantic). Marine Geology, 155 (1-2), 9-43

Mantovani, E. , Viti, M. , Babbucci, D. , Tamburelli, C. , Cenni, N. , Baglione, M. and D'Intinosante, V. (2014). Generation of Back-Arc Basins as Side Effect of Shortening Processes: Examples from the Central Mediterranean. International Journal of Geosciences, 5, 1062-1079. doi: 10.4236/ijg.2014.510091.

Medialdea, T., Vegas, R., Somoza, L., Vázquez, J.T., Maldonado, A., Díaz-del-Río, V., Maestro, A., Córdoba, D, M. C. Fernández-Puga, (2004). Structure and evolution of the "Olistostrome" complex of the Gibraltar Arc in the Gulf of Cádiz (eastern Central Atlantic): evidence from two long seismic cross-sections. Marine Geology 209, 1-4, 173-19

Medialdea T., Somoza L., Pinheiro L.M., Fernández-Puga M.C., Vázquez J.T., León R., Ivanov M.K., Magalhaes V., Díaz-del-Río V., Vegas R. (2009).Tectonics and mud volcano development in the Gulf of Cádiz.. Marine Geology 261 (2009) 48-63. doi:10.1016/j.margeo.2008.10.007.

McKenzie, D. (1972). Active Tectonics of the Mediterranean Region. Geophysical Journal Geophysical Journal of the Royal Astronomical Society, 30, pp. 109–185. doi:10.1111/j.1365-246X.1972.tb02351.x,

Miller, J.F., Mitra, S., (2011). Deformation and secondary faulting associated with basement-involved compressional and extensional structures. AAPG Bulletin, 95, 4, 675-689.

Monaco, C., Mazzoli, S., Tortorici, L. (1996). Active thrust tectonics in western Sicily (southern Italy): The 1968 Belice earthquake sequence. Terra Nova, 8 (4), pp. 372-381. DOI: 10.1111/j.1365-3121.1996.tb00570.x

Nigro, F., Renda, P. (2001). Oblique-slip thrusting in the Maghrebide chain of Sicily. Italian Journal of Geosciences, 120 (2-3), 187-200.

Nigro, F., Renda, P. (2002). Forced mode dictated by foreland fault-indenter shape during oblique convergence: the Western Sicily mainland. Boll. Soc. Geol. It., 121, 151-162

Palano, M., Ferranti, L., Monaco, C., Mattia, M., Aloisi, M., Bruno, V., Cannav, F., Siligato, G., (2012). GPS velocity and strain fields in Sicily and southern Calabria, Italy: Updated geodetic constraints on tectonic block interaction in the central Mediterranean. Journal of Geophysical Research: Solid Earth, 117 (7), art. no. B07401, DOI: 10.1029/2012JB009254

Paul, D., Mitra, S., (2013). Experimental models of transfer zones in rift systems. AAPG Bulletin, 97, 5, 759-780.

Ramberg, H., (1981). Gravity, deformation and the Earth's crust. Academic Press, London.

Reuther CD, Eisbacher GH (1985). Pantelleria rift-crustal extension in a convergent intraplate setting. Geol Rundsch 74, 585–597

Reuther, C-D., Ben-Avraham, Z. and Grasso, M. (1993). Origin and role of major strike-slip transfre during plate collision in the central mediterranean. Terra Nova, 5, 249-257.

Rotolo SG, Castorina F, Cellula D, Pompilio M (2006). Petrology and geochemistry of submarine volcanism in the Sicily Channel. J Geol 114:355–365

Roure, F., Howel, D.G., Muller, C., Moretti, I., (1990). Late Cenozoic subduction complex of Sicily. J. Struct. Geol. 12, 259–266

Sassi, W., Colletta, B., Balé, P., Paquereau, T., (1993). Modelling of structural complexity in sedimentary basins: the role of pre-existing faults in thrust tectonics. Tectonophysics 226, 97–112.

Scholz, C.H., Ando, R., Shaw, B.E., (2010). The mechanics of first order splay faulting: the strike-slip case. J. Struct. Geol. 32 (1), 118–126.

Soumaya, A., N. Ben Ayed, D. Delvaux, and M. Ghanmi (2015). Spatial variation of present-day stress field and tectonic regime in Tunisia and surroundings from formal inversion of focal mechanisms: Geodynamic implications for central Mediterranean, Tectonics, 34, 1154–1180, doi:10.1002/2015TC003895.

Toscani, G., Bonini, L., Ahmad, M.I., Di Bucci, D., Di Giulio, A., Seno, S., Galuppo, C., (2014). Opposite verging chians sharing the same foreland: kinematics and interaction through analogue models (Central Po Plain, Italy). Tectonophysics, 633, 268-282. doi:10.1016/j.tecto.2014.07.019.

Trincardi, F., and A. Argnani (1990). Gela submarine slide: A major basin-wide event in the Plio-Quaternary foredeep of Sicily, Geo Mar. Lett. , 10, 13 – 21, doi:10.1007/BF02431017.

Washington HS (1909). The submarine eruption of 1831 and 1891 near Pantelleria. Am J Sci 27:131–150

Zitellini N, E. Gràcia , L. Matias , P. Terrinha , M.A. Abreu , G. DeAlteriis J.P. Henriet J.J. Dañobeitia , D.G. Masson , T. Mulder , R. Ramella , L. Somoza , S. Diez . (2009). The quest for the Africa-Eurasia plate boundary west of the Strait of Gibraltar. Earth and Planetary Science Letters, doi:10.1016/j.epsl.2008.12.005

3- Numerical models

During my visiting research period at the University of Massachusetts (Amherst, USA), I worked with Prof. Michele Cooke who introduced me the numerical modelling used in geomechanics. This technique is used on 3D fault geometries obtained from seismic interpretation of Sciacca Fault. Within this research, we are trying to confirm our interpretation of seismic data by comparing fault activity and the uplift pattern obtained from the model and in the Sicilian Channel.

Subsurface data and numerical models: an integrated approach to reconstruct and constrain active fault systems (Sciacca Fault, Italy)

J.Fedorik[1], G. Toscani[1], M. Cooke[2], D. Civile[3], E. Lodolo[3], L. Bonini [4], S. Seno[1]

[1] *Università di Pavia*

[2] *University of Massachusetts*

[3] *OGS Trieste*

[4] *Università di Trieste*

***Corresponding author email**: *jakub.fedorik01@universitadipavia.it*

The analysis of an extensive number of multichannel seismic reflection profiles acquired in the northern part of the Sicilian Channel allowed a 3-D reconstruction of a regional NS-trending Transfer zone. This Transfer zone is composed of two major faults (Capo Granitola and Sciacca Fault) which display mainly a transcurrent tectonic regime (fig.1). This regional tectonic lineament is of broad interest for both geodynamic and seismotectonic implications having a complex tectonic evolution in an area that is a key point for Central Mediterranean geodynamics and locally showing evidences of ongoing tectonic activity. Along the Transfer zone, the maximum stress directions reoriented through times (Mantovani et al., 2014) and it separated different sectors of the Sicilian-Maghrebian Chain characterized by various tectonic evolution, deformation age and thrust vergence. Moreover, it separates in two portions the Sicilian Channel Rifting Zone (a

western area where the Pantelleria Graben took place and an eastern sector characterized by the presence of the Linosa and Malta troughs) where several recent submarine volcanic centers are present (Civile et al., 2008; Lodolo et al., 2012; Coltelli et al., 2016). A well-constrained 3D reconstruction of the Sciacca Fault (fig. 2) allowed us to define (i) the present day tectonic setting of this fault, (ii) its tectonic evolution and (iii) a possible interpretation of the seismic activity along it. Regarding the present day, tectonic setting data show that this tectonic lineament consists of a system of faults composed by a sub-vertical NNE-SSW trending master fault with several splays. The evidence of transcurrent tectonics along this fault is observable at least for 70 km, from the Sicily coastline to the southern margin of the Terrible Bank (fig.1). The Sciacca Fault probably developed along the offshore continuation of an inherited weakness zone identified in western Sicily and interpreted as a carbonate platform margin developed in Permo-Triassic times. It was probably active up to Miocene as a high angle normal fault testified by the considerable thickness variations of the Miocene succession. Under a NE-SW oriented maximum stress direction, the previous normal fault was re-activated in the Lower Pliocene as a right-lateral transcurrent fault with a compressive component producing positive flower structures. The maximum stress direction changed its orientation starting from the Late Pliocene (Mantovani et al., 2014), so that the present-day main compressive horizontal stress in the area of the Sicilian Channel has a NW-SE direction. This change in the orientation of the maximum stress field produced a kinematic change from right-lateral to present day left-lateral strike-slip motion. Instrumental seismicity shows that the Sicilian Channel is dominated by strike-slip focal mechanisms with left-lateral component (Calò and Parisi, 2014; Soumaya et al., 2015).

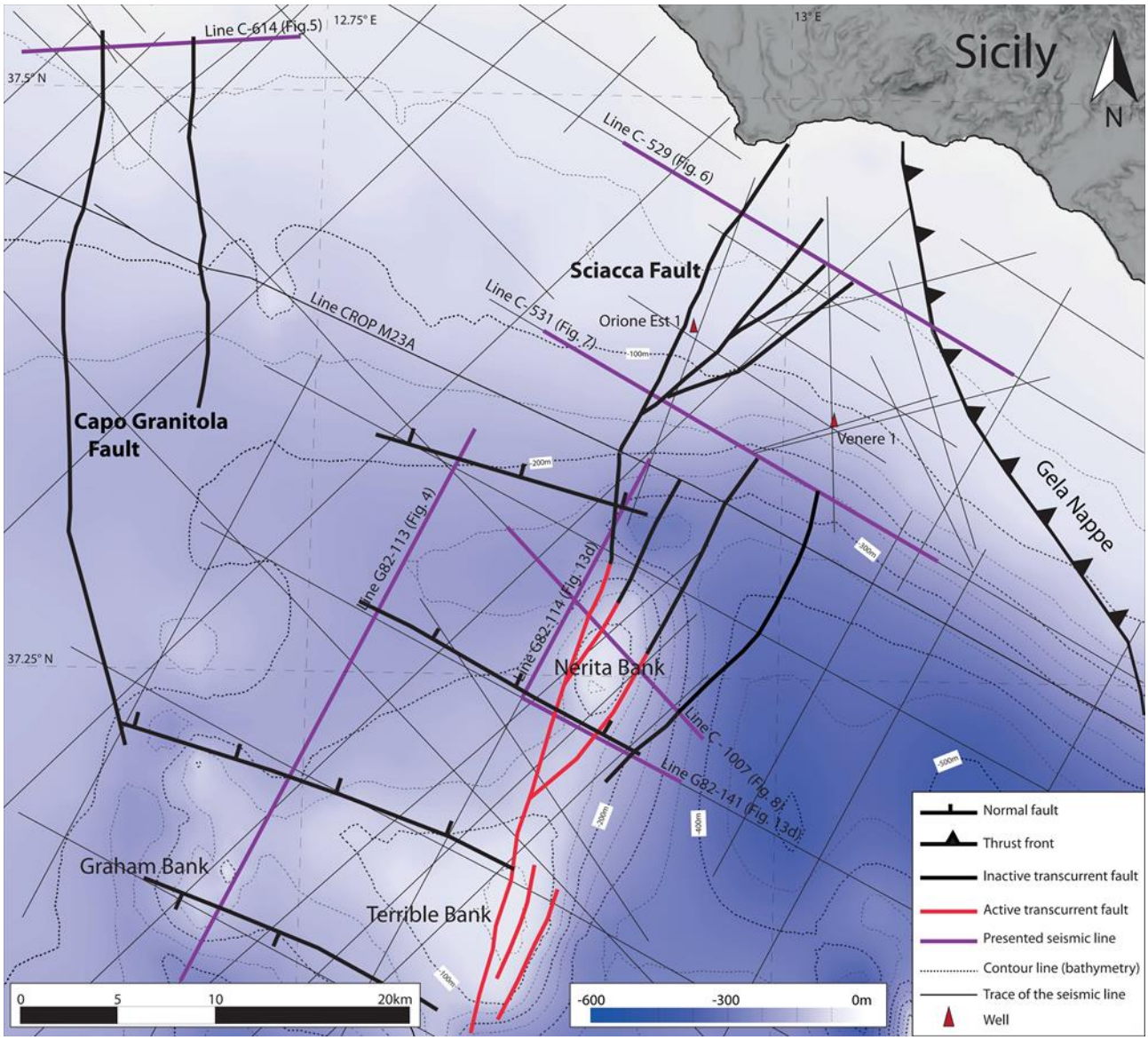

Fig. 1: Structural sketch of the study area (from Fedorik et al., 2018)

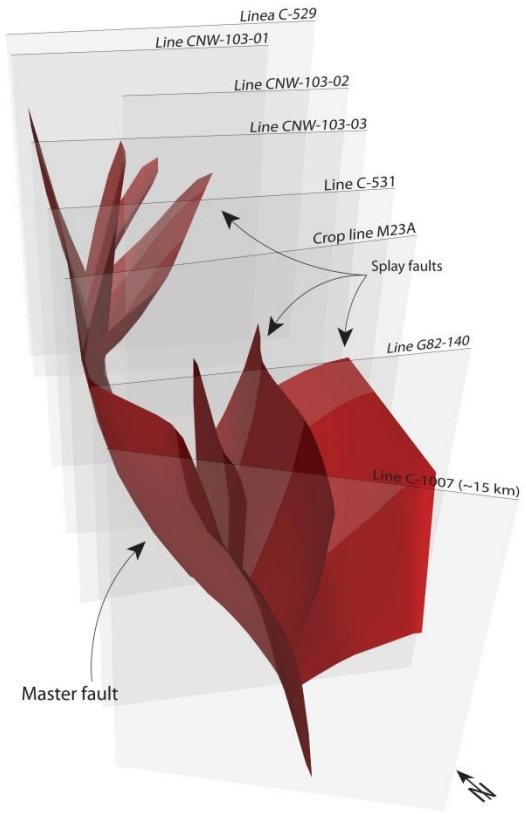

Fig. 2: 3D model of the Sciacca Fault (Fedorik et al., 2018)

Analyzing the seismic reflection profiles or more detailed chirp profiles (Lodolo et al., 2017), it is possible to highlight those faults or fault segments showing active tectonic evidence. Some of the faults belonging to the Sciacca Fault deform Quaternary deposits and cut the seafloor, especially in the area of the Nerita Bank and eastern side of the Terrible Bank. A structural map where recent and ongoing fault activity was detected was reconstructed. However, these kinds of reconstruction are necessarily dependent on the data (seismic reflection profiles) availability, quality and distribution/spacing.

To carry out a complete map where active faults (or active fault segments) are not limited to a restricted sector near the seismic reflection profiles, numerical models are needed in order to check and verify where strain is distributed. The digital 3D model of the Sciacca Fault has been used as input data in a Stress Analysis tool (Poly3D) to check the fault system response. According to available GPS and literature data, regional strain values were applied to the modelled fault system. The slip potential (fig. 3)on each fault and uplift pattern (fig. 4) was calculated. The numerical model outputs are in good agreement with the observations coming from the seismic

reflection profiles analysis and allow to constrain better and highlight which faults are most prone to be activated under the present day regional stress. The Sciacca Fault case study is a good example to test and verify how numerical models output fit with observed data and, at the same time, to constrain the seismic reflection profiles interpretation.

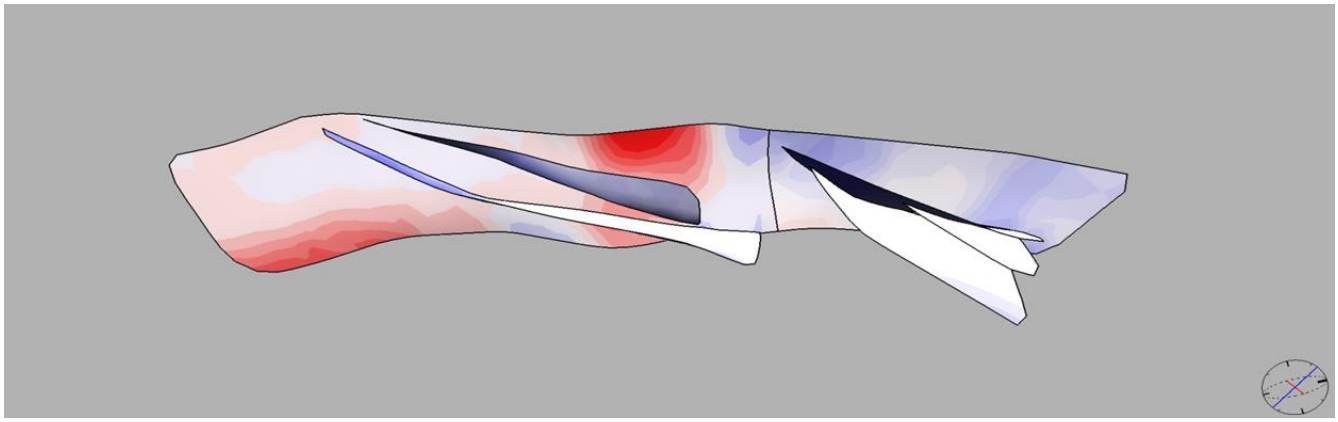

Fig. 3: a numerical model. On the main fault a slip tendency analysis was carried out in order to check where maximum slip is expected.

In a more general view, the case study once again highlights (i) the importance of 3D reconstructions that lead to well constrained geological reconstructions, (ii) the importance of a multidisciplinary approach using the best and most useful information coming from subsoil data, analogue and numerical models and (iii) how seismotectonic studies, in particular, can significantly be improved merging a different kind of data (seismicity, subsoil data, stress analysis, etc.).

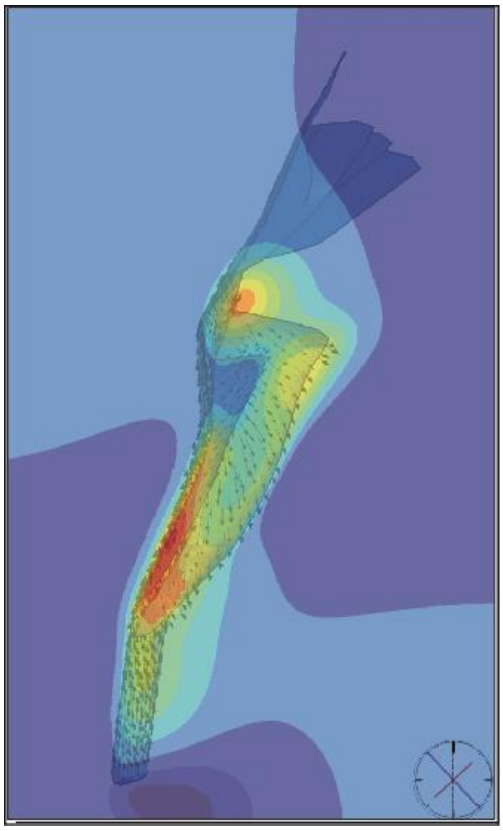

Figure 4: Uplift pattern along the Sciacca Fault obtained from tectonic loading applied at 148°. The northern segment of the Sciacca Fault is locked.

References

Calò M. and Parisi L.; 2014: *Evidences of a lithospheric fault zone in the Sicily Channel continental rift (southern Italy) from instrumental seismicity data*. Geophysical Journal International, **199 (1)**, art. no. ggu249, pp. 219-225. DOI: 10.1093/gji/ggu249

Civile D., Lodolo E., Tortorici L., Lanzafame and Brancolini, G.; 2008: *Relationships between magmatism and tectonics in a continental rift: The Pantelleria Island region (Sicily Channel, Italy)*. Marine Geology, **251**, 32-46.

Coltelli M., Cavallaro D., D'Anna G., D'Alessandro A., Grassa F., Mangano G., Patanè D. and Gresta S.; 2016: *Exploring the submarine graham bank in the sicily channel*. Annals of Geophysics, **59 (2)**, art. no. S0208,DOI: 10.4401/ag-6929

Lodolo E., Civile D., Zanolla C. and Geletti R.; 2012: *Magnetic signature of the Sicily Channel volcanism*. Marine Geophysical Research, **33 (1)**, 33-44. DOI: 10.1007/s11001-011-9144-y

Mantovani E., Viti M., Babbucci D., Tamburelli C., Cenni N., Baglione M. and D'Intinosante V.; 2014: *Generation of Back-Arc Basins as Side Effect of Shortening Processes: Examples from the Central Mediterranean.* International Journal of Geosciences, **5**, 1062-1079. doi: 10.4236/ijg.2014.510091.

Soumaya A., Ben Ayed N., Delvaux D. and Ghanmi M.; 2015: *Spatial variation of present-day stress field and tectonic regime in Tunisia and surroundings from formal inversion of focal mechanisms: Geodynamic implications for central Mediterranean. Tectonics*, **34**, 1154–1180, doi:10.1002/2015TC003895.

Lodolo E., Sanfilippo R., Rajola G., Canese S., Andaloro F., Montagna P., Rosso A., Macaluso D., DiGeronimo I., Caffaua M.; 2017: *The red coral deposits of the Graham Bank area: Constraints on the Holocene volcanic activity of the Sicilian Channel GeoResJ,* **13**, 126–133, https://doi.org/10.1016/j.grj.2017.04.003

4- Strike-slip dominated structural styles and its interaction with thrust belt structure.

A part of the PhD project was prepared with the collaboration of Prof. Guido Schreurs and Frank Zwaan (both from the University of Bern). The main reason for this collaboration and new analogue models was the lack of information of the internal structure within the strike-slip deformation. For this reason, the X-Ray Computed Tomography method was used to capture the internal development of the fault system during the model deformation. In Bern, we analyse the interaction between strike-slip dominated and thrust belt structures using the sandbox model. We compared pure strike-slipe, transpressional (10,20,30 degrees) and transtensional (10,20,30 degrees) models. The output of the research shows a significant change in the structural styles seen in the area of strike-slip deformation. We also propose a model for a formation of ,,splay faulting positioned on the one side of the primary fault", and lastly, the results bring some new inside in the understanding of geomechanics of Sicilian Channel and other natural examples.

4D analogue modelling of strike-slip dominated fault zones interacting with thrust belt structures

Jakub Fedorik[1]*, Frank Zwaan[2], Guido Schreurs[2], Giovanni Toscani[1], Lorenzo Bonini[3-4], Silvio Seno[1]

[1] *Dipartimento di Scienze della Terra e dell'Ambiente, Università di Pavia, Pavia, ITALY*

[2] *Institute of Geological Sciences, University of Bern, Bern, SWITZERLAND*

[3] *Dipartimento di Matematica e Geoscienze, Università di Trieste, ITALY*

[4] *INGV- Roma, ITALY*

***Corresponding author email**: *jakub.fedorik01@universitadipavia.it*

Abstract

The structural styles of strike-slip fault zones in the foreland of thrust belts are poorly understood. Here, we present scaled analogue models simulating the 4D evolution of strike-slip fault zones and their interaction with a thrust belt structure. An analysis of 7 different models setup applying pure

strike-slip, 10°-, 20°-, 30°-transtension and 10°-, 20°-, 30°-transpression kinematics shows important structural variations along the respective strike-slip fault zones. The experimental apparatus consists of a box with three independent rigid base plates. During the first phase of deformation, a thrust belt is created along the edge of a mobile plate that slides on top of two lower fixed plates inducing a first velocity discontinuity (VD1). In the second phase, a lower plate slides under the middle and upper plate that is now both fixed, creating the second velocity discontinuity (VD2). The shape of the fixed plates leads to the formation of a strike-slip dominated fault zone and simultaneous reactivation of the thrust front. The analogue models are analysed by X-Ray Computed Tomography (XRCT), providing a non-destructive visualisation of the internal structures during model evolution (4D analysis). Series of vertical sections and horizontal slices permit a full reconstruction of fault geometries. All transpressional models form pop-up structures along the strike-slip dominated fault zone, while the pure strike-slip model shows one sub-vertical fault only (above the VD2). The latter is bounded by two downward converging faults with different dip angles (37° and 52°). The 10˚-transtensional model develops a set of Riedel shear faults, which merge during the later stages of deformation along the fault tips above the VD2. The 20˚-transtensional model contains some Riedel shear faulting as well but is dominated by two faults with steep dip angles and some minor sub-vertical faults situated in between. This fault architecture is also observed in our 30˚-transtensional model. Our model results show resemblances with the fault geometries in natural settings, including the Sicilian Channel, the North Kuwait carbonate fields, Vienna Basin, Qaidam Basin and the Confidence Hills.

1- Introduction

Strike-slip motion is a fundamental tectonic process active around the world resulting in prominent surface expressions. In some areas strike-slip dominated fault zones are interacting with compressional structures. The Italian shoreline presents at least three examples where such interactions occur (Fig. 1). The Mattinata-Gondola fault zone (Di Bucci et al., 2007) in the northern end of the Calabrian arc is an example of oblique interaction, where strike-slip faulting occurs on both sides of the thrust front (Fig. 1a). The Vizzini-Scicli strike-slip fault zone, mapped in the Hyblean Plateau of Sicily (Di Bucci et al., 2010), is only observed in the thrust belt foreland (Fig. 1b). Fedorik et al. (2018) studied the offshore (foreland) part of the Sciacca Fault, an important strike-slip dominated fault zone observed on both sides of the Sicilian-Maghrebian thrust front (Fig. 1c). Their 3D Sciacca Fault model was obtained by seismic interpretation and was compared to analogue models in order to obtain the sense of strike-slip movement. However, it remains unclear whether the tectonic regime is dominated by pure strike-slip, transpressional or transtensional motion.

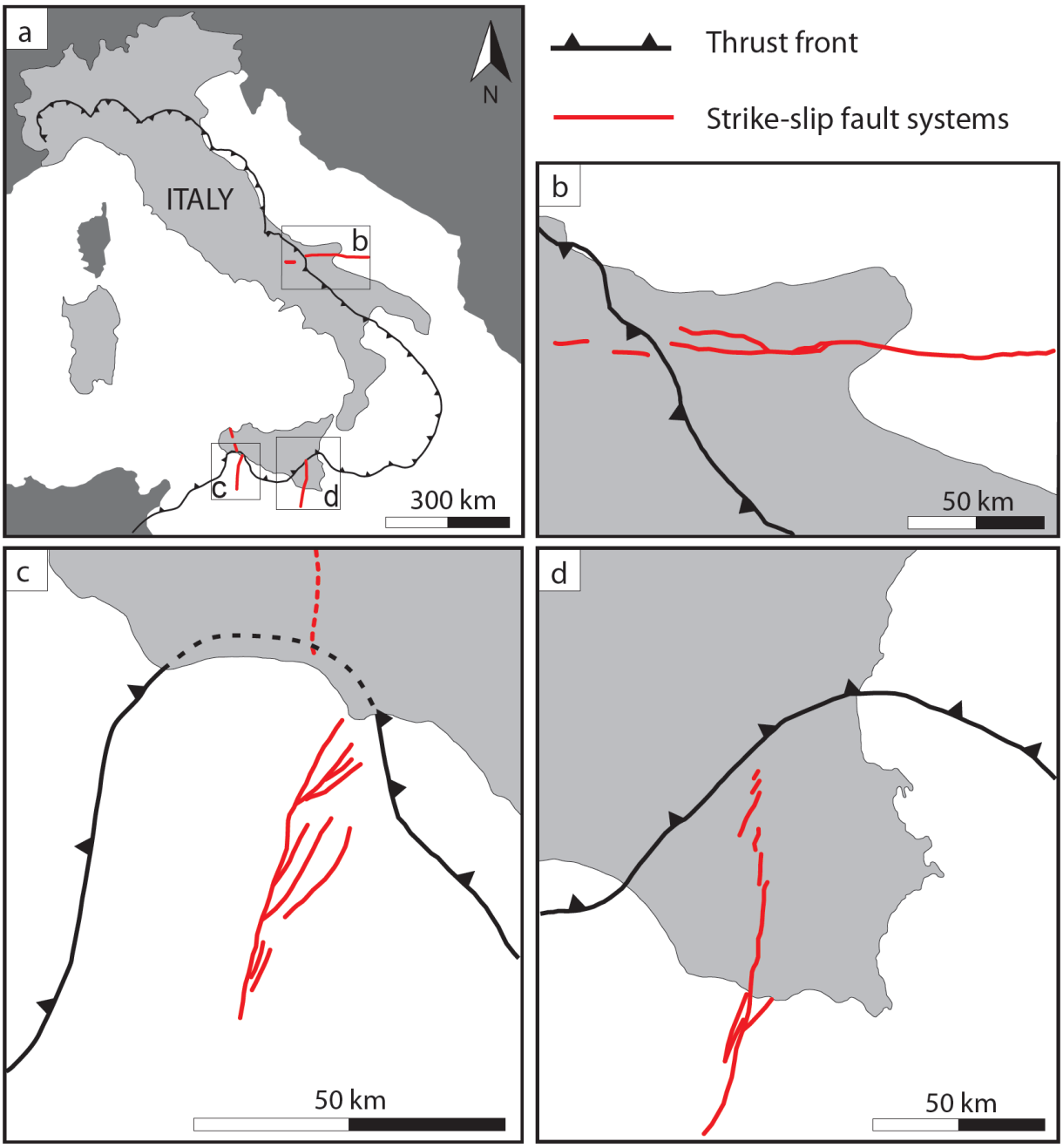

Figure 1: Examples of strike-slip dominated zones interacting with thrust belt structures in Italy. (a) Mattinata-Gondola shear zone (modified after Di Bucci et al., 2007). (b) Vizzini-Scicli shear zone (modified after Di Bucci et al., 2010). (c) Sciacca Fault (modified after Fedorik et al., 2018)

Analogue modelling studies have contributed significantly to our understanding of structures in strike-slip-dominated regimes (Dooley and Schreurs, 2012). Previous studies have simulated structures in setttings of pure strike-slip (e.g. Naylor et al., 1986; Mandl, 1988; Richard et al., 1995; Ueta et al., 2000; Xiao et al., 2017), transtension (e.g., Dooley et al., 2004; Smith et al., 2008; Wu et al., 2009) and transpression (e.g., Lowell, 1972; Casas et al., 2001; Leever et al., 2011; D' Adda et al., 2017). Seismic reflection profiles across regions that have undergone strike-slip dominated deformation are often difficult to interpret and reconstructing their structural evolution remains a

major challenge. Analogue modelling studies may help in constraining structural interpretations in such settings.

Here we present analogue models simulating strike-slip dominated fault zones interacting with thrust belt structures at a 90° angle. The 4D evolution of the models is analysed using X-Ray Computed Tomography (XRCT) which allows a detailed analysis of internal model structures with time (e.g. Colletta et al., 1991; Schreurs and Colletta, 1998; Schreurs et al., 2002, Zwaan et al., 2017; 2018). In total, we ran several models, in which pure strike-slip, 10°-, 20°- and 30°-transtensional, and 10°-, 20°- and 30°-transpressional tectonic regimes were simulated. Our specific model set-up provides different stress conditions along the limit of a fixed plate which simulates the strike-slip structure.

The analysis of model topography, CT sections and slices as well as 3D fault patterns are compared to well-described examples of pure strike-slip (eg.Tarim Basin: Cheng et al., 2017), transtensional (eg. Sicilian Channel: Fedorik et al., 2018; North Kuwait Carbonate Fields: Richard et al., 2014; Vienna Basin: Beidinger & Decker, 2011) and transpressional structures (eg. Confidence Hills: Dooley & McClay, 1996). Additionally, a model for formation of splay-primary faulting is discussed.

2- Experimental procedure

In order to model the interaction between strike-slip and thrust belt structures, our set-up consists of three different plates, which allow the simulation of two successive deformation phases (Fig. 2). Each of the three rigid plastic plates has a thickness of 1 mm. In the first phase, which is equal for all models, the uppermost plate is moved so that a thrust belt structure forms above its edge, where a first velocity discontinuity occurs (VD1). The total amount of displacement is equal to 3 cm. During the second phase, the lowermost plate moves and slides under both the fixed upper and middle plates. The latter has an L-shape geometry that allows simultaneous strike-slip and forethrust activation. The limit of the fixed plate along which strike-slip structures can be observed represents velocity discontinuity 2 (VD2). The third velocity discontinuity (VD3) is at the limit of the fixed plate, which is aligned with the limit of the upper moving plate. The VD3 assure the partial reactivation of pre-existing thrust belt structure and formation of new forethrusts. By applying different directions of movement to the lower plate, we simulate pure strike-slip, 10°-, 20°-, 30°-transpressional and 10°-, 20°-, 30°-transtensional tectonic regimes along the VD2. Total displacement during the second phase is 3.3 cm.

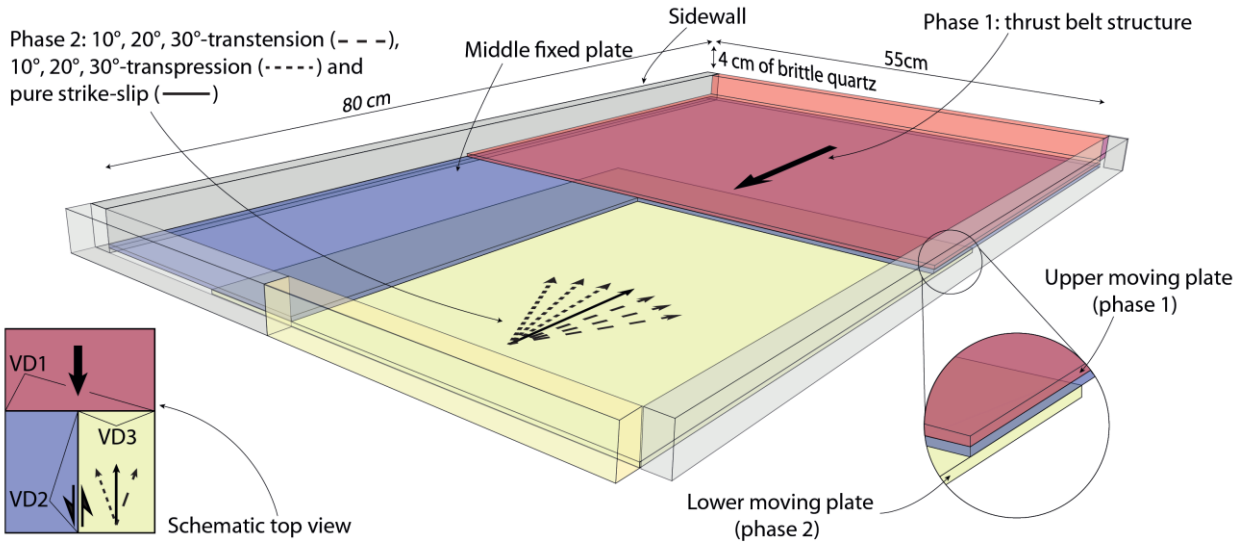

Figure 2: 3D and top view of base plate geometries, deformation directions and associated velocity discontinuities (VD) during the two deformation phases in our models

In each model, we use sand as it is a granular material generally applied for brittle upper crustal-scale modelling. The initial size of the model was approximately 80 x 55 x 4 cm. The model was confined on all sides by rigid walls and 4 cm thick layer of fine quartz sand (ø: 60 –250 µm, ρ: 1560 kg/m3) is sieved from ca. 30 cm height into the box. Granular materials typically show elastic-plastic, time-independent behaviour where increasing stress first results in strain-hardening, followed by failure at peak strength and a subsequent decrease in strength until the system reaches a state of dynamic, stable sliding (Lohrmann et al., 2003). Angles of peak- and stable friction are 36.1° and 31.4° for our quartz sand, with cohesion values in the order of several tens of Pa (Zwaan et al., 2016). The sand has a time-independent Mohr-Coulomb rheology, making it a suitable material to simulate upper crustal materials (e.g. McClay, 1990). The scaling of the model was set to a ratio of approximately 10-5, so that 1 cm in the model represents approximately 1 km in nature. Displacement of the moving plates, for both phases, occurred at a velocity of 10 cm/h. Top view images of the model surface were taken every 36 seconds - 1 mm increments and models were scanned with a 64 slice Siemens Somatom Definition AS X-ray CT-scanner at a 5-minute interval (every 0.83 cm of displacement).

We cut the 3D CT volumetric dataset (Fig. 3a) in three perpendicular directions and imported the data into Midland Valley's MOVE™ software for 3D structural analysis. Three horizontal slices taken at different depths (Fig. 3b) allow more accurate tracing of faults as surface effects (sand

fall, landslides, etc) are avoided. Vertical sections cut parallel and perpendicular to the VD1 at an interval of 3 cm (Fig. 3c) were added to the structural model. During the tracing of structures on sections and slices, the 3D volume was systematically checked to validate the interpretation. Fault auto tracking methods were not used as faults could not be extracted correctly in the high deformed areas (e.g. transtensional models). A digital elevation map (DEM) of the model surface (Fig. 3d) was obtained with DeVIDE open source software. Top view images of the model surface were referenced and plotted on the DEM. This data was especially useful for thrusts fault interpretation and reconstruction, as the traces of compressive faults were not as readily visible inside the model as the traces of faults formed during the second strike-slip dominated phase of deformation (Fig. 3e). The final 3D structural interpretation was obtained by interpolating the fault traces we digitised on horizontal and vertical sections. On the 3D fault geometries adaptive sampling was applied so that surface vertexes were homogeneously distributed permitting a homogenised size of surface faces (Fig. 3f). In total 27 3D structural interpretations were produced, each representing a time step during the second deformation phase (Table 1). For the pure strike-slip model we build only three 3D models as the scanned volume is not available for t = 5 min.

	Transpression 30°	Transpression 20°	Transpression 10°	Pure strike-slip	Transtension 10°	Transtension 20°	Transtension 30°
0.83 cm (5min)	X	X	X		X	X	X
1.66 cm (10 min)	X	X	X	X	X	X	X
2.5 cm (15 min)	X	X	X	X	X	X	X
3.33 cm (20 min)	X	X	X	X	X	X	X

Table 1: Overview of 3D structural interpretations derived from XRCT scans produced for this study, representing different deformation (time) steps during the second deformation phase, i.e along the VD2, when fore- and backthrust are formed yet.

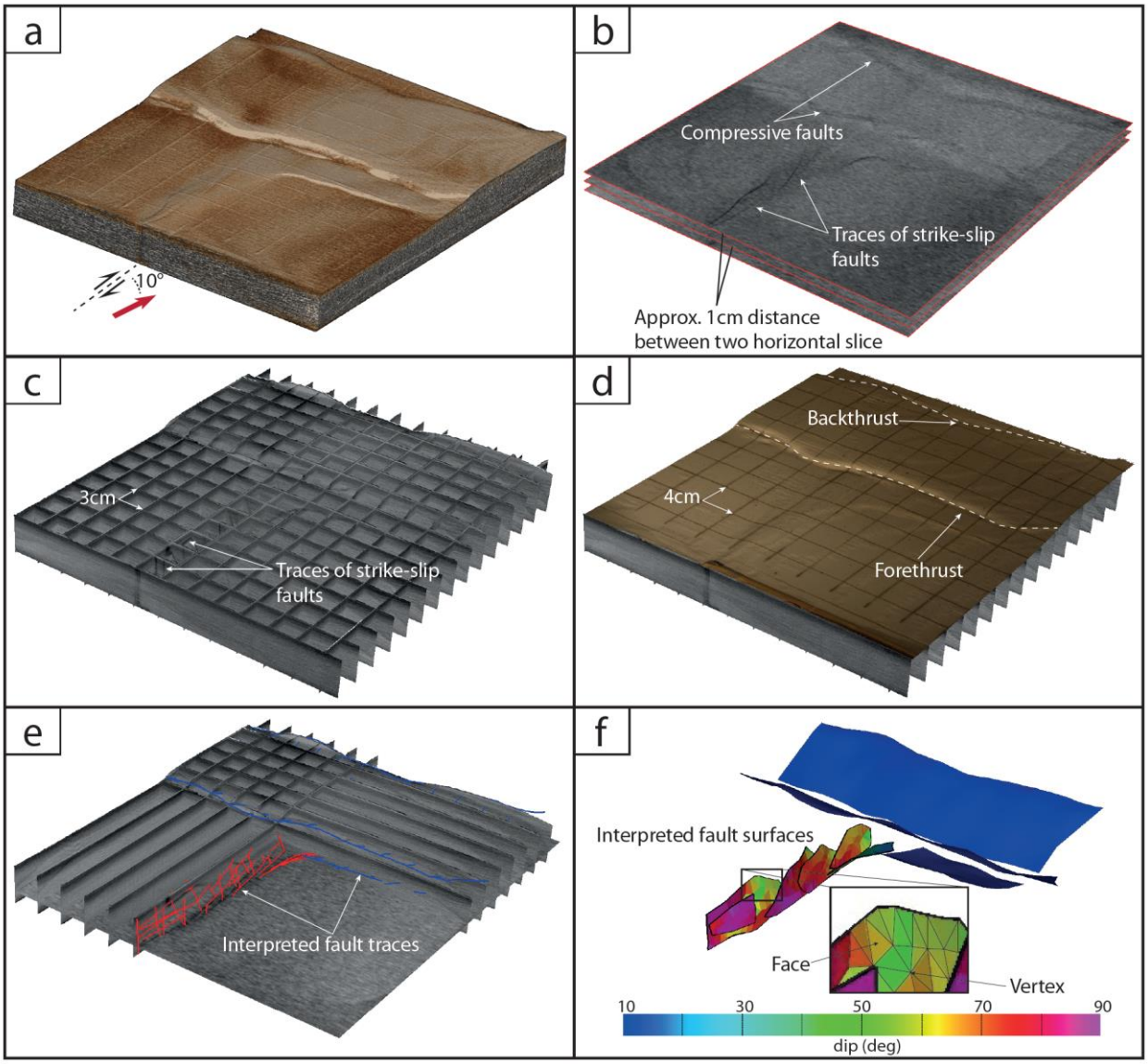

Figure 3: Analysis procedure. a) 3D volume rendering of a model; b) three CT-derived horizontal slices; c) grid of vertical sections; d) 3D model surface with georeferenced top view projected on it; e) several CT sections and one slice with the fault trace interpretation; f) final 3D fault surface interpretation.

3- Analogue modelling results

3.1 Plan view analysis

All models underwent a first identical phase of compression so that the same conjugate thrust system rooting at the velocity discontinuity develops in each model (Fig. 4). The second

deformation phase varies for each model as a function of the different tectonic regimes we tested (see Tab.1). Differences in the structural style are evident from top view images and the model's topography that formed during the second phase (Fig. 5). Transpressional models develop a central pop-up structure (positive relief) whose width decreases with decreasing obliquity (Fig. 5a-c). The pure strike-slip model experiment shows a similar, but narrower central pop-up structure, that is deformed in its central part by a single strike-slip fault (Fig. 5d). The transtensional models show even more concentrated deformation with increasing negative relief (graben formation), width and along-strike extent of the negative relief with increasing obliquity. It is worth noting that during its early stages of deformation, the 10°-transtensional model (Fig. 5e, 1.66 cm stage) develops a positive relief along the VD2. Subsequently, a small graben forms and widens in the distal area of the VD2 fault zone that was previously uplifted (Fig. 5e, 3.33 cm stage). In contrast, the more oblique 20°- (Fig. 5f) and 30°- (Fig. 5g) transtensional models display graben formation since the earliest stages of the second phase of deformation.

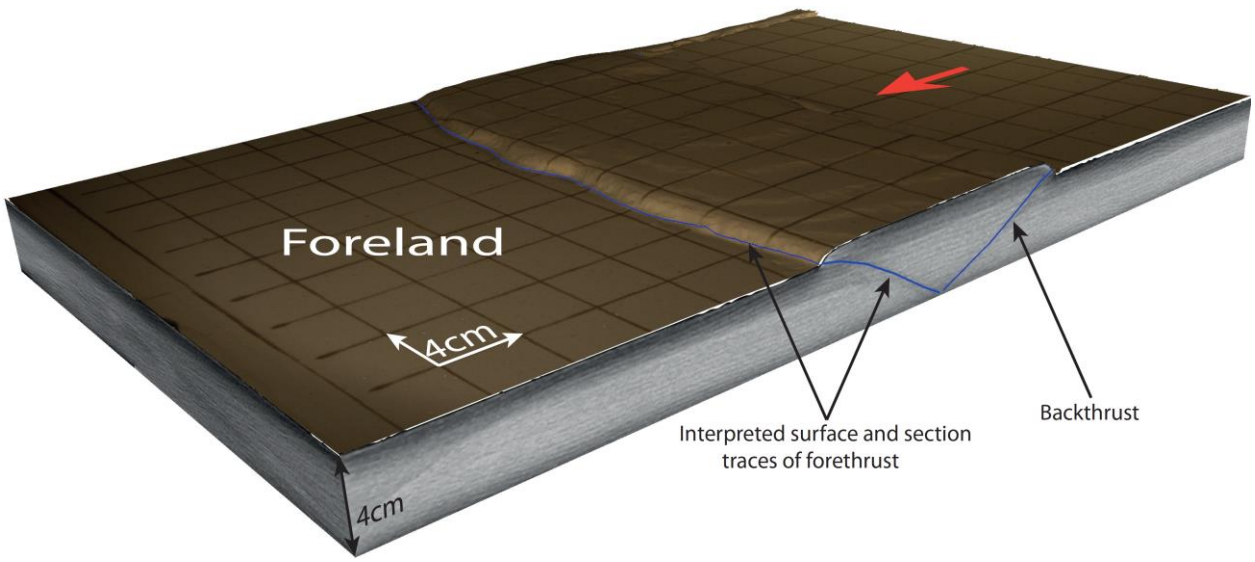

Figure 4: 3D view of the model after the first phase of the deformation. Red arrow show the direction of the displacement.

In all models, we observe re-activation of the pre-existing forethrust and the additional development of in-sequence thrust faulting along the VD3 as the right-hand part of the thrust is uplifted (Fig. 5, 3.33 cm stage). The similar linkage style between strike-slip faults and compressive-newly formed structures observed in top views and by topography analysis, implies that the same basic deformation mechanisms are active in pure strike-slip and transpressional

models, where the surface fault traces between the two fault systems form a ca. 90˚ angle (Fig. 5a-d). For transtensional models, the linkage between the two fault systems becomes more gradual, and the angle between the surface fault traces decreases with higher degrees of extension obliquity (Fig. 5e-f). Analysis of the view images also shows that the cross-cutting of the pre-existing or newly formed thrust fronts by the strike-slip dominated structures occurs earlier in pure strike-slip and transtensional models than in transtensional.

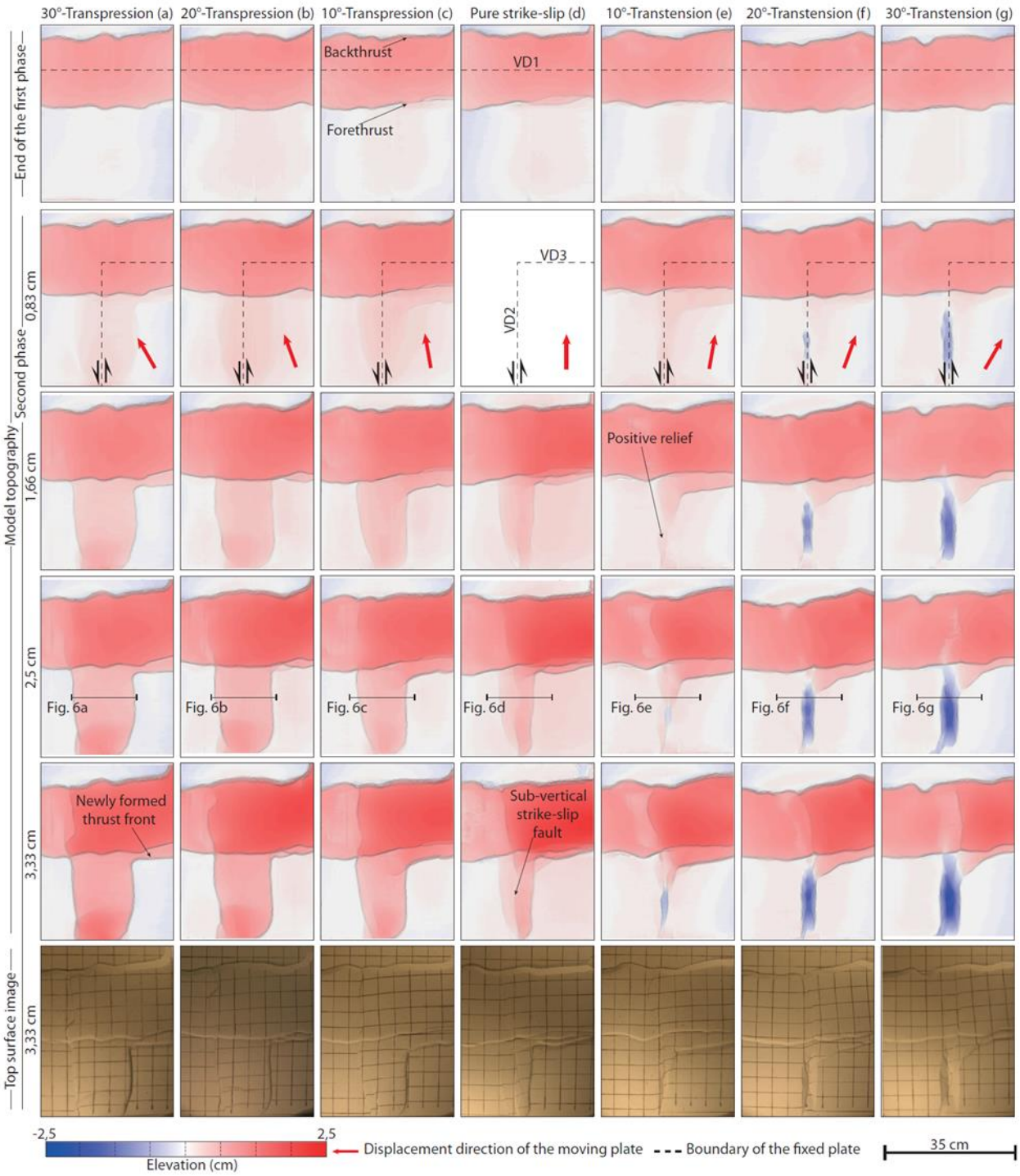

Figure 5: Top views depicting the topographic evolution of our models, calculated with DEMs derived from CT scans. The last row shows the top view images of the models after the final stage of the deformation (3,33 cm).

3.2 CT section analysis

Vertical sections perpendicular to the VD2 fault zones allow to better interpret and analyse structural features inside the sand pack (Fig. 6, left column). Geometrical properties (dip angle values of the surface faces of all faults except compressional structures) are plotted on histograms. Having observed that the dip angle values of thrust belt (first phase of deformation) and newly formed thrust fronts are approximately 30° for all models, they are not included in the histograms Every histogram (Fig. 6, right column) refers to the main faults above VD2, whose general attitude is shown by a cross section (see Fig. 5 for location). Figure 6 provides a general and synoptic view of how fault dips vary in accordance with the different tectonic regimes. A discrepancy of fault dip values observed in histograms is due to the areas where the strike-slip fault is linking with the newly formed thrust front; where the strike-slip fault are interacting; or reaching the top surface of the model where the dip decreases.

Cross-sections of transpressional models (Fig. 6a-c) show a pop-up structure. It is quite evident from the cross sections that the fault dip angle decreases with increasing angle of transpression. Dip angle analysis shows that the most frequent dip angle values for the 10˚-, 20˚- and 30°-transpressional models are 34°, 33°, and 26°, respectively, typical for reverse slip and the pop-up development observed in these models (Fig. 6a-c).

As in the transpressional models, the pure strike-slip (Fig. 6d) model contains a pop-up structure visible in cross-section, but both faults have a steeper dip and a sub-vertical strike-slip fault occurs in between. This is expressed in the histogram by three fault dip frequency spikes. The fault on the side of the moving plate (right-hand side of the cross-section) shows a higher dip angle value (52°) than the reverse fault situated on the side (left) of the fixed plate (37°).

Transtensional models (Fig. 6e-g) are characterised by faults with steep dip angles. However, the model simulating a 10°-transtensional regime (Fig. 6e), the most similar to the strike-slip one, shows a wider dip angle range (40°-90°). The 20°- and 30°-transtensional models contain several

sub-vertical faults with dip angles ranging between 70°-90° and 75°-90°, respectively (Fig. 6f, g). The 10°-transtensional model shows some faults with a reverse slip component at the location of the CT section, creating a positive vertical relief (Fig. 6e). In contrast, the steep faults in the 20°- and 30°-transtensional models have a normal dip-slip component, resulting in the development of a depression.

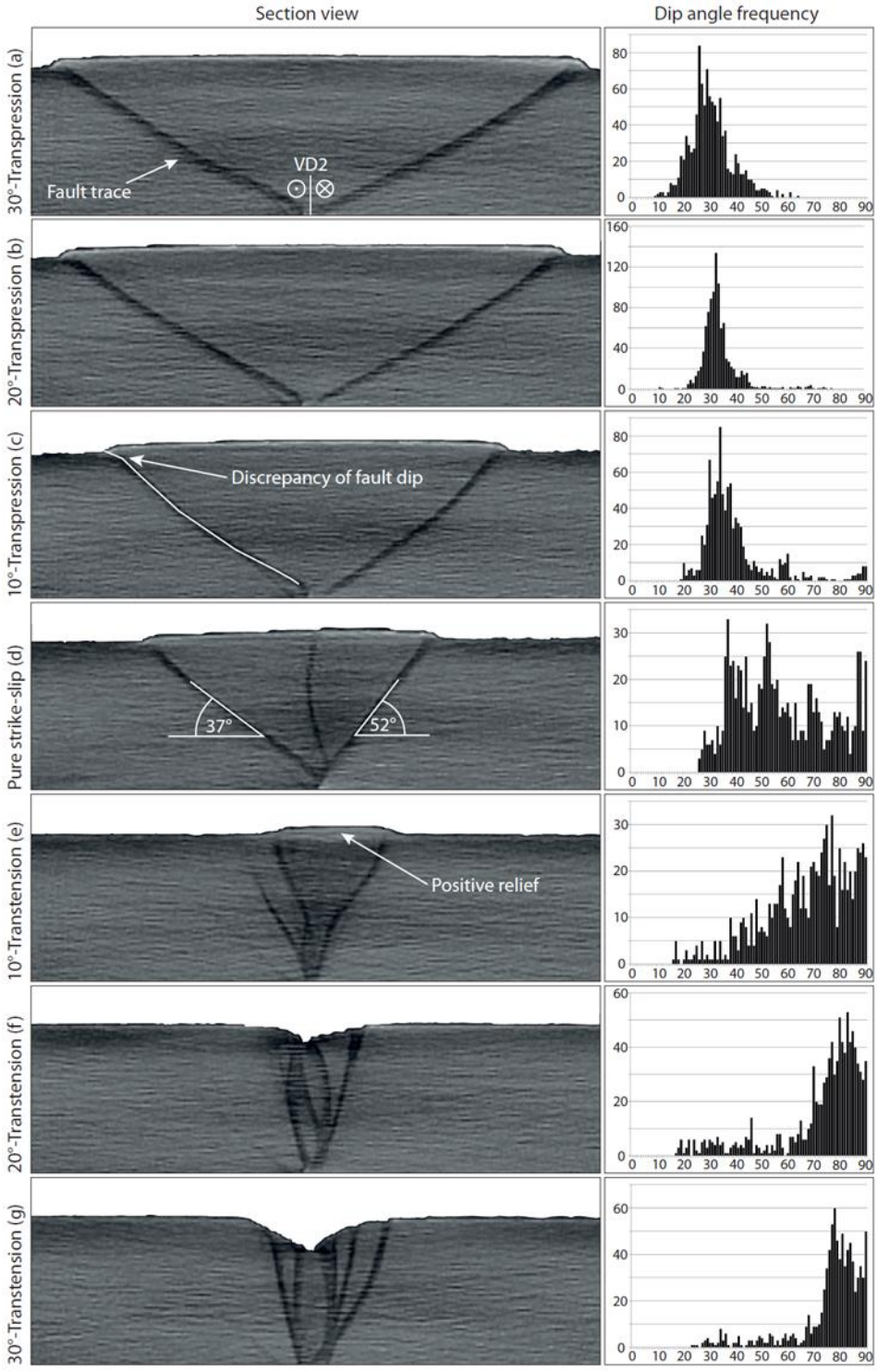

Figure 6: Left side: section views of all models obtained within the same distance from the backstop wall and same amount of displacement (1,66cm). Right side: histograms with geometrical properties- dip angle values of the surface faces of all strike-slip dominated faults.

3.3 3D fault geometries

The interpretation of cross sections and horizontal slices allows the reconstruction and digitisation of 3D fault geometries at different time steps, thus allowing a 4D analysis of our models. Figures 7 and 8 show the 3D fault reconstruction of all models during the second deformation phase at 5-minute intervals equivalent to 0.83 cm displacement increments.

The fault system occurring in the pure strike-slip model (Figs. 7a, Fig. 8a) contains two conjugate faults, but in addition a well-developed subvertical central fault occurs, positioned above the VD2. Of the three mainly strike-slip faults with some dip-slip component, the central one is the only fault crosscutting the pre-existing forethrust (Figs. 7a, 8a). This central fault is subvertical along the VD2, but its dip rapidly decreases to less than 40° between the fore- and backthrusts. The dip-slip component of the fault increase in this area.

All transpressional models show similar fault complexity initiating during the very early stages of model phase 2 as two main oblique-slip reverse faults form a pop-up structure rooting at the limit between the fixed and moving plate (VD2). During progressive deformation, the fault situated on the side of the fixed plate cuts and displaces the forethrust and terminates against the backthrust of the thrust belt created during the first deformation phase, in addition, the fault segment inside of the thrust belt show mostly reverse dip-slip component. These are a common features observed in all transpressional models (Fig. 7b-d). However, the forethrust is cut at about the same moment in models with 10° and 20° transpression, while it occurs at an earlier stage for the 30°-transpressional model (Fig. 7b-d, 1.66 and 2.5 cm stages). In contrast, the fault above the moving plate never displaces the pre-existing forethrust in any transpressional model (Fig. 7b-d). This can be explained considering the peculiar kinematics of these models. The moving plate always induces a compressive stress in front of the pre-existing forethrust (VD3). This is evident from the structures forming above the moving plate in all models (Fig. 7): a new thrust fault develops above the moving plate only, striking parallel to the previously existing one. This new thrust forms more or less at the same time as the oblique-slip reverse fault above the moving

plate (Fig. 7b-d, 0.83 cm stage). In the late stages of deformation, this fault and the newly formed thrust fault are well developed and link up, thus preventing the cutting of the pre-existing forethrust (Fig. 7b-d, 3.33 stage). During the latest stage of deformation in the 10°-transpressional model (20 min or 3.33 cm, Fig. 7b) a small sub-vertical fault occurs above VD2, which is not observed in other transpressional models.

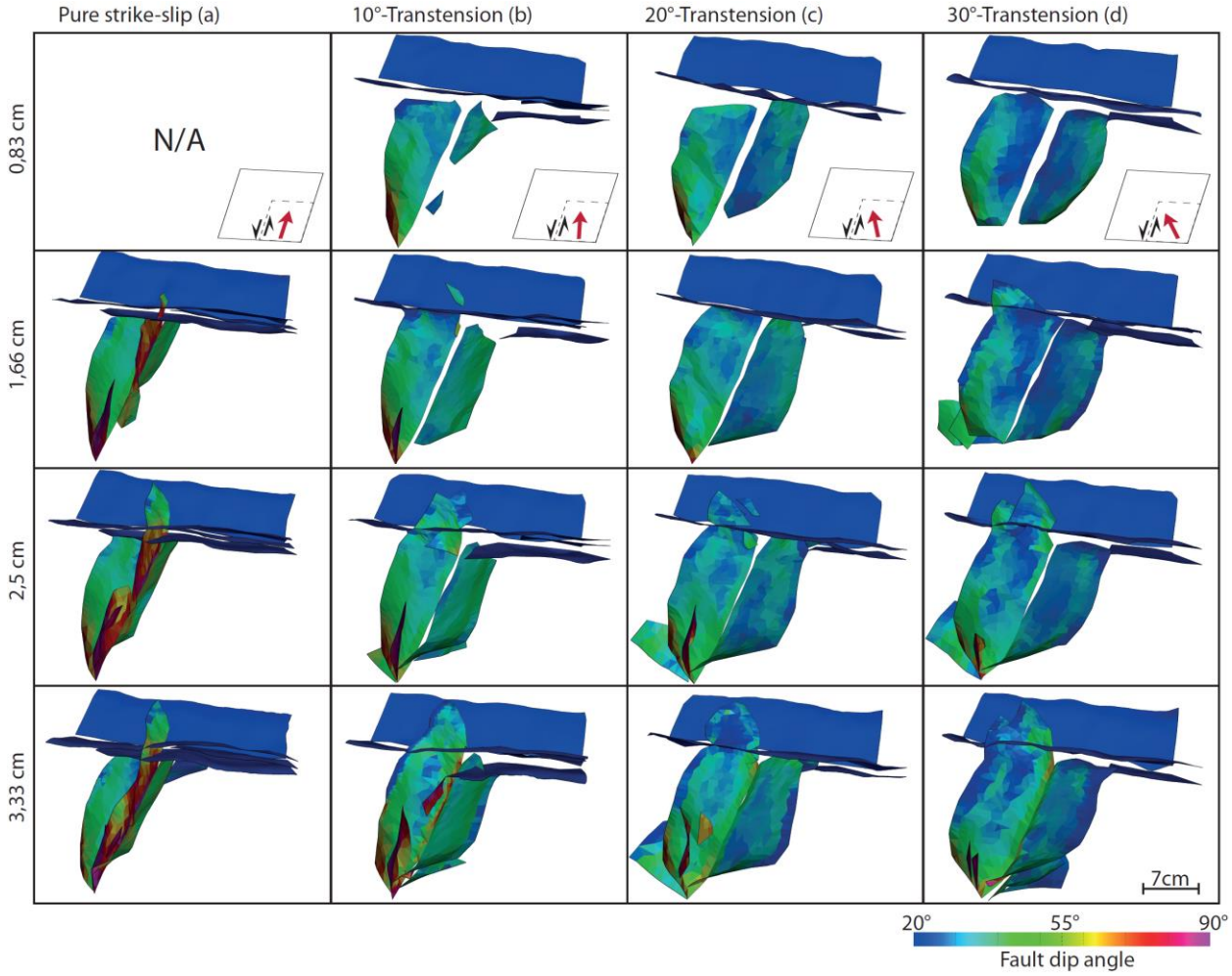

Figure 7: 3D interpretation of fault geometries in the pure strike-slip fault model (3 steps of deformation) and the transpressional models (4 steps of deformation for each model). All faults except thrust belt and newly formed thrust fronts are plotted with the dip angle values.

The transtensional experiments develop the highest fault system complexity and important differences between the 10°, 20° and 30° models can be observed (Fig. 8b-d). All faults along the VD2 have dip angles within the range of 50° to 90° (Fig. 6e-g). The 10°-transtensional model contains one highly dipping (~70°) strike-slip dominated fault with a reverse dip-slip component

along with several Riedel shear faults situated above the fixed plate and in between a subvertical strike-slip dominated fault above the VD2 (Fig. 8b). The latter fault is the only one crosscutting the pre-existing forethrust and shows similar geometry and kinematics to the central fault in the pure strike-slip model (Fig. 8a, b, 3.33 cm stage). In the 20˚-transtensional model, some Riedel shear faults develop close to the thrust front, whereas two steep strike-slip dominated faults with a normal dip-slip component mark the edge of a graben system along the VD2 containing internal sub-vertical strike-slip faults (Fig. 8c). The VD2 fault system in the 30°-transtensional model (Fig. 8d) is also bordered by two steep strike-slip dominated faults with a normal dip-slip component. Between these two faults, several sub-vertical strike-slip faults occur, while faults between the fore- and backthrust show an important decrease of dip angle with reverse dip-slip component (similarly to pure strike-slip models).

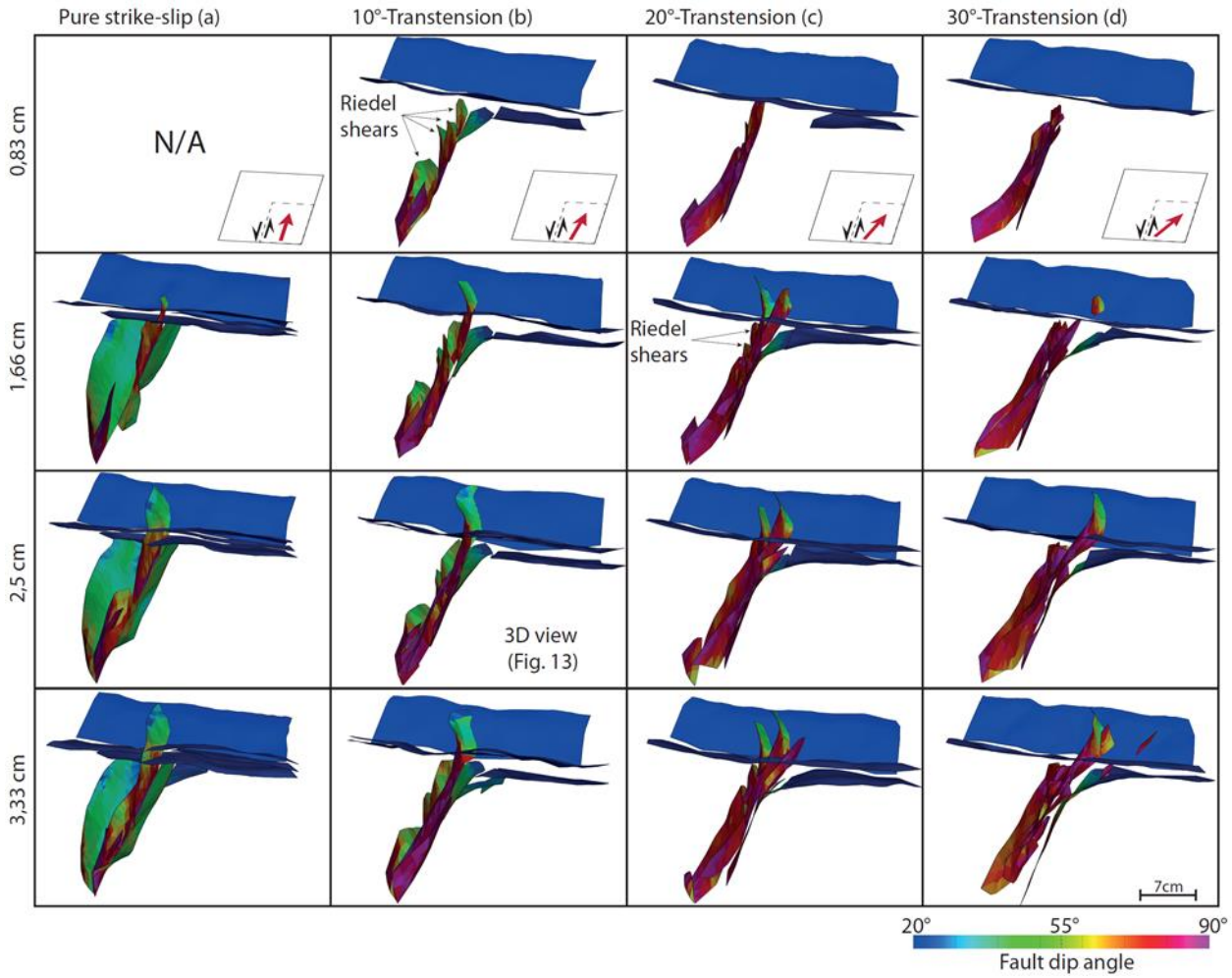

Figure 8: 3D interpretation of fault geometries in the pure strike-slip fault model (3 steps of deformation) and the transtensional models (4 steps of deformation for each model). All faults except thrust belt and newly formed thrust fronts are plotted with the dip angle values.

3.4 3D fault geometries and horizontal slices – transpressional models

The CT data allow a map-view analysis of a model's internal fault systems at different timesteps so that we can assess the evolution of faults on slices at various depths in the sand pack. As mentioned earlier, the three transpressional models show similar structural styles. The horizontal slices presented in Fig. 9 illustrate the structural evolution of our 20°-transpressional model, which we selected as representative of transpressional and strike-slip models. The slices in this picture are taken at the half height of the sand-pack, i.e. at 2 cm above the fixed middle plate. The first slice, taken after 5 min or 0.83 cm of deformation (Fig. 9a), shows two primary parallel-oriented oblique-slip reverse faults. The fault situated above the moving plate (right-hand side) reaches the pre-existing thrust front earlier than the fault located above the fixed plate (left-hand side). After 1.66 cm of deformation, both faults reach the thrust front (Fig. 9b). At the 2.5 cm stage, the fault above the fixed plate splits in two faults, which crosscut and deform the sand volume between fore and backthrust (Fig. 9c), while the fault above the moving plate connects with a newly formed forethrust (developed in front of the pre-existing pop-up structure) (Fig. 9c). The last stage of deformation highlights how only the oblique-slip reverse faults above the fixed plate crosscut the pre-existing forethrust (Fig. 9d and 9d').

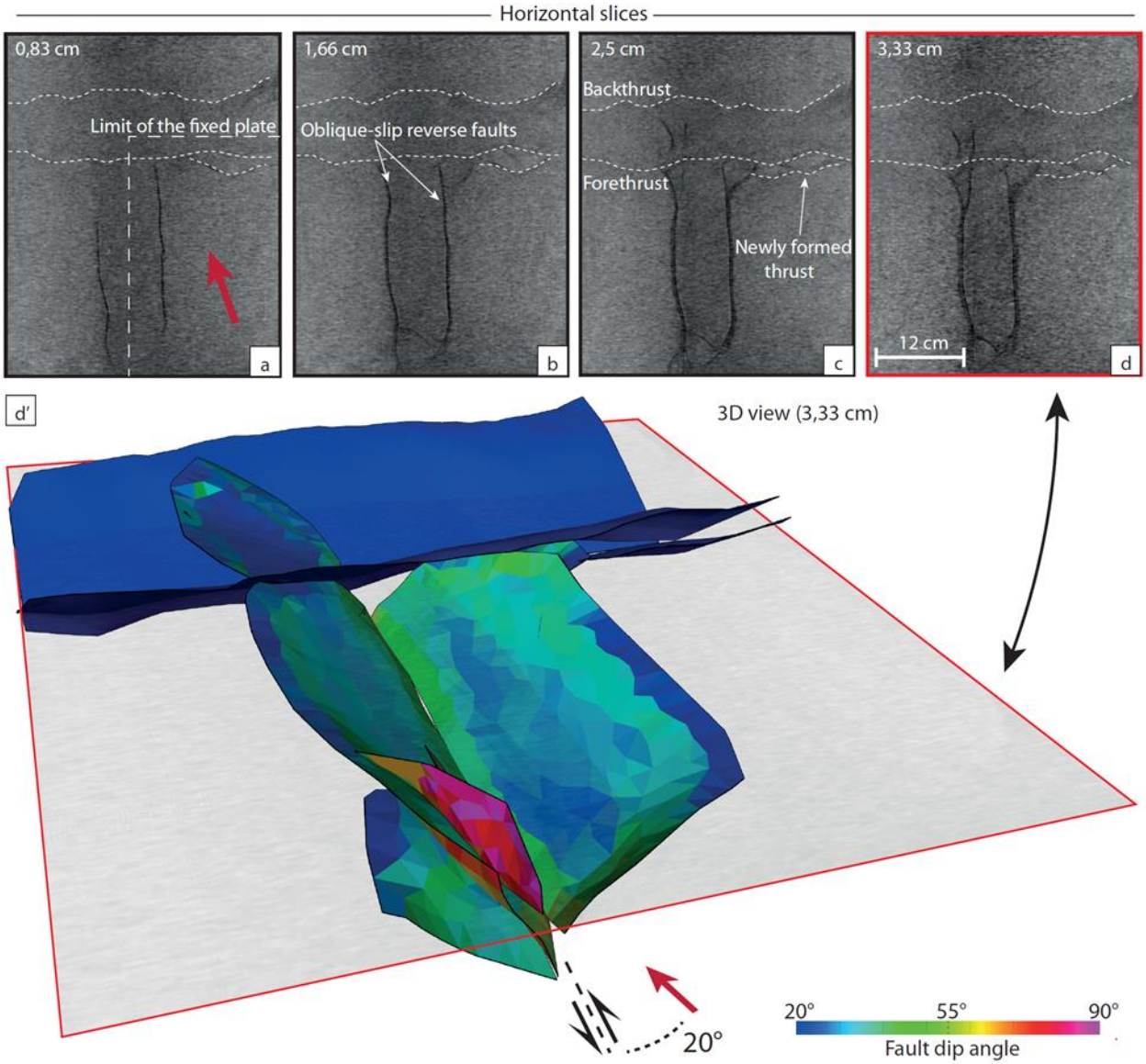

Figure 9: The evolution of the 20°-transpressional model illustrated by four horizontal slices (extracted at the same location) and 3D view of the last step of the second deformation phase.

3.5 3D fault geometries and horizontal slices - transtensional models

In the 10°-transtensional model (Fig. 10) initial Riedel shears occur after 0.83 cm of displacement (Fig. 10a and 10a'). At the level of the horizontal slice, these faults do not seem to be connected and are located on the side of the fixed plate only. Due to the convergence between the moving plate and the fixed one, a newly formed thrust, parallel to the forethrust, takes place. After 1.66 cm of deformation, the Riedel shear fault tips positioned above the VD2 merge creating a primary strike-slip fault (Fig. 10b). This fault clearly displaces the forethrust of the pre-existing pop-up structure. In the following deformation step (2.5 cm of displacement, Fig. 10c) another well-

developed strike-slip fault located above the VD2 is visible on the horizontal slices, and the newly formed thrust continues its development above the moving plate, parallel to the pre-existing forethrust. The last stage (3.33 cm of displacement) also shows the linkage between the newly formed thrust fault (striking parallel to the pre-existing pop-up) and the strike-slip dominated zone (Fig. 10d and 10d').

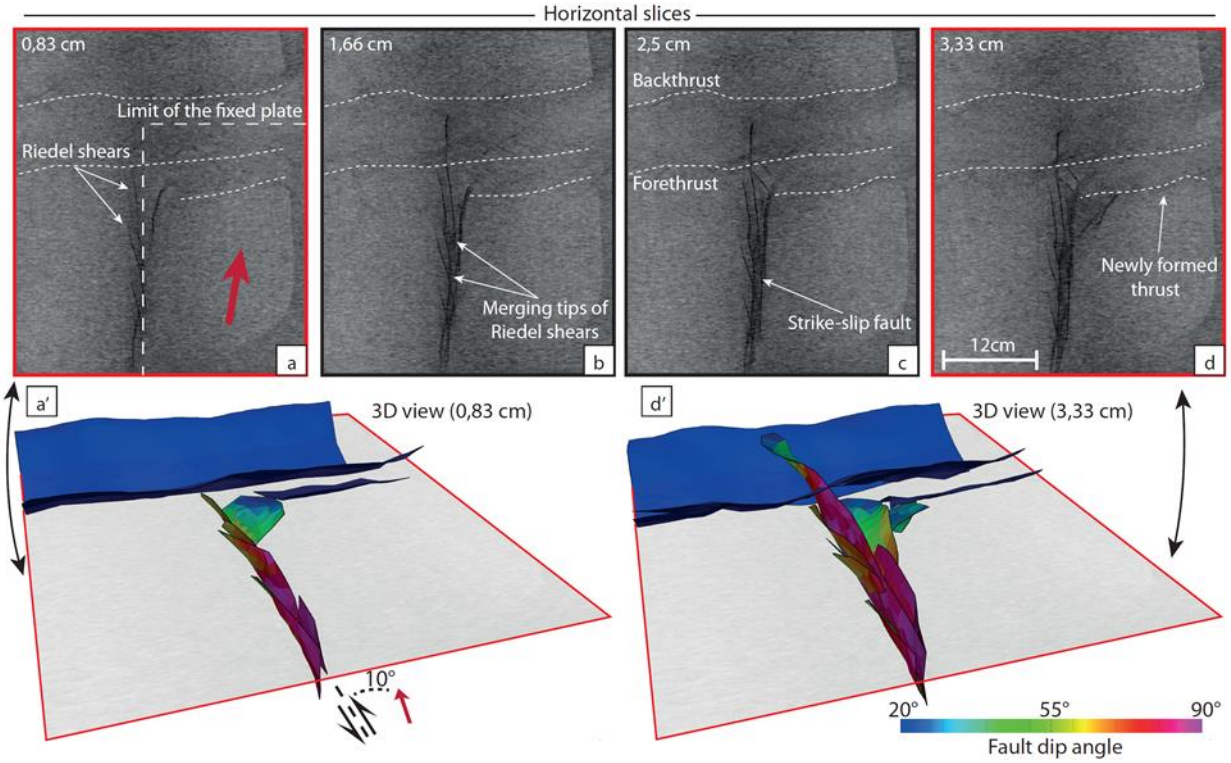

Figure 10: The evolution of the 10°-transtensional model illustrated by four horizontal slices (extracted at the same location) and 3D views of the first and the last steps of the second deformation phase.

In fig. 11 four horizontal slices of the 20°-transtensional model at different deformation stages are shown. At 0.83 cm of displacement, similar Riedel shears as in the 10°-transtensional model can be observed (Fig. 11a and 11a'). These structures are present only in the area close to the forethrust and link up with the two major steep strike-slip dominated faults (with a dip-slip component) running parallel to the VD2. In the following deformation step (at 1.66 cm of displacement) one of the steep strike-slip dominated faults positioned above the VD2 propagates towards the forethrust trace, branching into two separate fault splays that both crosscut the forethrust. The fault patterns at 2.5 and 3.33 cm of displacement (Fig. 11c and 11d) illustrate how these two

splays, that never crosscut the backthrust, evolve. Simultaneously, a secondary thrust in front of the main forethrust continues its development, as well as the several minor faults between the major steep strike-slip faults along the VD2. The last stage of deformation also shows the new linkage between the two fault systems (Fig. 11d, and 11d').

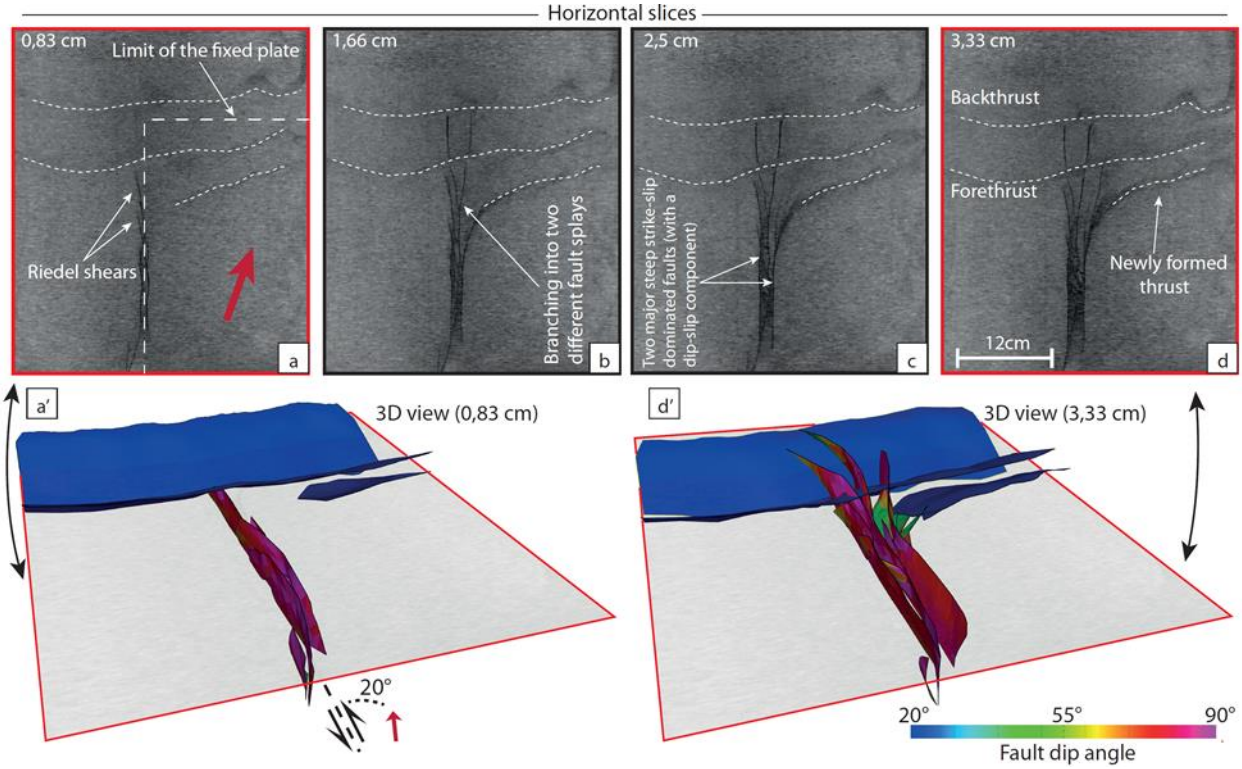

Figure 11: The evolution of the 20°-transtensional model illustrated by four horizontal slices (extracted at the same location) and 3D views of the first and the last steps of the second deformation phase.

The model simulating transtension with 30° obliquity is presented in figure 12. The first 3D fault pattern and slice image (after 0.83 cm of displacement) show two. The following intervals (slices after 1.66 and 2.5 cm of displacement, Fig.12b and 12c) highlight the propagation of a sub-vertical strike-slip fault which crosscuts the forethrust. Also some sub-vertical faults develop in the last deformation stages (Fig. 12d and 12d'). The newly formed thrust front continues its activity, and the 3D view (Fig. 12d') of fault pattern reveals two new strike-slip faults appearing in the area between fore- and backthrust.

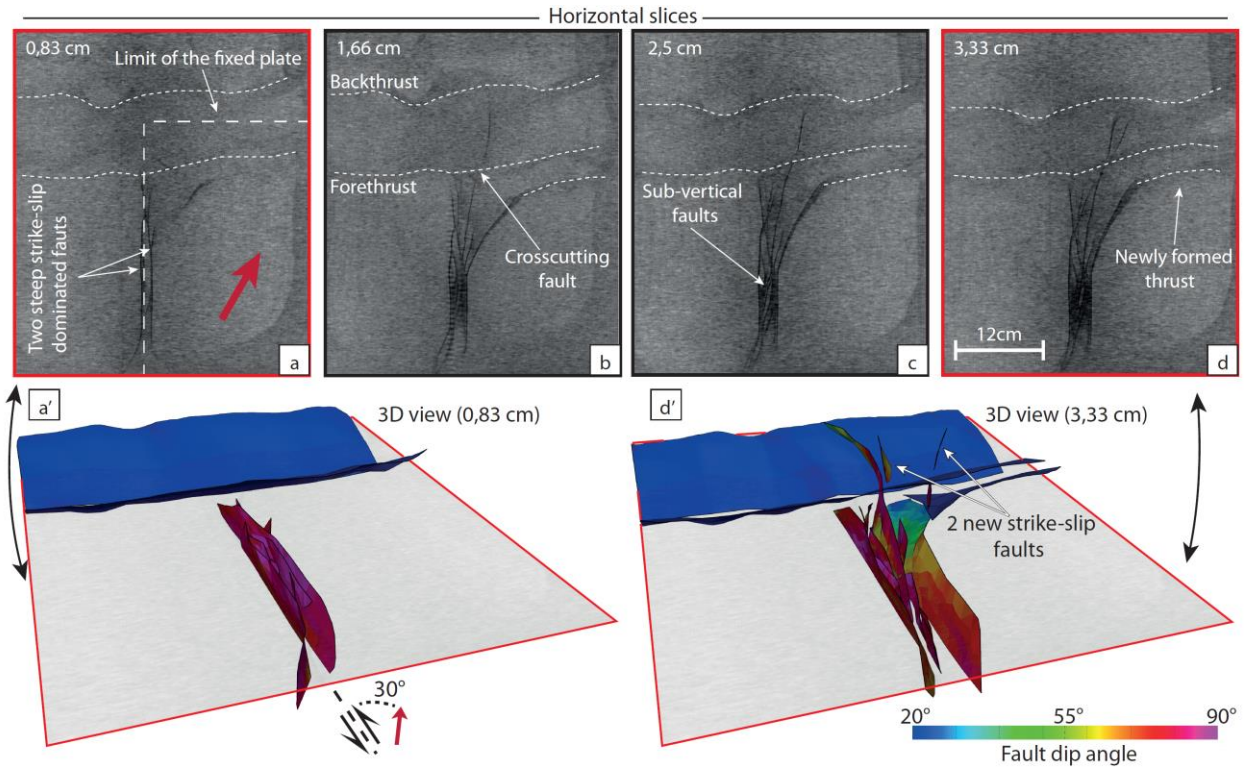

Figure 12: The evolution of the 30°-transtensional model illustrated by four horizontal slices (extracted at the same location) and 3D views of the first and the last steps of the second deformation phase.

Increasing the obliquity in transtensional models causes an important change of structural styles accommodating deformation. The less oblique model (10° transtension, Fig. 9) develops several Riedel shears (splay faults) connected by one primary fault. The 20°-transtension model identically develops some Riedel shears, but the main part of deformation in the foreland is accommodated by two steep strike-slip dominated fault system (with normal dip-slip components along the main boundary faults), containing some minor steep faults situated in between. The most oblique model (30° of transtension) shows a wider shear zone all along the VD2. In all transtensional models, the pre-existing fore-thrust is crosscut by strike-slip faults.

4- Discussion

A comparison of pure strike-slip, transpressional and transtensional fault geometries

Transpressional models (Fig. 7) all show similar structural styles and fault pattern, developing two oblique-slip reverse faults between which a pop-up forms (Fig. 5a, b, c and 6a, b, c). Comparable structures have been observed in clay models (Lowell, 1972; Wilcox et al., 1973) and sand models of transpression (Leever et al., 2011; D'Adda et al., 2017). However, our transpressional models do not develop any Riedel shears as seen in previous pure strike-slip and 15°-transpressional models by Casas et al. (2001) or Di Bucci et al., 2007. These differences are considered to be related to differences in the model setup: in almost all previous studies the basal plate boundary is straight, while our model set-up is designed to simultaneously produce strike-slip and compressive structures. This particular set-up imposes a general compression within the sand-pack situated above the moving plate, which may explain the absence of Riedel shears that should otherwise occur in pure strike-slip and transpressional settings. Differently, as expected for transpressional tectonic systems, our models develop pop-up structures bounded by oblique-slip reverse faults, whose dip angle increases with decreasing transpressional obliquity (Fig. 6a-d). The absence of sub-vertical strike-slip faults in transpressional models, might be explained by high compressional component in a direction parallel to thrust belt structure. This is produced by transpressional kinematics itself and as a secondary effect of compression along the VD3. More compression is built from transpressional kinematics, smaller dip angle of the two downward converging oblique-slip reverse faults is observed.

Transtensional models show a complicated and variable fault system (Fig. 6d-f). The most deformed area above the VD2 is only a few centimetres wide, but several sub-vertical faults develop and interact during deformation. Fault traces on the model surface do not provide sufficient information about the 3D complexity of the fault system, however, the angle between strike-slip dominated faults and newly formed thrust faults in front of the pre-existing fore, and backthrust decreases with the higher angle of obliquity of transtensional models (Fig. 6e-f). The angle variation is probably produced to accommodate more efficiently the lateral displacement (along the VD3) of the moving plate.

CT images are an important asset to describe and reconstruct these fault systems allowing visualisation of sections or construction of 3D fault patterns at depth. The 3D fault pattern of the transtensional models shows the evolution from a splay-primary faults mechanism seen within the 10-transtensional model to two highly dipping conjugate oblique-normal faults bounding several minor sub-vertical faults system observed in the 30°-transtensional model. The 20°-transtensional model shows some splay faulting as well, however, the strike-slip dominated area is deformed mostly with the fault system seen in the 30°-transtensional model. Furthermore, the model

topography data clearly illustrates the difference between the 10°-transtensional and the 20°- and 30°-transtensional models (Fig. 5e-g). The latter two models develop an expected negative relief change along the VD2, while the 10°-transtensional model produces a positive relief in the area close to the thrust belt. The unexpected occurrence of this positive relief and positive flower structures in transtensional tectonic regimes is related to our particular model set-up, which creates different stress conditions along the VD2.

Splay faults

In Scholz et al. (2010), the authors describe and explain the asymmetry of splay faults and show several natural cases where fault splays are present only on one side of the primary fault (e.g. the Alpine Fault in New Zealand, the San Andreas Fault in California and the Denali Fault in Alaska). Analogue models by Fedorik et al. (2018) with a clay set-up show similar results, where splay faults only develop on one side of the primary fault within pure strike-slip, 10°-transpressional and 10°-transtensional models. Similarly, splay faults occur within our transtensional models (10° and partially for 20° obliquity) carried out using quartz sand only. Our 4D model analysis of 10°-transtensional shows that Riedel shear faults form in the early stages of deformation above the fixed plate only (fig. 13). When deformation increases, the fault tips above the VD2 merge creating a primary strike-slip fault. We do not observe any new splay fault after the primary fault is formed.

We suggest that the observed asymmetry of splay faults (always and only in the area of the fixed plate) is due to more favourable stress conditions as the area of the moving plate is, in fact, always under compression due to its movement toward the pre-existing forethrust. Xiao et al. (2017) present a model with equal stress conditions on the two sides of the velocity discontinuity, and their results show equally distributed Riedel shear faults on both sides of the plate boundary. In their models, the primary fault crosscuts Riedel shear faults in the late stages of deformation in their central area. This “ideal” stress condition equally distributed on both side of the plate boundary is not present in our models where the different plate shape and pre-existing structures produce a stress re-organisation and more asymmetric/complex structures.

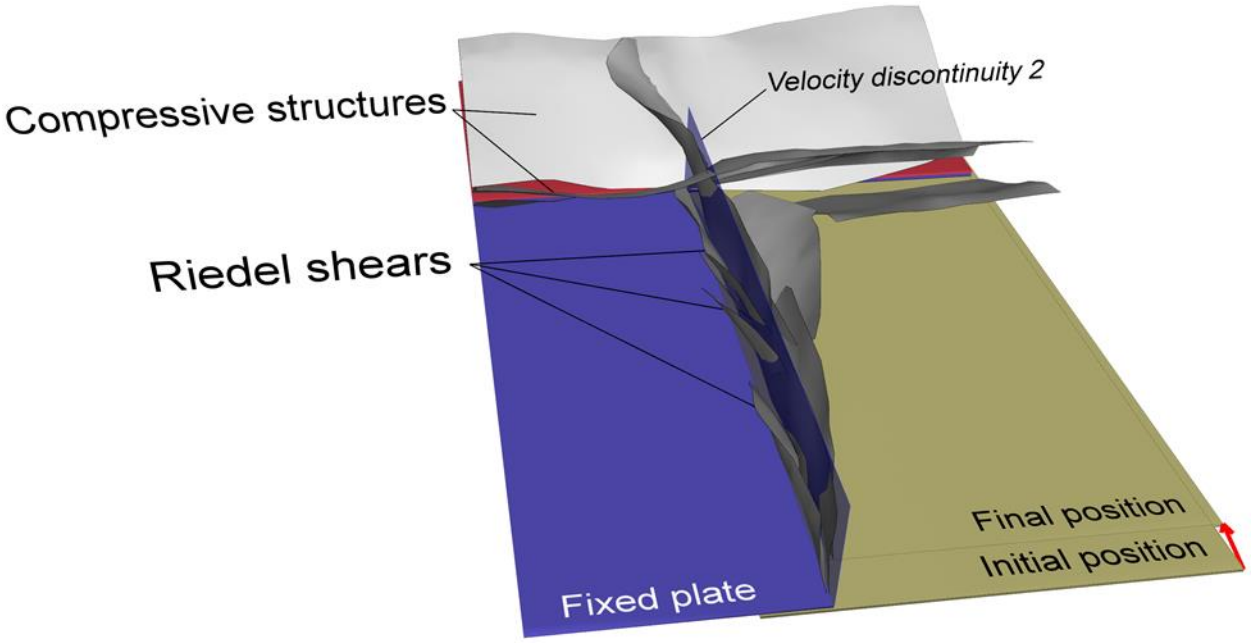

Figure 13: 3D pdf figure of transtensional 10° model (after 10min/1,66 cm of displacement) with the base plate and fault geometries. This figure can be rotated with Adobe Reader or other adapted pdf reader.

Comparison with natural examples

Our models results can be of help for the interpretation and reconstruction of interacting compressional and strike-slip dominated structures, and to analyse the associated kinematics. However, presented natural cases intend to be compared to structural styles seen only in the area of our models which are dominated by strike-slip tectonics, more precisely along the VD2.

With our modelling results, we now have better constraints on which tectonic mechanism may have produced the Sciacca Fault in the Sicilian Channel, where several splay faults connect to a primary strike-slip fault (Fig. 14a).These splay faults are localizsed on one side only of the primary fault. In addition, positive flower structures are observed on seismic lines crossing the Sciacca Fault (Argnani, 1990; Ghisseti et al., 2009). Fedorik et al. (2018) ran clay analogue models which simulate pure strike-slip and 10°-transtensional and transpressional tectonic regimes. These models produce the same structural styles (splay faulting positioned on one side only of primary fault) and positive flower structures. However, the internal structures within these models could not be analysed and compared to seismic sections. Also our 10°-transtensional analogue sand model produces splay faulting associated with a primary strike-slip fault and positive relief,

comparable to the structural style seen in the Sicilian Channel. Therefore we suggest that the Sciacca Fault was built as a right-lateral fault system under the transtensional tectonics regime.

Richard et al. (2014) describe the North Kuwait carbonate fields where Riedel shear faults formed in a transtensional tectonic regime (Fig. 14b). These authors show Riedel shear structures which are connected at depth by a single fault which is positioned along the SW tips of the before mentioned Riedel structures. Comparable fault system, similarly build in a transtensional tectonic regime, can be observed in the Vienna basin (Fig. 14c), where surface faults are interpreted as Riedel shears, which converge into single fault structure at greater depths (Beidinger & Decker, 2011). These faults mostly occur on one side of the primary displacement zone (PDZ). Both examples present similar structural styles as seen in our 10°-transtensional models, where tips of the Riedel shear faults are positioned exactly above the VD2.

The strike-slip dominated area in our pure strike-slip model (Fig. 7a and 8a) shows comparable fault patterns as observed by Cheng et al. (2017) in the Qaidam Basin, China. The authors's interpretation highlights one sub-vertical strike-slip fault which is bounded by two conjugate faults with different dip angle values (Fig. 14d). Our pure strike-slip model presents comparable fault architecture as the difference of the dip angle value between the two conjugate faults is equal to 15°.

The Confidence Hills in eastern California, USA contains a well exposed, composite, positive flower structure (Dooley & McClay, 1996, Fig. 14e). The flower structure is formed by a doubly plunging anticline that is striking roughly parallel to the bounding oblique-slip reverse faults. In 3D, the faults are inferred to link at depth to a single basal strike-slip fault. This structure shows similar structural styles in comparison to our transpressional models where the pop-up structure is not internally deformed (Fig. 9). Thus, we can suggest that the Confidence Hills might by produced by transpressional tectonic regime.

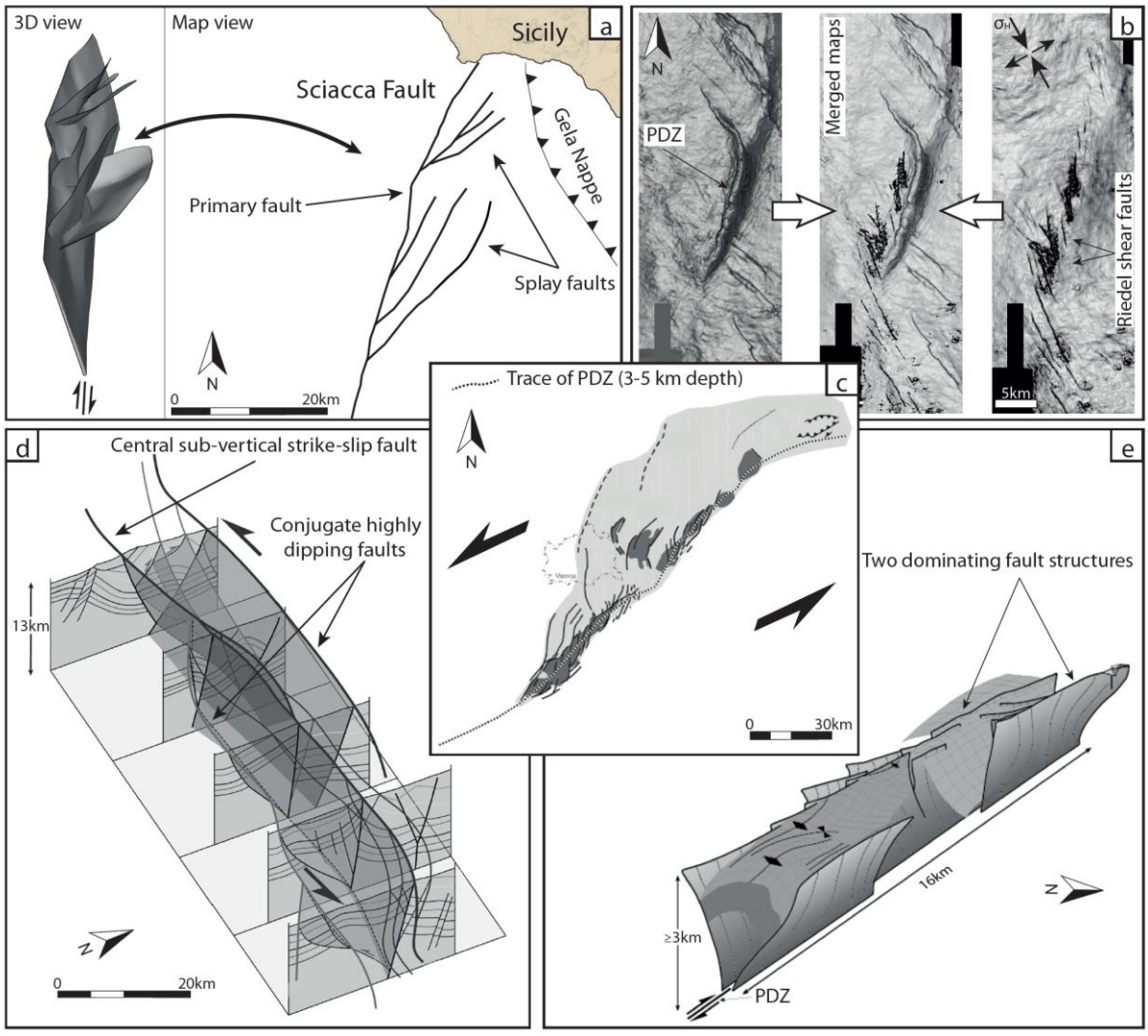

Figure 14: Natural examples of strike-slip dominated areas with similar structural styles as seen in our analogue models: a) Structural framework of the Sciacca Fault (3D seismic interpretation and map view). The most important splay faults are observed on the eastern side of the primary fault; b) Coherence maps obtained from 3D seismic from North Kuwait carbonate fields. Najmah horizont - early Jurassic (left) showing the lower primary displacement zone (PDZ) in the area, Ahmadi horizont - late Jurassic (right) present Riedel shears faults. Merged maps (middle) show the position of the splay faults to the primary fault (Modified from Richard et al. 2014); c) Tectonic sketch map summarising the active kinematics and geometrical fault segmentation of the Vienna Basin strike-slip fault. The lower PDZ of the strike-slip fault is located on the southern tips of the upper Riedel shear faults (Modifier from Beidinger & Decker, 2011); d) 3D conceptual model illustrating structural styles of the Huangshi left-lateral strike-slip structural system in map-view and cross-section (Modified from Cheng et al., 2017); e) 3D synoptic model of the Confidence Hills, constructed with surface data. The fault segments are thought to link at depth to a common PDZ.

The flower structure is formed by doubly plunging anticlines that are oriented roughly parallel the boundary fault segments (Modified after Dooley & McClay, 1996)

5- Conclusion

In this paper we use analogue models to investigate the interaction between strike-slip dominated tectonics and thrust belt structures in a range of tectonic settings (from transpression to transtension). Our main conclusions are as follows:

-The area where strike-slip deformation is concentrated shows an important variation of structural styles. All transpressional models produce pop-up structures along the VD2, whose boundary fault dip angle values decrease with higher degrees of obliquity (Fig. 7b, c, d). The pure strike-slip model forms two conjugate oblique-slip reverse faults, which are steeper than their equivalents in the transpressional models, plus a sub-vertical fault situated above the VD2 (Fig. 7a). The transtensional models (Fig. 8b, c, d) show the change from a splay and primary faults system typical for lower angles of extension obliquity to two highly dipping conjugate oblique-normal faults bounding several minor sub-vertical fault system (higher angle of extension obliquity).

- The pure strike-slip model illustrates the possibility of developing compressional structures in a non-compressive regime, whereas the 10°-transtension model indicates that such structures can form even within a transtensional setting, due to the presence of a thrust front nearby.

-Only the 10°-transtension model develops a splay and primary faults system (Fig. 13). Here early Riedel shear faults preferentially appear in the most extended area, which is on the side of the fixed plate, while no strike-slip structures are formed on the moving plate. Later on, the tips of the Riedel shear faults which are closer to the limit of the VD2 are connected and create the structural style which can be interpreted as a splay- primary faults system.

-The 90˚ linkage (Fig. 5) between fault zones along the VD2 and newly-formed compressive structures associated with the trust belt in pure strike-slip and transpressional models implies that similar kinematics occur in these settings. In transtensional settings, the angle between both fault trends seen on the model surfaces decreases with higher angles of extension obliquity.

We believe our model set-up is well suitable for simulating natural conditions where usually regional stress are not equal on either side of a strike-slip fault system that acts as a physical discontinuity.

-Similar structural styles we observe in the strike-slip part of our models are also present in natural settings such as the Sicilian Channel, the North Kuwait carbonate fields, the Vienna Basin, the Qaidam Basin and the Confidence Hills.

Aknowledgements

Many thanks to Nicole Schwendener for her help with the CT-scanning. The research period of J.F at the University of Bern was funded by the University of Pavia, Bando Mobilità Internazionale. Midland Valley Exploration Ltd. is kindly acknowledged for providing Move licenses to the University of Pavia within the ASI (Academic Software Initiatives).

References

Argnani, A., 1990. The Strait of Sicily rift zone: foreland deformation related to the evolution of a backarc basin, J. Geodyn., 12, 311-331.

Beidinger A., Decker K., 2011. 3D geometry and kinematics of the Lassee flower structure: Implications for segmentation and seismotectonics of the Vienna Basin strike–slip fault, Austria. Tectonophysics 499, 22–40, doi:10.1016/j.tecto.2010.11.006

Billi, A., R. Gambini, C. Nicolai, Storti, F., 2007. Neogene-Quaternary intraforeland transpression along a Mesozoic platform-basin margin: The Gargano fault system, Adria, Italy, Geosphere, 3, 1–15, doi:10.1130/GES00057.1.

Casas, A.M., Gapais, D., Nalpas, T., Besnard, K., Román-Berdiel, T., 2001. Analogue models of transpressive systems. Journal of Structural Geology 23, 733–743

Cheng, X., Zhang, Q., Yu, X., Du, W., Liu, R., Bian, Q., Wang, Z., Zhang, T., Guo, Z., 2017.Strike-slip fault network of the Huangshi structure, SW Qaidam Basin: insights from surface fractures and seismic data. J. Struct. Geol. 94, 1–12

Colletta, B., Letouzey, J., Pinedo, R., Ballard, J.F., Balé, P., 1991. Computerized X-ray tomography analysis of sandbox models: examples of thin-skinned thrust systems. Geology 19, 1063–1067. http://dx.doi.org/10.1130/0091-7613(1991)019b1063:

D'Adda P., Longoni R., Magistroni C., Meda M., Righetti F., Cavozzi C., Nestola Y., Storti F., 2017. "Extensional reactivation of a deep transpressional architecture: Insights from sandbox analogue modeling applied to the Val d'Agri basin (Southern Apennines, Italy)." Interpretation, 5(1), SD55-SD66.

Di Bucci, D., Ravaglia, A., Seno, S., Toscani, G., Fracassi, U., Valensise, G., 2006. Seismotectonics of the Southern Apennines and Adriatic foreland: insights on active regional E–W shear zones from analogue modeling. Tectonics 25, TC4015. http://dx.doi.org/10.1029/2005TC001898.

Di Bucci, D., Ravaglia, A., Seno, S., Toscani, G., Fracassi, U., Valensise, G., 2007. Seismotectonics of the Southern Apennines and Adriatic foreland (Southern Italy): a short note on active E–W shear zones from analogue modeling. Quat. Int. 171–172, 2–13. http://dx.doi.org/10.1016/j.quaint.2007.01.005.

Di Bucci, D., P. Burrato, P. Vannoli, Valensise, G., 2010. Tectonic evidence for the ongoing Africa-Eurasia convergence in central Mediterranean foreland areas: A journey among long-lived shear zones, large earthquakes, and elusive fault motions, J. Geophys. Res. 115, no. B12404, doi 10.1029/2009JB006480.

Dooley, T., McClay, K., 1996. Strike-slip deformation in the Confidence Hills, southern Death Valley fault zone, eastern California, USA. Journal of the Geological Society 153, 375–387.

Dooley, T., Monastero, F., Hall, B., McClay, K.R., Whitehouse, P., 2004. Scaled sandbox modelling of transtensional pull-apart basins: applications to the Coso geothermal system. Geothermal Research Council Transactions 28, 637–641.

Dooley, T.P., Schreurs, G., 2012. Analogue modelling of intraplate strike-slip tectonics:a review and new experimental results. Tectonophysics 574-575, 1-71.

Fedorik, J., Toscani, G., Lodolo, E., Civile, D., Bonini, L., Seno, S., 2018. Structural analysis and Miocene-to-Present tectonic evolution of a lithospheric-scale, transcurrent lineament: The Sciacca Fault (Sicilian Channel, Central Mediterranean Sea) Tectonophysics, 722, pp. 342-355. DOI: 10.1016/j.tecto.2017.11.014

Ghisetti, F. C., A. R. Gorman, M. Grasso, Vezzani, L., 2009. Imprint of foreland structure on the deformation of a thrust sheet: The Plio-Pleistocene Gela Nappe (southern Sicily, Italy), Tectonics, 28, TC4015, doi:10.1029/2008TC002385.

Klinkmüller, M., 2011. Properties of analogue materials, experimental reproducibility and 2D/3D deformation quantification techniques in analogue modeling of crustal-scale processes. Unpublished PhD Thesis, University of Bern, Switzerland.

Leever, K. A., Gabrielsen R. H., Faleide J.I., Braathen A., 2011. A transpressional origin for the West Spitsbergen fold-and-thrust belt: Insight from analog modeling, Tectonics, 30, TC2014, doi:10.1029/2010TC002753.

Lohrmann, J., Kukowski, N., Adam, J., Oncken, O., 2003. The impact of analogue materialproperties on the geometry, kinematics, and dynamics of convergent sand wedges. J. Struct. Geol. 25, 1691–1711. http://dx.doi.org/10.1016/S0191-8141(03)00005-1.

Lowell, J.D., 1972. Spitsbergen Tertiary orogenic belt and the Spitsbergen fracture zone. Geological Society of America Bulletin 83, 3091-3102.

Mahoney L., Hill K., McLaren S., Hanani A., 2017.Complex fold and thrust belt structural styles: Examples from the Greater Juha area of the Papuan Fold and Thrust Belt, Papua New Guinea, Journal of Structural Geology 100, 98-119. https://doi.org/10.1016/j.jsg.2017.05.010

Mandl, G., 1988. Mechanics of Tectonic Faulting. Elsevier.

Naylor, M.A., Mandl, G., Sijpesteijn, C.H.K., 1986. Fault geometries in basement-induced wrench faulting under different initial stress states. Journal of Structural Geology 8, 737–752.

Panien, M., Schreurs, G., Pfiffner, A., 2006. Mechanical behaviour of granular materials used in analogue modelling: insights from grain characterisation, ring-shear tests and analogue experiments. J. Struct. Geol. 28, 1710–1724. http://dx.doi.org/10.1016/j.jsg.2006.05.004.

Richard, P., Naylor, M.A., Koopman, A., 1995. Experimental models of strike-slip tectonics.Petroleum Geoscience 1, 71–80.

Richard, P., Bazalgette L., Kidambi V., Laiq K., Odreman A., Al Qadeeri B., Narhari R., Pattnaik C., Al Ateeqi K., 2014. Structural Evolution Model for the North Kuwait Carbonate Fields and its Implication for Fracture Characterisation and Modelling, presented at the International Petroleum Technology Conference, Doha, Qatar, 20–22 January 2014. IPTC 17620.

Schreurs, C., Colletta, B., 1998. Analogue modelling of faulting in zones of continental transtension and transpression. In: Holdsworth, R.E., Strachan, R.A., Dewey, J.F. (Eds.), Continental Transpressional and Transtensional Tectonics. Geol. Soc. London Spec. Publ. Vol. 135, pp. 59–79. http://dx.doi.org/10.1144/GSL.SP.1998.135.01.05.

Schreurs, G., Hänni, R., Vock, P., 2002. Analogue modelling of transfer zones in fold and thrust belts: a 4-D analysis. In: Schellart, W.P., Passchier, C. (Eds.), Analogue Modelling of Large-scale Tectonic Processes. J. Virt. Expl. Vol. 7, pp. 67–73. http://dx.doi.org/10.3809/jvirtex.2002.00047.

Scholz, C.H., Ando, R., Shaw, B.E., 2010. The mechanics of first order splay faulting: the strike-slip case. J. Struct. Geol. 32 (1), 118–126.

Ueta, K., Tani, K., Kato, T., 2000. Computerized X-ray tomography analysis of threedimensionalfault geometries in basement-induced wrench faulting. Engineering Geology 56, 197–210.

Xiao, Y., Wu, G., Lei, Y., Chen T., 2017. Analogue modeling of through-going process and development pattern of strike-slip fault zone. Petroleum Exploration and Development 44(3), 368–376.

Wilcox, R.E., Harding, T.P., Seely, D.R., 1973. Basic wrench tectonics. Association of Petroleum Geologists Bulletin 57 (1), 74-96.

Zwaan, F., G. Schreurs, J. Naliboff, S., Buiter, S.J.H., 2016. Insights into the effects of oblique extension on continental rift interaction from 3D analogue and numerical models: Tectonophysics, 693 Part B, 239–260, doi: http://dx.doi.org/10.1016/j.tecto.2016.02.036.

Zwaan, F., Schreurs, G., 2016. How oblique extension and structural inheritance influence rift segment interaction: Insights from 4D analog models. Interpretation, 5 (1), pp. SD119-SD138. DOI: 10.1190/INT-2016-0063.1

Zwaan, F., Schreurs, G., Adam, J., 2017. Effects of sedimentation on rift segment and transfer zone evolution in orthogonal and oblique extension settings: Insights from analogue models analysed with 4D X-ray computed tomography and digital volume correlation techniques,Global and Planetary Change, doi.org/10.1016/j.gloplacha.2017.11.002.

5- Conclusions

This thesis first study focus was a natural case (Sicilian Channel, see chapter 2) where available data and seismic activity is present to describe the structural setting of the study area. Interpretation of the seismic dataset reveals a positive flower structure along the Sciacca Fault, which is constituted of one primary and several splay faults positioned mostly on its one side. Analogue clay models were carried out to understand better the kinematics under which this fault complex was built. Numerical models (see chapter 3) have been run to test the consistency of the seismic interpretation and they also provided preliminary results which explain the different tectonic activity along the Sciacca Fault. The observation of splay faults in clay analogue models and Sicilian Channel forced us to think about more about the general process which creates such structures. To obtain an internal image and the evolution of the fault pattern, sand models have been analysed with XRCT technique (see chapter 4). Main conclusions and results of the thesis are:

-Structural map completion of the study area in the Sicilian Channel, where a part of a Transfer zone is seen through the seismic profiles. Two primary transcurrent lineaments were identified (Sciacca and Capo Granitola faults) and for the Sciacca Fault, a 3D model was built.

-Active and non-active segments of Sciacca Fault were mapped through the seismic profiles, while preliminary results from the numerical models produce the same outcome, where the southern segment of the Sciacca Fault show more slip potential that the northern one.

-Moreover, numerical models provide validation of the seismic interpretation through the comparison of the uplift pattern seen in the model and along the Nerita Bank.

-The CT-scan analogue models give the new insides of the internal structural styles of different strike-slip dominated kinematics during the interaction with the thrust belt structure. These models also show the importance of an induced stress differences in analogue modelling.

-The model of splay faults evolution, which are positioned only on the one side of the primary fault is proposed.

- Structural styles observed in the analogue models are compared to natural settings such as Sicilian Channel, two sectors of the Adriatic-Hyblean foreland of the Apennine-Maghrebian chain, North Kuwait carbonate fields, Vienna Basin, Qaidam Basin and Confidence Hills.

Acknowledgments

I would like to thank Dr. Giovanni Toscani, for his guidance, encouragement and advice he has provided throughout my time as his student. I have been extremely lucky to have a supervisor who cared so much about my personal and work life. I would also like to thank Prof. Silvio Seno who created this PhD project. Dr. Lorenzo Bonini is also acknowledged for his suggestions within analogue modelling. In particular, I would like to thank Dr. Emanuele Lodolo and Dr. Dario Civile for their neverending corrections on the manuscript, which significantly improved the final result. I am extremely grateful to Prof. Michele Cooke who supervised me and let me work in her laboratory at the University of Massachusetts. I would like to acknowledge Prof. Guido Schreurs and Dr. Frank Zwaan who allowed me to use the tectonic laboratory at the University of Bern and significantly improved obtained results. I would like to express my gratitude toward my PhD colleagues for their friendship and for their translating skills. I am grateful to the PhD committee of the Earth and Environmental Sciences at the University of Pavia, who financed and selected me for this PhD project. Most of all, I am fully indebted to my wife Michaela and my son Chris, for being my motivation and helped me survive all the stress from these three years.